

**MODELLING THE RESPIRATORY CONTROL
SYSTEM IN HUMAN SUBJECTS FOR
EXERCISE CONDITIONS**

A THESIS
SUBMITTED TO THE FACULTY OF ENGINEERING
OF THE UNIVERSITY OF GLASGOW
FOR THE DEGREE OF
DOCTOR OF PHILOSOPHY

by
Husni Thamrin
October 2008

© Copyright 2008 by Husni Thamrin
All Rights Reserved

Abstract

A model is a very helpful tool to describe, interpret and explain the behaviour of a highly complex system such as the human respiratory system. The research work presented in this thesis is concerned with the development of a nonlinear dynamic simulation model of the respiratory control system in human subjects for exercise conditions.

Modelling the respiratory system is not a new activity but the development of a general model that takes into account the conditions above the lactate threshold has not been attempted previously because of a number of problems that arise for these particular operating conditions. Many variables become increasingly non linear in terms of their temporal pattern and magnitudes. Also metabolic acidosis, which is negligible below the lactate threshold, cannot be neglected for exercise conditions that take the system above the lactate threshold.

The current work has established a general model that applies for exercise conditions below and above the lactate threshold. The model takes into account the factor of metabolic acidosis, which is calculated by estimating the production and consumption of lactate in body tissues and its kinetics in the blood. The slow component increase of muscle energetics and O_2 extraction is also considered. Well established algorithms are employed to estimate the O_2 and CO_2 dissociation curves and the Siggaard-Andersen nomogram is used to calculate blood pH. The model is able to reproduce the main features of the system response in terms of ventilation and pulmonary gas exchange during moderate and heavy exercise. It is also able to reproduce the characteristics of several blood quantities including arterial gas partial pressures, arterial O_2 and CO_2 concentrations, mixed-venous and arterial pH and also lactate and bicarbonate concentrations.

Potential applications of the model include describing the contribution of haemoglobin to performance in exercise conditions, estimating how cardiac output should change during heavy exercise, describing the effect of acidosis, and describing the

changes of body CO₂ stores during exercise. Assumptions, limitations and procedures for testing and evaluating the model are discussed, along with suggestions for further developments that could lead to possible improvements of the model and thus to an extension of the range of problems to which the model could be applied.

Acknowledgements

I would like to express my sincere gratitude to my supervisor, Prof. David J. Murray-Smith for his continued guidance, sincere encouragement, thoughtful support, kindness and understanding during my doctoral studies. I would also like to express my gratitude to Prof. Susan A. Ward of the School of Sport and Exercise Sciences, University of Leeds, who guided this research in terms of its direction from a physiological point of view. I am also grateful to my second supervisor Dr. Bernd Porr for his support and advice. I appreciate the assistance provided by Dr. Andy Cathcart during the early period of this research.

I have also greatly benefited from scientific discussions with research colleagues especially Dr. Jiang Zhang and Dr. Carrie Ferguson. I would like to thank other personnel in the Centre for Systems and Control, Mr. Tom O'Hara and Ms Vi Romanes for help and assistance in technical and administrative aspects of the work.

I would like to show gratitude to the Rectorate of Universitas Muhammadiyah Surakarta for their support to the TPSDP project, from which the funding for this research has come. I would also like to thank to the personnel in TPSDP Sub-Project Management, Mr. Sarjito, Mr. Patna Partono and Mr. Tri Tjahyono for their kind assistance in relation to the financial and other matters.

A million thanks to my family members especially Emak for support, love and care. Also to Elda, Sarah, Hanif and Ihsan; thank you all for your patience, love and understanding. This is all about you.

Also to others who have not been named but nevertheless have been helpful, thank you very much.

Contents

Abstract.....	ii
Acknowledgements.....	iv
Contents.....	v
List of Figures.....	viii
List of Tables.....	xi
List of Symbols.....	xii
Chapter 1 Introduction.....	1
1.1. Modelling and Simulation of the Respiratory System.....	2
1.2. Overview of the Respiratory System.....	5
1.3. Models of the Respiratory System.....	6
1.4. Models of the Respiratory Control System for Exercise Conditions.....	7
1.5. Objectives, Originality and Contributions of the Thesis.....	8
1.6. Outline of the Thesis.....	9
Chapter 2 Physiology of Exercise.....	11
2.1. The Lung.....	12
2.2. Muscle.....	14
2.3. Transport of Oxygen in Blood.....	16
2.4. Transport of Carbon Dioxide.....	18
2.5. Control of ventilation.....	20
2.6. Exercise domains.....	22
2.7. Summary.....	23
Chapter 3 Implementation of a Model for the Respiratory Control System under Exercise Conditions.....	24
3.1. Structure of the Saunders, Bali and Carson model.....	25
3.2. Simulation of the Saunders, Bali and Carson model under rest conditions.....	28
3.2.1. CO ₂ loading by increasing the inspired fraction.....	28
3.2.2. Step increase in CO ₂ inflow in inspired gas.....	30
3.2.3. Step increase in CO ₂ inflow in mixed venous blood.....	31
3.2.4. Hypoxic gas mixtures.....	32
3.3. Simulation of the model under exercise conditions.....	32
3.4. Discussion.....	35
3.5. Summary.....	37
Chapter 4 A Model of the Respiratory System for Conditions of Moderate Exercise.....	38
4.1. Model structure.....	39
4.2. Cardiac output and muscle blood flow.....	40
4.3. Ventilation.....	44

4.3.1. Ventilatory efficiency.....	45
4.3.2. Ventilation profile in the model.....	46
4.4. Pulmonary oxygen uptake.....	48
4.5. Muscle oxygen consumption.....	50
4.6. Carbon dioxide production	51
4.6.1. Carbon dioxide storage in muscle.....	52
4.6.2. Calculation of pH.....	52
4.7. Arterial partial pressure.....	55
4.8. Simulation Results.....	56
4.8.1. Parameter Values.....	56
4.8.2. General Model Behaviour.....	57
4.8.3. Relationship between the $V'CO_2$, $V'O_2$, $V'E$ and Q' variables during phase 1.....	62
4.8.4. Kinetics of blood gas variables during phase 2.....	64
4.8.5. Does muscle have capacity to store CO_2 ?.....	66
4.9. Model Assessment and Discussion.....	68
4.9.1. General Impressions of the Model Behaviour.....	69
4.9.2. Relationship between the $V'CO_2$, $V'O_2$, $V'E$ and Q' variables during phase 1.....	70
4.9.3. Kinetics of blood gas variables during phase 2.....	70
4.9.4. Does muscle have capacity to store CO_2 ?.....	71
4.9.5. Early acidosis.....	72
4.10. Summary.....	73
Chapter 5 Model for Lactate Metabolism.....	74
5.1. Lactate metabolism.....	75
5.2. Model of Lactate Metabolism.....	78
5.3. Parameter values.....	79
5.4. Simulation Results.....	81
5.5. Discussion.....	85
5.6. Summary.....	88
Chapter 6 Model of Respiratory System for Conditions above the Lactate Threshold.....	89
6.1. Model structure.....	90
6.2. Energetics of the muscle.....	90
6.3. Oxygen consumption and maximum oxygen consumption.....	93
6.4. Cardiac output at high intensity exercise.....	96
6.5. Carbon dioxide production.....	98
6.6. Metabolic acidosis.....	99
6.7. Muscle fibre type recruitment.....	100

6.8. Hyperventilation.....	101
6.9. Simulation Results.....	102
6.9.1. Simulation with incremental exercise.....	102
6.9.2. Simulation with constant work rates.....	108
6.9.3. Lactate kinetics at different work rates.....	111
6.9.4. Sensitivity to changes of [Hb].....	112
6.9.5. Effect of changes in cardiac output.....	113
6.9.6. Changes in CO ₂ Stores During Exercise.....	115
6.10. Discussion.....	117
6.10.1. General Impressions.....	117
6.10.2. Potential Application.....	118
6.10.3. Limitation and Improvement.....	119
6.11. Summary.....	120
Chapter 7 Overall Discussion, Conclusions and Future Work.....	122
7.1. Summary, Model Assumptions and Limitations.....	123
7.1.1. Reconstruction of Saunders, Bali and Carson model.....	123
7.1.2. Model for exercise conditions below the lactate threshold.....	124
7.1.3. Lactate metabolism.....	126
7.1.4. Model for exercise above the lactate threshold.....	126
7.1.5. Limitation and potential application.....	127
7.2. Conclusions.....	128
7.3. Suggestions for Further Work.....	129
Bibliography.....	131
Appendix.....	138

List of Figures

Figure 1.1. The respiratory system.....	5
Figure 1.2. Conceptual model of the human respiratory system.....	6
Figure 2.1. ATP supplies phosphate during muscle contraction.....	14
Figure 2.2 Oxygen dissociation curve.....	18
Figure 2.3 Carbon dioxide dissociation curves (at 37°C) for different O ₂ saturation showing Haldane effect.....	20
Figure 2.4 Response of respiratory system to changes of gas tension (at rest)	21
Figure 2.5. Hypothetical response of O ₂ uptake for several constant work rates.....	23
Figure 3.1. Controlled system of the Saunders, Bali and Carson model.....	26
Figure 3.2. Controller used in the Saunders, Bali and Carson model.....	27
Figure 3.3. Simulation result from the Simulink model for an abrupt increase in the fraction of inspired CO ₂ (FICO ₂).....	30
Figure 3.4. Response to step increase in CO ₂ inflow in inspired gas.....	31
Figure 3.5. Response to step increase in CO ₂ inflow in mixed venous blood.....	31
Figure 3.6. Profile of ventilation for 100 W exercise.....	33
Figure 3.7. Changes in arterial gas partial pressures during 100 W exercise	34
Figure 3.8. Response of the modified model for PaCO ₂ and PvCO ₂ during transition from rest to 100 W exercise.....	34
Figure 3.9. Response of the modified model for ventilation during transition from rest to 100 W exercise.....	35
Figure 4.1 Structure of the Respiratory System Model.....	39
Figure 4.2. The two phase response of cardiac output as suggested by some investigators.....	43
Figure 4.3. Kinetics of pulmonary oxygen uptake (V'O ₂) at the onset of a step increase in moderate intensity exercise.....	49
Figure 4.4. Siggaard Andersen nomogram.....	54
Figure 4.5. Changes of the ratio of dead space volume to tidal volume (V _D /V _T) over the range of ventilation considered.....	56
Figure 4.6 Response for exercise in moderate intensity domain: Ventilation (V'E) and CO ₂ output (V'CO ₂) from simulation.....	58
Figure 4.7 Response for cardiac output (Q') and pulmonary oxygen uptake (V'O ₂) from simulation	59
Figure 4.8 Arterial and venous CO ₂ partial pressures from simulation.....	60
Figure 4.9 Arterial and venous O ₂ partial pressures from simulation.....	60
Figure 4.10 Simulation result for bicarbonate concentration and arterial lactate concentration.....	61

Figure 4.11 Arterial and venous pH during 100 W exercise.....	62
Figure 4.12. Kinetics of $V'CO_2$ for different phase-1 kinetics of Q'	63
Figure 4.13. Kinetics of $V'O_2$ for different phase-1 kinetics of Q'	63
Figure 4.14. Kinetics of $V'CO_2$ for different phase-1 magnitudes of VE'	64
Figure 4.15 Kinetics of $V'O_2$ for different phase-1 magnitudes of VE'	64
Figure 4.16. Concentration of blood oxygen at the onset of exercise.....	65
Figure 4.17 Muscle vascular gas content at the onset of exercise.....	65
Figure 4.18 Simulation result for blood oxygen concentration in artery, muscle venous and mixed venous blood.....	66
Figure 4.19. CO_2 output for two simulation conditions: with and without muscle CO_2 storage.....	67
Figure 4.20. RER for two simulation conditions: with and without muscle CO_2 storage..	67
Figure 4.21. Arterial PCO_2 for two simulation conditions: with and without muscle CO_2 storage.....	68
Figure 5.1. Lactate concentration in the artery during a step increase in work rate for moderate, heavy and very heavy exercise	76
Figure 5.2. Structure of the model for lactate metabolism.....	78
Figure 5.3. Lactate concentration in blood and muscle compartment during unloaded exercise.....	82
Figure 5.4. Lactate concentration in blood and muscle compartment during 100 W exercise starting at time = 0 min on the base line of unloaded exercise.....	82
Figure 5.5. Lactate concentration in blood and muscle compartment during unloaded exercise.....	83
Figure 5.6. Arterial [La] after a sudden increase of muscle [La] at the 20th minute on the base-line of unloaded exercise.....	84
Figure 5.7. Lactate concentration in blood and muscle compartment during 100 W exercise.....	85
Figure 5.8. Arterial [La] after 3 minutes maximal exercise.....	86
Figure 6.1. Two samples of individual data taken during cycle ergometer exercise at a level 50W less than the ventilatory threshold.....	91
Figure 6.2. Model response of muscle O_2 extraction ($Q'O_2$) for exercise at 200 watt where LT is assumed to be 100 watt.....	96
Figure 6.3. Model response for arterial and mixed venous O_2 content during incremental exercise from unloaded condition to 300 W in 10 minutes.....	104
Figure 6.4. Model response for arterial and mixed venous CO_2 content during incremental exercise from unloaded condition to 300 W in 10 minutes.....	105
Figure 6.5. Model response for arterial and mixed venous CO_2 partial pressure during incremental exercise from unloaded condition to 300 W in 10 minutes.....	105

Figure 6.6. Model response for arterial and mixed venous pH during incremental exercise from unloaded condition to 300 W in 10 minutes.....	106
Figure 6.7. Model response for kinetics of pulmonary gas exchange during incremental exercise.....	107
Figure 6.8. Model response for kinetics of ventilatory equivalent during incremental exercise.....	107
Figure 6.9. Breath by breath measurement of pulmonary gas exchange of a relatively fit subject during incremental exercise.....	108
Figure 6.10. Model response for pulmonary oxygen uptake at different work rates.....	109
Figure 6.11. Model response for ventilation at different work rates.....	109
Figure 6.12. Model response for CO ₂ output at different work rates.....	110
Figure 6.13. Second by second response of a subject conducting exercise at several constant work rates from the base line of unloaded exercise.....	110
Figure 6.14. Model response for arterial [La] at work rates below LT.....	111
Figure 6.15. Model response for arterial [La] at work rates above LT.....	112
Figure 6.16. Pulmonary gas exchange during 150W exercise for different [Hb].....	112
Figure 6.17. Mixed-venous gas content during 150 W exercise for different [Hb].....	113
Figure 6.18. Arterial and mixed venous O ₂ content in simulation for different cardiac output levels.....	114
Figure 6.19. Arterial mixed venous O ₂ content difference against the ratio of V'O ₂ to V'O ₂ max as determined from simulation studies with different cardiac output values..	115
Figure 6.20. Kinetics of the total body CO ₂ stores during 60 W exercise.....	116
Figure 6.21. Kinetics of body CO ₂ stores calculated from experimental data.....	116
Figure 6.22. Kinetics of CO ₂ stores during exercise above LT (150W).	117

List of Tables

Table 2.1. Characteristics of muscle fibre types.....	16
Table 3.2. Comparison of Simulink model parameters with those of Saunders, Bali and Carson (SBC)	28
Table 3.3. Result of examination of CO ₂ loading by increasing the inspired fraction.....	29
Table 3.4. Result of experiment using hypoxic gas mixtures.....	32
Table 3.5. Values of cardiac output and metabolic rates for the simulation of exercise....	32
Table 5.6. Lactate concentration after 30s maximal exercise and during recovery.....	77
Table 5.7. Muscle volume in kg of several body organs (Kida et al., 2006).....	79
Table 6.8. Mean values of variables as presented in Sun et al. (2001).....	103
Table 6.9. Base line value of O ₂ uptake, CO ₂ output and cardiac output.....	104

List of Symbols

[Hb]	Haemoglobin concentration
[La]	Lactate concentration
BB	Buffer base
BE	Base excess
C	Concentration
CaCO ₂	Arterial CO ₂ concentration (content)
CaO ₂	Arterial O ₂ concentration (content)
CCO ₂	CO ₂ content
CMO ₂	Muscle oxygen content
CO ₂	Carbon dioxide
C _{O₂}	O ₂ content
CP	Critical point
FACO ₂	Alveolar CO ₂ fractional concentration
FAO ₂	Alveolar O ₂ fractional concentration
FICO ₂	Inspired fractional concentration of CO ₂
FIO ₂	Inspired fractional concentration of O ₂
HR	Heart rate
LT	The lactate threshold
MyoO ₂	Myoglobin O ₂ concentration
NBB	Normal buffer base
O ₂	Oxygen
P	Production (of lactate)
PACO ₂	Alveolar CO ₂ partial pressure
PaCO ₂	Arterial CO ₂ partial pressure
PAO ₂	Alveolar O ₂ partial pressure
PaO ₂	Arterial O ₂ partial pressure
PB	Barometric (air) pressure
PCO ₂	CO ₂ partial pressure
PMO ₂	Oxygen partial pressure in the muscle compartment
PO ₂ , P _{O₂}	O ₂ partial pressure
Q' , Q̇	Cardiac output
Q'B , Q̇B	Brain blood flow
Q'CO ₂ , Q̇CO ₂	Muscle CO ₂ production
Q'M , Q̇M	Muscle blood flow
Q'O ₂ , Q̇O ₂	Muscle O ₂ extraction

$Q'OT, \dot{Q}OT$	Other tissue blood flow
$RBCO_2$	Brain CO_2 production
RBO_2	Brain O_2 consumption
RER	Pulmonary respiratory exchange ratio
$ROTCO_2$	Other tissue CO_2 production
$ROTO_2$	Other tissue O_2 consumption
RQ	Muscle respiration quotient
SO_2	Blood O_2 saturation
SV	Stroke volume
T	Body temperature
TD	Fundamental component time delay
U	Utilization (of lactate)
V	Volume
$V'A, \dot{V}A$	Alveolar ventilation
$V'CO_2, \dot{V}CO_2$	Pulmonary CO_2 output
$V'E, \dot{V}E$	Ventilation
$V'O_2, \dot{V}O_2$	Pulmonary oxygen uptake
VD	Dead space volume
VD/VT	Ratio of dead space to tidal volume
VM	The muscle volume
VT	Tidal volume
WR	Work rate
α	Solubility (of O_2 or CO_2)
αMO_2	O_2 solubility of the muscle compartment
$\Delta V'O_2/\Delta WR$	Ratio of oxygen uptake to work rate
μ, Φ_1	Phase 1 magnitude relative to steady-state (final) value
σ	Partition coefficient
τ	Time constant
τ_c	Muscle CO_2 storage kinetics

Meaning of indexes

i	Initial (or phase 1) component
f	Fundamental (or phase 2) component
s	Slow component
bl	Base line value
M, m	Of muscle
max	Maximum value

OT, o	Of other tissue
La	Of lactate

Chapter 1

Introduction

1.1. Modelling and Simulation of the Respiratory System

Physiological systems are very complex and hierarchical in structure and the complexity is present in every level including the organs, the cells and biochemical molecules. The great complexity of physiological systems makes it difficult to describe, interpret or explain their behaviour without the assistance of some form of model. Dynamic models are particularly helpful in discussing physiological systems as living systems are seldom in a steady state. Also, it is often impossible to measure a quantity directly from a living subject and a good dynamic model can sometimes help in the process of making a feasible estimate for the value of the quantity of interest. Many applications of physiological models in biology and medicine can be identified and these include aiding understanding, testing hypotheses, developing inferential measurement techniques, teaching, simulating and experimental design (Cobelli and Carson, 2001).

Modelling and simulation has a long history when related to applications in physiology including the respiratory system. The notion of control of respiration emerged as early as the 1900s, as recognized through the works of, for example, Krogh and Lindhard (1913) and Douglas and Haldane (1909). However, the use of formal mathematical control systems theory in describing the control of respiration did not start until the around 1950s, for instance through the works by Gray (1946), Grodins et al. (1954) and Defares (1964).

Model development and simulation of physiological systems is an interdisciplinary process involving biomedical scientists, physiologists, physicians, engineers and computer experts. Mathematical, biochemical and physical models of physiological systems, e.g. the circulatory system, the renal system, the cardiovascular system and the respiratory system have been derived and their dynamical behaviour have been studied by simulation. Some of these models have been successfully applied to the development of parameter estimation techniques either to optimize the parameter sets or to estimate those parameters that are important for monitoring or treatment in health care units. Taking the case of the respiratory system for example; several methods have been developed to estimate cardiac output without the need to sample blood (e.g. Capek (1988), also see review by Olszowka et al. (2003)); efforts have also been made to use gas exchange models to estimate cardiopulmonary quantities (e.g. (Bache, 1981)).

Modelling and simulation in engineering and in physiology, or in the life sciences in general have some common problems so that the possibility is open to apply similar methods in solving problems across these various disciplines. For example, the characteristics of the respiratory system have been studied using several test signal stimuli, such as step functions, ramps, impulses, and even pseudo random signals that are usually applied when interrogating engineering systems, e.g. (Fujihara et al., 1973a;

Fujihara et al., 1973b). Also stability theory that is normally applied to engineering control systems has been used to describe a respiratory dysfunction called Cheyne-Stokes respiration which is indicated by periodic breathing (Batzel and Tran, 2000a; Batzel and Tran, 2000b). The cardiovascular system has been observed to have equivalence with electrical circuits and this fact can be used with benefit in the analysis of the cardiovascular profile during exercise through the use of electric circuit principles (e.g. Ohm's Law and Kirchhoff's Laws) (Dolensek et al., 2007).

However, it must be noted that modelling of a physiological system is generally the reverse of the modelling process in engineering science and systems theory in that the physiological system is already created and has been optimized through natural processes. The main goal of engineering modelling is system synthesis and optimization where the mathematical model may be used, for example, to develop an optimal control strategy for a process or keep a process within a range of "normal" operating conditions. On the other hand, modelling and simulation of physiological systems is an iterative process involving model development, computer simulation, and then repeatedly adjusting the structure of the model and its parameters in order to match the real biological system in some specific way. The derived model is said to be successful if, for the intended application of the model, an appropriate level of match is obtained between the simulation results and data obtained from the real physiological system for the variables that are deemed important for that application. In certain circumstances, the physiologists are more interested in developing a model that adequately describes the pathological behaviour in disease, outside the normal range of conditions for the system under investigation (Moeller, 1993) and modelling and simulation principles can again be useful in such cases.

Once a physiological model is set up, a process needs to be conducted to assess the accuracy and suitability of the model for the intended application. The procedures depend on the principles of model validation which include the following aspects (Murray-Smith and Carson, 1988):

- a). Empirical validity in which an adequate level of agreement is shown between the model and the corresponding data.
- b). Theoretical validity in the sense that the model shows overall consistency with the accepted theories
- c). Pragmatic validity such that the model satisfies all the requirements of the intended application.
- d). Heuristic validity in the sense that the model can be shown to have potential for explanation and hypothesis testing.

Application of the appropriate methods of model validation leads to three possible outcomes (Murray-Smith, 1995):

- 1). The experimental data sets used in the assessment of the model cannot be explained by any combination of the model structures and parameter values considered. The candidate models are therefore all falsified and it is essential to reconsider the structure of the model and the underlying assumptions.
- 2). One or more combinations of model structure and parameter values produce a match that is considered adequate for the intended application but the level of uncertainty is excessive for some parameters. In this case the model may be of little predictive value and reassessment of the model structure may be necessary.
- 3). A model produces satisfactory agreement with experimental results obtained from the real system and involves parameter values that are considered plausible. In this case the model is of acceptable validity in terms of the specific tests applied and may be used for the intended application until such time that further evidence is found that falsifies the model.

In the development of complex physiological models it is inevitable that the information upon which a specific model is based comes from a variety of sources. Even if there is close collaboration between an experimental physiologist and the model developer it is almost inevitable that, in a practical model development project, at least some sub-models will be developed on the basis of published results of experiments carried out by others. In such situations the data sets available are limited and the data must be looked at carefully in order to ensure that there is some separation between data used for the estimation of model parameters and other forms of model tuning and the data used eventually for testing of the model or sub-model to ensure that it is fit for the intended purpose. Attempts to validate a model using data which have been used already for purposes of model tuning or parameter estimation generally leads to false and usually over-optimistic conclusions.

In cases where a model has been developed and tested using limited experimental data sets for the sub-models it is important that there should be extensive testing of the overall model and that as many situations as possible be considered and that evidence from a number of different sources should be used. Even in cases of this kind where a large amount of data may exist from experiments carried out on the complete system, there may be significant problems in terms of any form of detailed external validation because information is inevitably lacking about the parameter values appropriate to each of the subjects used in the experimental investigations. In many situations the most appropriate form of external validation for complex physiological models involves qualitative feature matching rather than detailed point-by-point comparisons over the whole experimental record. At best it may be possible to compare trends, or make comparisons of steady state levels, or consider peak values and their times of occurrence,

or assess the frequency and rate of decay or growth of an oscillatory response. Although the application of some techniques of model validation that have been found useful in engineering applications may be inappropriate in physiology, the general principles of model validation are similar in all fields of application whatever the level of uncertainty in the model structure and parameters. Modelling is always an iterative process involving repeated steps which include model formulation, tuning and parameter estimation and repeated testing. The details of all these iterative steps depend on the nature of the application and the purpose for which the model is being developed.

1.2. Overview of the Respiratory System

Respiratory system can be defined as a group of organs involved in drawing oxygen into and removing carbon dioxide out of the body or cell. Oxygen is required to enable living cells to conduct aerobic metabolism (or respiration) to obtain energy and carbon dioxide is the waste product of the metabolism.

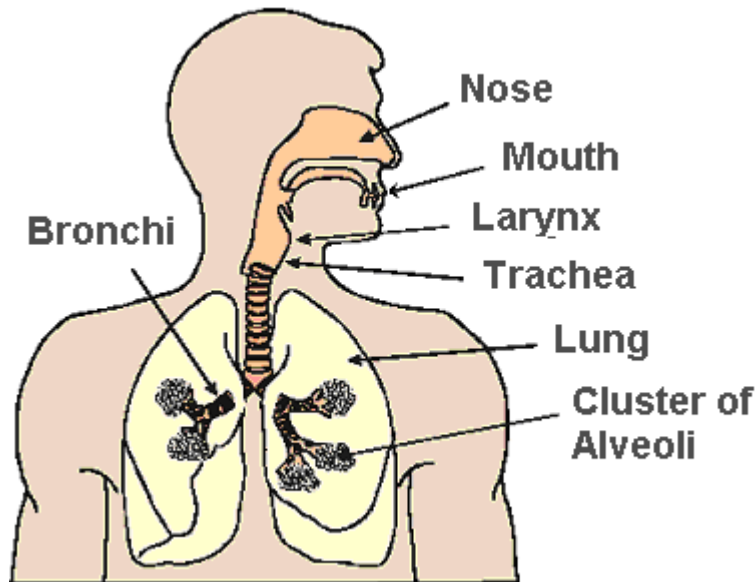


Figure 1.1. The respiratory system

In human, respiratory system consists of several organs. The nose or mouth, the trachea and the bronchi serve as the air passage (Figure 1.1). The lung with its alveoli facilitates oxygenation of the blood with a concomitant removal of carbon dioxide.

The context of respiratory system can be extended further to reach body tissues because respiration, which utilizes oxygen and produces carbon dioxide, takes place in the body tissues. Within this context, the heart plays a part in the respiratory system because it drives the blood pass through the lung and the body tissues to transports O_2 and CO_2 (Figure 1.2).

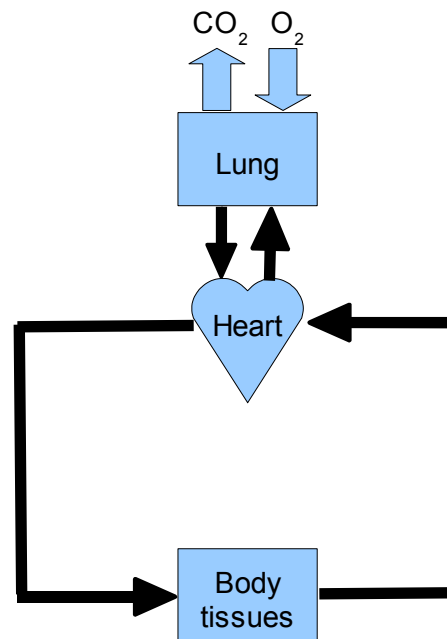


Figure 1.2. Conceptual model of the human respiratory system

1.3. Models of the Respiratory System

Many models to describe the behaviour of respiratory systems have been developed and more are still in development. Some of them are intended to be general models in an effort to describe the whole functionality of the respiratory system, but many are designed to describe a specific function within the large system of respiration.

For example, Barstow and Mole have developed a model consisting of a muscle compartment and a lung compartment where oxygen exchange between them is provided by the arterial and venous blood circulation (Barstow and Mole, 1987). The model was intended to demonstrate the effect of blood circulation on the kinetics of pulmonary oxygen uptake ($\dot{V}O_2$). With the use of an assumed first-order exponential as the kinetics of muscle oxygen consumption ($\dot{Q}O_2$) and appropriate physiological values for other parameters, they were able to show that the kinetics of $\dot{V}O_2$ should contain two components. The first component was determined by the cardiovascular system (the blood circulation) and the second was a reflection of $\dot{Q}O_2$. They then suggested that $\dot{Q}O_2$ could be estimated from $\dot{V}O_2$.

Stuhmiller and Stuhmiller (2006) designed a model that describes the respiration, circulation, oxygen metabolism, and ventilatory control during exposure to carbon monoxide in both human and animals. Their model reaffirms the role of brain hypoxia on hyperventilation during carbon monoxide exposures.

Khoo et al. (1982) proposed a general model which includes controller non-linearity. The model was specially developed to study the stability property of the system, and was able to account for several kinds of periodic breathing resulting from instability in

respiratory control: in normalcy during sleep and on acute exposure to high altitude, in sleeping infants, and in patients with cardiovascular or neurological lesions.

Probably the work of Grodins et al. (1967) is the first to design the general model of the respiratory control system. Their model consists of the brain and other tissues compartments as an O_2 consumer and CO_2 producer, the blood that transports the respiratory gases to and from the tissues and the lung, and a controller function that depends on the partial pressure of O_2 and CO_2 . Their model performs well in terms of reproducing the response to normal conditions as well as hypoxia at sea level, hypoxia at altitude, inhalation of carbon dioxide and metabolic acidosis.

1.4. Models of the Respiratory Control System for Exercise Conditions

Several models have also been created to simulate the actions of the respiratory control system when the subject is performing exercise. Until the 1970s, arterial partial pressure of CO_2 and O_2 and arterial pH were the only variables that were identified as taking part in the control of ventilation. In exercise conditions, those variables change very little while ventilation may increase many times. Feedback control theory suggests that as the controller is assumed to be proportional, the error should be related to the controlled system gain. However, if the controller gain is estimated from the system response at rest, the error is too small to account for the ventilation during exercise.

The model developed by Grodins et al. (1967) thus fails when tested under exercise conditions. Grodins continued his work by adding a term to his controller equation which is proportional to CO_2 output. However this had no physiological basis and, as a result, the resulting model was not widely accepted.

Saunders et al. (1980) modified Grodins' model to include cyclic ventilation, respiratory dead space volume, variable lung volume, a blood shunt, a separate muscle compartment and a different controller equation. They tested their model for several different situations, including increased inspired CO_2 fraction, a step increase in mixed-venous blood CO_2 concentration, breath-holding and exercise tests. They obtained mixed results overall and the exercise test result was poor. Saunders (1980) himself used the model to propose other controller equations that calculate ventilation based on the rate of rise (not the mean value) of arterial CO_2 partial pressure and he was apparently successful in describing the increase of ventilation during exercise.

Cabrera et al. (1998, 1999) developed a model having 4 compartments consisting of an alveolar compartment, a skeletal muscle compartment and a splanchnic and other tissues compartment. Unlike previous models which focused the modelling on respiratory gases, these authors included biochemical reactions of several metabolic substances, such as lactate, pyruvate and glycogen, which highly complicated their model. They tried

ventilation controller equations that were similar to those developed previously by Grodins et al. (1967) and Saunders (1980). The model is intended primarily to investigate the response of lactate concentration against changes in hypoxia and exercise but it is not concerned with respiratory dynamics. The model is able to show the kinetics of many metabolic species during hypoxia and exercise with generally fair results.

Recently, scientists began to consider that potassium may fulfil the criteria as the controller variable that stimulates ventilation during exercise (see Paterson (1992) and McCoy and Hargreaves (1992) but see McLoughlin et al. (1994) for a slightly contrasting suggestion). Ursino and Magosso (2004) have developed a model incorporating arterial potassium concentration as a variable that controls ventilation among other variables such as gas partial pressure in the artery and brain. A chemoreceptor is sensitive to changes in magnitude and rate of rise of arterial $[K^+]$ and it serves as a feedforward control element that manipulates ventilation. The model may be used to highlight the role of each factor that contributes to control of ventilation but the simulation result has not been well verified.

1.5. Objectives, Originality and Contributions of the Thesis

In this research, a general model will be developed, which put emphasis on the reproduction of the responses of the human respiratory control system under exercise conditions below and above the lactate threshold. In particular, the research aims at several objectives below:

- Reconstruction of the Saunders, Bali and Carson (SBC) model using currently popular simulation software and study the possibility to modify or extend the SBC model to apply for conditions of exercise.
- Development of a model of respiratory control system that is valid for condition of moderate exercise, i.e. below the lactate threshold.
- Construction of a model of lactate metabolism that has a valid profile of blood lactate concentration in the conditions of exercise.
- Development of a model of respiratory control system for conditions above the lactate threshold, which has the same structure with the model for moderate exercise condition but with additional features that apply for conditions above the lactate threshold.

For each constructed and developed model, validation will be conducted against data and information that is obtained from published sources.

The work described in this thesis is original. To our knowledge, developing a general and comprehensive model that incorporates conditions above the lactate threshold has never been done before. For example, models that were developed by Cabrera et al. (1998), Saunders et al. (1980) were tested for exercise below the lactate

threshold. The model by Ursino and Magosso (2004) describes the control of ventilation but does not show the effect on the kinetics of respiratory gases.

Several modelling efforts for incremental exercise, which means its applicability spans from below to above the lactate threshold, have been conducted to describe specific functions. This means that the developed models are not general models. For example, Lamarra et al. (1989) developed a model that describes the kinetics of arterial partial pressure of CO₂ and O₂. Rowlands (2005) developed a compartmental model that incorporates CO₂ and several blood biochemical ions to describe behaviour of CO₂ stores.

The main contributions of this research are as follows:

- A general model of respiratory control system for a human subject under exercise conditions is developed. The model is applicable for exercise conditions in all domains of exercise below and above the lactate threshold.
- The model is able to reproduce the characteristics of pulmonary gas exchange during exercise, i.e. ventilation, oxygen uptake and carbon dioxide output for at least two exercise forcing functions, i.e. a ramp and a step, which are already widely used in interrogating the respiratory control system.
- The model is able to reproduce the characteristics of several arterial blood quantities: partial pressure of oxygen and carbon dioxide, oxygen and carbon dioxide concentration, pH, lactate and bicarbonate concentration.

1.6. Outline of the Thesis

This thesis is divided into 7 chapters and is organized as follows:

Chapter 1 outlines the background aspects of modelling and simulation in the field of the respiratory system and the contribution of the thesis. In addition, this chapter gives a brief review of some models that have been developed in previous investigations.

Chapter 2 describes several body compartments, i.e. the lung, the muscle and the blood, that have major involvement during the course of exercise, along with related mathematical relationships. In addition, this chapter describes the physiological basis for the control of ventilation and provides an explanation of the basic terminology commonly used in exercise physiology.

Chapter 3 reviews a model of the respiratory control system that was developed by Saunders et al. (1980). The model is reconstructed using currently available modern software tools and is assessed in terms of possible modifications to make it applicable for a wider range of exercise conditions.

Chapter 4 describes the development of a model of the respiratory control system that is applicable for exercise in the moderate intensity domain. The chapter provides a more in-depth discussion of respiratory parameters and variables and includes mathematical equations that relate those variables and parameters. The resulting model structure is also shown and discussed. Simulation results are presented and analysis is provided firstly to compare the simulation results with experimental results and secondly to illustrate possible uses of the model.

Chapter 5 investigates lactate metabolism. A model for lactate metabolism is developed which is suitable in form to incorporate as an integral part of the general model. The lactate model focuses on the reproduction of the kinetics of arterial lactate concentration during exercise. The modelling is important to simulate metabolic acidosis that arises during the early period of exercise and during exercise in the heavy intensity domain. Simulation is conducted to demonstrate that the model produces responses that have an appropriate form.

Chapter 6 describes the development of the general model that applies for exercise conditions above the lactate threshold. Basically, the structure is similar to the model described in Chapter 4 but several additional elements are introduced to make the model suitable for the heavy exercise domain, for example hyperventilation. This chapter presents the simulation result for two different stimuli, i.e. incremental exercise and for various levels of constant work rate below and above the lactate threshold. The model response is assessed and possible applications are discussed.

Chapter 7 summarises the main features of the resulting model and presents the overall conclusions of the research study. Several suggestions are made for future research work.

Chapter 2

Physiology of Exercise

This chapter provides description of several body compartments that have major involvement during the course of exercise. It also describes several basic terminologies that are commonly found in exercise physiology.

2.1. The Lung

The lung is the respiratory organ which has the main function to transport oxygen from the atmosphere into the bloodstream, and to excrete carbon dioxide from the bloodstream into the atmosphere. Gas exchange is accomplished in the specialized cells that form thin-walled air sacs called alveoli. From the atmosphere to the alveoli, the respiratory gases go through conducting airways from the nose or mouth termed the trachea, bronchi and bronchioles. The huge number of alveoli provides an enormous surface area for the gas exchange. A large number of fine blood capillaries surround the alveoli allowing oxygen from the air inside the alveoli to diffuse into the bloodstream, and carbon dioxide to diffuse from the blood to the alveoli.

The construction of alveoli is so effective for the purposes of gas exchange that in only one third of its journey through the lung, the blood becomes saturated with oxygen. In a short time, the partial pressure of oxygen and carbon dioxide in the blood capillaries become equal to that in the corresponding alveoli. Even during exercise, when blood flows with higher speed, the blood can still be fully oxygenized before it leaves the lung.

Not all the gas that is inhaled fills the alveoli, some fills the conducting airways where gas exchange cannot take place. The volume of inhaled gas that does not participate in gas exchange is called the anatomical dead space and it amounts to about 150 ml of the 500 ml which forms the typical tidal volume, i.e. the volume of gas that is inhaled and exhaled in one breath. The anatomical dead space increases as the tidal volume is increased. The physiological dead space is defined as being equal to the anatomical dead space plus the alveolar dead space. The alveolar dead space results from the fact that there is a region in the alveoli that does receive air to be exchanged, but for which there is not enough blood flowing through the capillaries for any exchange to be effective. It is a very small volume in a normal subject (5 ml) but can increase due to some lung diseases.

As mentioned above, the anatomical dead space volume increases with the increase of tidal volume. The ratio of dead space volume (VD) to tidal volume (VT) at rest is typically:

$$VD/VT = 0.35 \quad (2.1)$$

During exercise, the ratio of dead space to tidal volume decreases depending on the work rate and can drop to values as low as 0.17 (Wasserman et al., 1967).

The volume of gas that is inhaled and exhaled in a minute is called the ventilation. The ventilation ($V'E$) depends on the tidal volume (VT) and the frequency of breathing (f):

$$\dot{V}E = V_T \cdot f \quad (2.2)$$

Because not all the ventilated air is involved in the gas exchange, a term called alveolar ventilation ($\dot{V}'A$) has been introduced. This represents the portion of the ventilated air that fills the alveoli and takes part in gas exchange. The alveolar ventilation is equal to the ventilation minus the dead space ventilation:

$$\dot{V}'A = \dot{V}E - \dot{V}D \quad (2.3)$$

or

$$\dot{V}'A = \dot{V}E(1 - V_D/V_T) \quad (2.4)$$

If the rate of respiratory gas exchange is known, the fraction of the gas in the alveoli can be calculated and thus the arterial partial pressure can be estimated. For example, for carbon dioxide:

$$F_{ACO_2} = \dot{V}CO_2 / \dot{V}'A \quad (2.5)$$

where F_{ACO_2} is the fractional concentration of alveolar CO_2 , $\dot{V}'CO_2$ is the volumetric rate of CO_2 output where both $\dot{V}'CO_2$ and $\dot{V}'A$ are expressed in terms of STPD (standard temperature and pressure dry). Equation (2.5) can be converted in terms of more commonly used physiological variables and units to give the equation:

$$P_{ACO_2} = 863 \cdot \dot{V}CO_2 / \dot{V}'A \quad (2.6)$$

where P_{ACO_2} is the partial pressure of alveolar CO_2 in mmHg, $\dot{V}'CO_2$ in STPD and $\dot{V}'A$ in BTPS (body temperature and pressure saturated with water vapour) and 863 is the conversion factor between the different gas measurement units.

For an ideal lung, in which the ventilation-perfusion ratio is uniformly normal, where there is no diffusion limitation and where no right to left shunt exists, the partial pressure of O_2 and CO_2 in the artery will be equal to the partial pressure in the alveoli:

$$P_{aCO_2} = 863 \cdot \dot{V}CO_2 / \dot{V}'A \quad (2.7)$$

or

$$P_{aCO_2} = \frac{863 \cdot \dot{V}CO_2}{\dot{V}E(1 - V_D/V_T)} \quad (2.8)$$

Similarly, the fractional concentration of oxygen in the alveoli may be calculated as:

$$F_{AO_2} = F_{IO_2} - \dot{V}O_2 / \dot{V}'A \quad (2.9)$$

where F_{IO_2} is the fractional concentration of inspired oxygen. Equation (2.9) can be converted so that it is expressed in terms of partial pressures as:

$$PAO_2 = 147 - 863 \cdot \dot{V}O_2 / \dot{V}A \quad (2.10)$$

where 147 is the partial pressure of the inspired oxygen. For an ideal lung,

$$PaO_2 = 147 - \frac{863 \cdot \dot{V}O_2}{\dot{V}E(1 - VD/VT)} \quad (2.11)$$

The above derivation has been presented and explained in a number of earlier publications such as in (Whipp, 1990; Whipp, 1998).

2.2. Muscle

Skeletal muscles are the part of human body that transform potential biochemical energy into mechanical movement when we exercise. Fibres in muscles, where each unit is called a myofibril, perform contraction and relaxation by a process that involves establishing certain chemical bonds and breaking other bonds (Johnson, 1991). The process requires a source of energy which is immediate and durable. Immediate energy is available in the form of adenosine triphosphate (ATP) in the muscle cytosol. The amount of ATP in cytosol is limited and an intensely contracting muscle can consume it in less than a second (Hultman and Greenhaff, 1991).

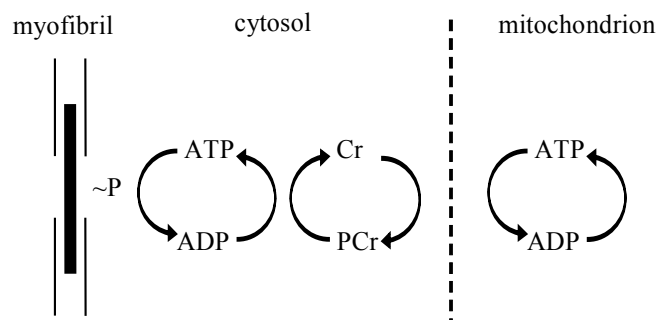


Figure 2.1. ATP supplies phosphate during muscle contraction. The myofibril is the muscle fibre unit, the cytosol is the internal fluid of cells and a mitochondrion is a part of a cell which produces most ATP. A cell contains at least one mitochondrion and can have thousands mitochondria (adapted from Wasserman et al., 2005).

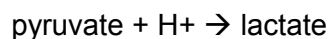
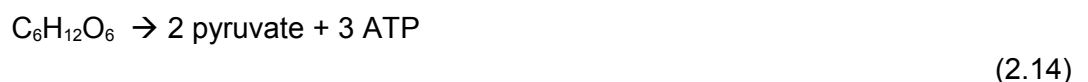
When utilized, ATP is transformed into adenosine diphosphate (ADP) and an inorganic phosphate. This process produces high energy. In turn, muscle phosphocreatine (PCr) is ready to break into creatine and phosphate, with which ADP combines in the resynthesis of ATP. The concentration of intracellular PCr is about 5 times greater than the concentration of ATP (Wasserman et al., 2005) so it can take several seconds of intense exercise before the phosphocreatine is fully utilized. Creatine will then combine with phosphate from the mitochondria to reproduce phosphocreatine. These cycles are depicted in Figure 2.1.

In mitochondria ATP is produced through oxidation of metabolic substrates such as carbohydrates and lipids. Different substrates use different amounts of oxygen and produce different quantities of ATP. The following equations show the oxidation of glycogen, which is a form of carbohydrate that is stored in muscle, and palmitate, which is a form of lipid. Oxidation of glycogen provides enough energy to resynthesize 36 mol of ATP while oxidation of palmitate provides energy to produce 130 mol of ATP.



As may be seen from the above equations, complete oxidation requires a large amount of oxygen. This is also known as an aerobic reaction. Aerobic metabolism always produces carbon dioxide and the amount is dependent on the substrate used. For each molecule of glycogen, 6 molecules of oxygen are used and 6 molecules of carbon dioxide are produced. In contrast, each palmitate molecule needs 23 molecules of O_2 in its oxidation and produces 16 molecules of CO_2 . It is common to express the relative amount of CO_2 produced to the O_2 consumed as a quantity known as the respiratory quotient (RQ). Hence, the RQ of glycogen usage is 1 and the RQ of palmitate usage is 0.7. The actual RQ of muscle lies between these two values.

It is important to note that the oxidation of glycogen or glucose proceeds through the deformation of the substrate into pyruvate producing ATP. This deformation takes place outside the mitochondria. Pyruvate is then oxidized into CO_2 using oxygen. In cases where the mitochondria do not have sufficient oxygen, no pyruvate oxidation may take place. In this situation, pyruvate converts into lactate. This conversion requires a hydrogen ion which is provided by the conversion of a molecule called NADH^+ into NAD^+ . The latter molecule takes part in the breakdown of glycogen into pyruvate. Hence without oxygen, ATP is still produced, but at the expense of producing lactate:



This is called anaerobic metabolism.

Two types of muscle fibres have been identified: the slow twitch fibres (Type I) and the fast twitch fibres (Type II). The latter group has been further divided into Type IIa and Type IIx. These different types of muscle fibres differ in structure and biochemical properties (see Table 2.1). Type I fibres take a relatively long time (about 80ms) to develop peak tension following their activation, compared to Type II fibres which take only 30 ms to achieve the peak tension after activation (Wasserman et al., 2005). Slow twitch fibres and Type IIa fast twitch fibres are rich in myoglobin and this gives them a red colour whereas Type IIx fibres are white. Slow twitch fibres also tend to have a higher level of oxidative enzymes so that oxidative reactions can take place more easily. Oxidative

reaction is a complete cycle of fuel oxidation (equations 2.12 and 2.13) which produces more ATP from the same amount of substrate and glycolytic reaction is the partial cycle which produces pyruvate (Equation (2.14)).

Table 2.1. Characteristics of muscle fibre types (Wasserman et al., 2005)

	Type I	Type IIa	Type IIx
Contraction	Slow twitch	Fast twitch	Fast twitch
Fibre size	Small	Intermediate	Large
Colour	Red	Red	White
Myoglobin concentration	High	High	Low
Mitochondrial content	High	High	Low
Fuel utilization	Oxidative	Oxidative	Glycolytic

One important fact is that slow twitch fibres are more efficient than fast twitch fibres, which means that they can perform more work or develop more tension from the same amount of substrate. In other words, fast twitch fibres need more oxygen and substrate than slow twitch fibres to perform the same work. Slow twitch fibres are also more resistant to fatigue and therefore slow twitch fibres are more involved in sustained movement, such as endurance exercise.

2.3. Transport of Oxygen in Blood

The metabolic processes of our body, even at rest, require oxygen and substrate and produce carbon dioxide (CO_2). Anaerobic exercise also produces lactate. These species need to be moved from muscle to other parts of body. Oxygen is transported from the lung where it is taken from the air during each breath cycle. Carbon dioxide is transported to the lung and released to the air. Lactate is slowly recycled in the liver.

The partial pressure of oxygen (PO_2) in the lung alveoli is typically about 104 mmHg, whereas the PO_2 of the (mixed) venous blood entering the pulmonary capillaries is only 40 mmHg. This pressure difference causes oxygen to diffuse from the alveoli into the pulmonary capillaries. The diffusion is sufficiently fast to ensure that by the time the blood has moved one third of the distance through the capillaries of the lung, the blood PO_2 has risen to approximately 104 mmHg. Even during high intensity exercise, where the demand of the body for oxygen increases enormously and the blood flows more rapidly through the capillaries, the blood is still almost completely saturated with oxygen when it leaves the pulmonary capillaries.

A small percentage of oxygenated blood passes through the bronchial circulation to supply the lung tissues. It mixes in the pulmonary veins with the oxygenated blood (venous admixture) and causes the PO_2 of the blood pumped into the aorta to fall to approximately 96 mmHg.

When the arterial blood reaches the main tissues, its oxygen partial pressure is still 96 mmHg. The tissue PO_2 is normally about 40 mmHg so that when blood passes through the tissues, oxygen diffuses quickly from the arterial blood into the tissues. The PO_2 of the blood entering the veins from the tissue capillaries become almost equal to 40mmHg. During exercise, muscle PO_2 can drop to a level as low as 5 mmHg which makes oxygen diffuse even more quickly.

The content of oxygen in blood depends on the capability of oxygen to bind to and release from blood proteins (its affinity) and how much it can dissolve into blood plasma (its solubility). The dissolved amount of oxygen depends on its partial pressure which, according to Henry's law, involves a linear relationship. The dissolved amount of oxygen contributes only about 3% of the oxygen content in the blood. The other 97% is bound to blood proteins, especially the haemoglobin. Oxygen affinity in blood depends very much on its partial pressure but also to other factors such as temperature, acidity and the partial pressure of carbon dioxide. A high oxygen partial pressure ensures a high affinity of oxygen to haemoglobin; for example at normal arterial PO_2 of 100 mmHg, haemoglobin is almost fully saturated with oxygen.

The relationship between oxygen content and its partial pressure is described by the oxygen dissociation curve in blood. When plotted graphically, the dissociation curve has an S shape where the slope is small for higher PO_2 levels and steep for lower PO_2 levels (Figure 2.2). Therefore, a large variation of PO_2 in the higher range (such as occurs in the lung) only produces a slight change in oxygen content and the blood is still almost saturated, whereas a small decrease of PO_2 in the lower range (such as in muscles) stimulates large amounts of oxygen to be released. An empirical expression for the oxygen dissociation curve was proposed by Kelman as follows (Kelman, 1966):

$$x = 0.024(37 - T) + 0.4(\text{pH} - 7.4) + 0.06(\log(40) - \log PCO_2)$$

$$z = PO_2 \cdot 10^x$$

$$SO_2 = \frac{0.204 \cdot (-8.5322289 \cdot 10^3 z + 2.1214010 \times 10^3 z^2 + -6.7073989z^3 + z^4)}{9.3596087 \times 10^5 + -3.1346258 \times 10^4 z + 2.3961674 \times 10^3 z^2 + -6.7104406z^3 + z^4} \quad (2.15)$$

where SO_2 , T, pH and PCO_2 are the blood oxygen saturation (%), temperature ($^{\circ}C$), pH and partial pressure of carbon dioxide in mmHg respectively.

Another important factor that affects blood oxygen content is the concentration of haemoglobin [Hb]. Subjects with low [Hb] have low blood content (anaemia) although their blood volume and arterial PO_2 are normal. Blood content in the artery is calculated as follows:

$$CaO_2 = 1.34 \cdot [Hb] \cdot SaO_2 + 0.003 \cdot PaO_2$$

where CaO_2 , SaO_2 , PaO_2 are arterial oxygen content (in ml/dl), blood oxygen saturation (%) and arterial partial pressure (mmHg) respectively, $[Hb]$ is in gm/dl and 1.34 is the binding capacity of haemoglobin (in ml O_2 /g Hb),

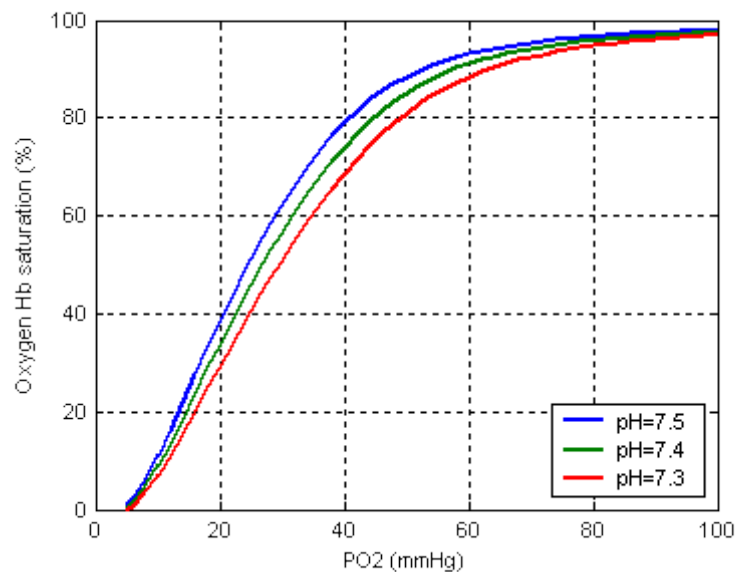


Figure 2.2 Oxygen dissociation curve (Levitzky, 2003); Effect of acidity on oxygen affinity is shown as a shift of the dissociation curve.

Other factors that influence the oxygen affinity support the release of oxygen in tissues for conditions in which the tissues require more oxygen. During exercise, for instance, muscle has a high concentration of CO_2 so that the CO_2 partial pressure (PCO_2) is higher, as is its acidity. Higher PCO_2 values and stronger acidity reduces the oxygen affinity to blood so enhances its release to muscle. The influence of PCO_2 on the oxygen dissociation curve is called Bohr Effect.

2.4. Transport of Carbon Dioxide

Carbon dioxide diffuses in the same way as oxygen, flowing from regions with higher partial pressure to regions with lower partial pressure. However, CO_2 has a value of diffusibility 20 times higher than O_2 which means that CO_2 diffuses more rapidly for the same pressure difference. Thus CO_2 needs a smaller pressure difference than O_2 to produce the same gas flow rate.

The PCO_2 level in the alveoli is about 40 mmHg while the PCO_2 of mixed venous blood entering the pulmonary capillaries is about 45 mmHg. This pressure difference of 5 mmHg is large enough to ensure that, by the time blood passes one third of the distance through the lung capillaries, the blood PCO_2 level has dropped to about 40 mmHg.

Carbon dioxide is present in the blood in several different forms:

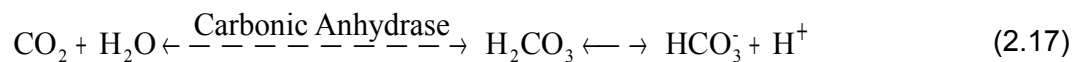
1. As carbon dioxide dissolved in plasma. The solubility of carbon dioxide is 0.075 ml CO_2 /dl/mmHg. At a PCO_2 level of 45 mmHg, the dissolved CO_2 concentration is 3.4 ml/dl.

2. As carbon dioxide bound with plasma protein. The plasma protein concentration is about 7% of blood. CO₂ binds the amine groups to form carbamino compounds:



In equation (2.16), R-NH₂ and R-NH-COO represent the molecule formula of the amine and carbamino compound, respectively.

3. As carbon dioxide dissolved in the blood cells. CO₂ can cross the red cell membrane and dissolve in red blood cell water.
4. As carbon dioxide bound to haemoglobin (Hb). Approximately 30% of the red blood cell content is haemoglobin. CO₂ can form carbamino haemoglobin on amine groups. CO₂ affinity to Hb is less than that of O₂ so that less CO₂ is bound to Hb. However, the oxygen partial pressure influences CO₂ affinity, through what is termed the Haldane effect, where lower PO₂ promotes higher CO₂ affinity and higher PO₂ downgrades the CO₂ affinity.
5. As bicarbonate. Carbon dioxide reacts with water to form carbonic acid. The reaction is slow unless it is catalyzed by a certain enzyme called carbonic anhydrase. Red blood cells contain carbonic anhydrase so CO₂ forms much carbonic acid in the cells. Carbonic acid then dissociates into bicarbonate and hydrogen ions as shown in the relationship (14) below. A large portion of CO₂ is stored in the form of bicarbonate. In the artery, for example, bicarbonate amounts to approximately 90% of CO₂.



The amount of CO₂ stored in the blood is dependent on several factors, primarily the gas partial pressure. Figure 2.3 depicts the blood CO₂ pressure – content relationship. As seen in the figure, the dissociation curve is affected by blood haemoglobin oxygen saturation (and consequently O₂ partial pressure). Higher SO₂ levels shift the curve to the right, which means the same content of CO₂ will have higher CO₂ partial pressure. This is called the Haldane effect.

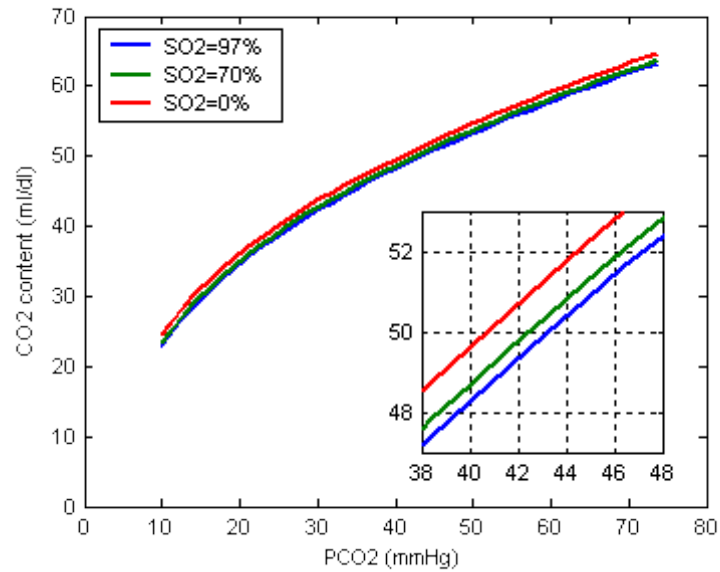


Figure 2.3 Carbon dioxide dissociation curves (at 37°C) for different O₂ saturation showing Haldane effect (Levitzky, 2003); Inset shows the curves for PCO₂ values within the range of rest condition.

The best known algorithm to describe the CO₂ dissociation curve is one first selected by Douglas et al (1988), where it has been stated that the algorithm is applicable to exercise conditions. The calculation of blood CO₂ content involves two steps. Firstly, plasma CO₂ content (CCO_{2,p}) and plasma bicarbonate concentration [HCO₃⁻]_p are calculated from the Henderson-Hasselbach equation:

$$\begin{aligned} \text{CCO}_{2,p} &= \text{PCO}_2 \cdot s \cdot [1 + 10^{(\text{pH} - \text{pK}')}] \\ [\text{HCO}_3^-] &= \text{CCO}_{2,p} - \text{PCO}_2 \cdot s \end{aligned} \quad (2.18)$$

where s is the plasma solubility coefficient (in mM/mmHg) of CO₂ and pK' is the apparent dissociation constant of the CO₂-HCO₃⁻ system. The variable s is 0.0307 in plasma at 37°C and pH 7.4 in normal human subjects. The variable pK' is calculated using Kelman's equation (Kelman, 1967).

$$\text{pK}' = 6.086 + 0.042 (7.4 - \text{pH}) + (38 - \text{TEMP}) (0.00472 + 0.00139 (7.4 - \text{pH}))$$

Secondly, the total blood content of CO₂ is calculated from the modified Visser's equation:

$$\text{CCO}_2 = \text{CCO}_{2,p} \cdot \left(\frac{1 - 0.0289[\text{Hb}]}{(3.352 - 0.456\text{SO}_2)(8.142 - \text{pH})} \right) \quad (2.19)$$

where [Hb] is the haemoglobin concentration and SO₂ is the oxygen saturation value.

2.5. Control of ventilation

Two sensors are involved in controlling the ventilation: central chemoreceptors and peripheral chemoreceptors. Central chemoreceptors on the surface of the medulla are sensitive to the partial pressure of carbon dioxide (PCO₂) and acidity (pH level). This type

of sensor is responsible for driving 70-80% of the resting ventilation. In hyperoxic conditions, i.e. when the subject inhales 100% oxygen, the respiratory controller produces a level of ventilation ($\dot{V}E$) that exhibits linearity to arterial carbon dioxide partial pressure ($PaCO_2$), with a slope of approximately 0.1-0.2 l/min/kPa (Ward, 2004a):

$$\dot{V}E = S \cdot (PaCO_2 - PaCO_2(0)) \quad (2.20)$$

where S is the slope.

Peripheral chemoreceptors lie in the carotid bodies and are sensitive primarily to an increase in $PaCO_2$, a decrease in arterial pH or a decrease in arterial oxygen partial pressure (PaO_2). This type of sensor is responsible for driving 20-30% of the steady state ventilation at rest. Carotid body chemoreceptors are responsible for a hyperbolic $\dot{V}E$ - PaO_2 relationship:

$$\dot{V}E = \dot{V}E(0) + \frac{A}{(PaO_2 - C)} \quad (2.21)$$

where $\dot{V}E(0)$ is the response during hyperoxia, A is a constant known as the hypoxic sensitivity with an average value of about 17.5 l/min/kPa at normal $PaCO_2$, and C is a constant parameter having a value of 4.3 kPa. If the $PaCO_2$ level is increased, the hypoxic sensitivity is increased (the hyperbolic area is increased, see Figure 2.4), which results in a proportional increase of ventilation. It is important to note that when ventilation is expressed in terms of oxygen saturation level (SaO_2) rather than PaO_2 , the relationship is linear:

$$\dot{V}E = G \cdot SaO_2 - \dot{V}E(0) \quad (2.22)$$

Figure has been removed due to Copyright restrictions.

As inferred from equations (2.8) and (2.11), changes in $V'E$ have an effect on the values of $PaCO_2$ and PaO_2 , thus those variables are involved in a closed loop system. The activity of the respiratory controller, as described previously in this section, is extracted when the ventilation is prevented from feeding back the $PaCO_2$ and PaO_2 , i.e. the system senses one stimulus by keeping the other stimulus constant. When both stimuli are allowed to change simultaneously, the outcomes in terms of the arterial blood gas composition are not always ideal. When someone accustomed to living at sea-level is brought to high altitude, ventilation increases to restore PaO_2 , which in the short term "ignores" the changes of $PaCO_2$ and pH until acid-base adaptation occurs to overcome the "error".

The exact activity of the controller is not well understood during exercise (Ward, 2004b). Here, the respiratory control system not only functions to maintain normal arterial blood gas partial pressures at, or close to, resting condition, but also changes the alveolar ventilation rate to adapt to the increasing metabolic needs. It is now agreed that the general features of ventilation response during exercise involves $V'E$ increasing sufficiently to maintain arterial PCO_2 and pH (Whipp, 1990) within normal levels.

2.6. Exercise domains

Exercise work rate can be grouped into several domains according to how the human body responds to exercise. The domains are moderate, heavy, very heavy or severe exercise. In several situations, however, scientists simply distinguish two domains, i.e. the moderate (below the lactate threshold) and heavy exercise domains (above the lactate threshold).

In moderate exercise, the steady state increase of O_2 uptake ($V'O_2$) is proportional to the increase of work rate, with a proportionality gain of approximately 10 ml/min/watt (Whipp, 1994a). For example, an increase in work from "zero" watt (unloaded exercise) to 100 watt leads to an increase of O_2 uptake by 1000 ml/min. The O_2 uptake can be well characterized by a single exponential after a short tissue - lung transport delay (Note that in this thesis, an exponential characteristic refers to a first-order linear system response). In the blood, lactate concentration ($[La]$) may increase at the onset of exercise but after a while $[La]$ decreases back to the base line level or to a level slightly higher.

Heavy exercise is characterized by the accumulation of $[La]$ in blood. After a large increase at the onset of exercise, blood $[La]$ may decrease to a value well above the base line or it may be sustained at the high level. Oxygen uptake increases with kinetics similar to (or slightly slower than) the increase during moderate exercise. This increase projects to the level of O_2 uptake as estimated by the proportionality gain in the moderate domain. Several minutes (some 2 -3 minutes typically) after exercise onset, a slow phase of O_2 uptake occurs which results in a much later attainment of the steady state and a higher

proportionality gain (Whipp, 1994b) (see Figure 2.5). There is no exact border between moderate and heavy exercise but because lactate accumulation becomes the discriminator of the two domains, the border is called the lactate threshold (LT). The lactate threshold is also called the anaerobic threshold because lactate is produced in an anaerobic metabolism (a metabolism that does not use oxygen).

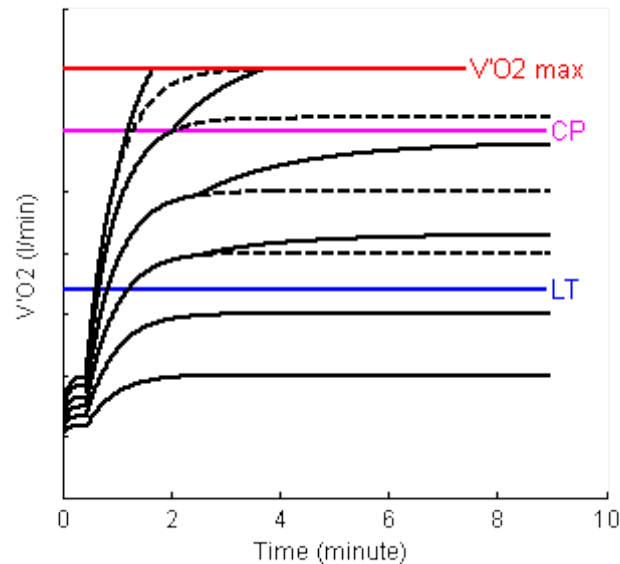


Figure 2.5. Hypothetical response of O₂ uptake for several constant work rates; LT = lactate threshold, CP = critical power. For work rates below LT, V'O₂ increases exponentially after a short delay. For work rate between LT and CP, V'O₂ stabilizes at a value higher than that predicted by the underlying exponential (dashed line). For work rate higher than CP, V'O₂ does not stabilize and attains V'O₂ max. Figure is redrawn from Whipp (1994a).

An exercise work rate is in the very heavy or severe exercise domain when the body cannot attain a steady state condition. Lactate keeps accumulating and oxygen uptake keeps increasing until a point where the body reaches a state of fatigue and exercise is halted. At this point, the level of O₂ uptake attained is called maximum O₂ uptake (V'O_{2,max}). The work rate that discriminates heavy and very heavy exercise is called the critical power (CP).

2.7. Summary

The lung is the organ that draws O₂ into the blood stream and expels CO₂ out. Muscle is the main body tissue that increases the utilization of O₂ and the production of CO₂ during exercise. Transport of O₂ and CO₂ between lung and body tissues is maximized by the way blood binds O₂ and CO₂ molecules. The partial pressures of O₂ and CO₂ in blood are involved in the control of lung ventilation.

Chapter 3

Implementation of a Model for the Respiratory Control System under Exercise Conditions

This chapter discusses the structure of a model developed by Saunders, Bali and Carson (Saunders et al., 1980) in the late 1970s. Reimplementation of the model using modern Simulink software is described and an assessment is conducted. The purpose of the implementation and subsequent investigation of the model was to evaluate whether or not it could be modified to make it applicable for exercise conditions.

3.1. Structure of the Saunders, Bali and Carson model

Saunders and his colleagues developed a model consisting of four compartments: a lung compartment, a brain compartment, a muscle compartment, and an additional compartment representing other tissues. This model was based on an earlier well established model of Grodins et al. (1967) but with the lung compartment modified to include cyclical respiration, respiratory dead volume, variable lung volume, blood shunt, a separate muscle compartment and a different controller equation. Simplification of the brain compartment was also introduced by omitting the effects of the cerebrospinal fluid reservoir and ignoring the effect of nitrogen gas concentration.

The inclusion of a muscle compartment is essential for investigation of a respiratory control system model under exercise conditions because muscle O₂ consumption and CO₂ production change greatly during exercise. The muscle compartment in the model features a myoglobin dissociation curve to express the muscle oxygen storage capability. It is mathematically in the form of three-piece linear model which implies a maximum oxygen carrying capacity for myoglobin of about 0.5 litre (STPD). These three linear descriptions have the form:

$$\begin{aligned} \text{MyoO}_2 &= 0.045 \cdot \text{PMO}_2 && \text{for } 0 < \text{PMO}_2 \leq 6.93 \\ &= 0.004167 \cdot \text{PMO}_2 && \text{for } 6.93 < \text{PMO}_2 \leq 33.96 \\ &= 0.0005555 \cdot \text{PMO}_2 && \text{for } 33.96 < \text{PMO}_2 \end{aligned} \quad (3.1)$$

where

$$\text{CMO}_2 = (\text{PMO}_2 \cdot \alpha \text{MO}_2) / \text{PB} + \text{MyoO}_2 / \text{VM}$$

In the above equation, MyoO₂, CMO₂, PMO₂ represent muscle myoglobin concentration, O₂ content and O₂ partial pressure, respectively, αMO_2 is the solubility of O₂ in muscle compartment, PB is the barometric pressure, and VM is the muscle volume. The muscle and all other compartments also have the capacity to store carbon dioxide. Saunders et al. (1980) used a similar dissociation curve for those compartments as for blood but reducing the Haldane effect and eliminating the role of haemoglobin.

The storage capacity of oxygen in the brain and other tissues compartment was described in terms of the partial pressure and a solubility coefficient (using Henry's law):

$$\text{C}_{\text{O}_2} = (\text{P}_{\text{O}_2} \cdot \alpha) / \text{PB} \quad (3.2)$$

where P_B is the barometric pressure, which is normally 760 mmHg, and C_{O_2} and P_{O_2} are the concentration and partial pressure of oxygen in the corresponding compartment, respectively. The constant α is the solubility coefficient.

A special feature of the Saunders, Bali and Carson (SBC) model is the representation of the lung compartment. In this model the lung has a variable volume to allow it to represent the cycle of inspiration and expiration. A sinusoidal wave is used to represent the respiratory cycle with the same period for inspiration and expiration. Such a cyclic representation allows investigation of the system characteristics based on breath by breath events.

The lung alveolar compartment represents the part of the lung where gas exchange with the blood takes place. The lung dead space volume is represented as a variable in recognition of the fact that the volume of the upper portions of the lung, where gas exchange does not take place, changes with the changing volume of the lung (see Figure 3.1). The fixed part of the dead space volume is the anatomical dead space and the variable part is the alveolar dead space which expands towards the alveolar compartment. The cyclic nature of the processes within the lung makes the mathematical representation fairly complicated. The model of the lung involves 14 equations, some of which are first order differential equations.

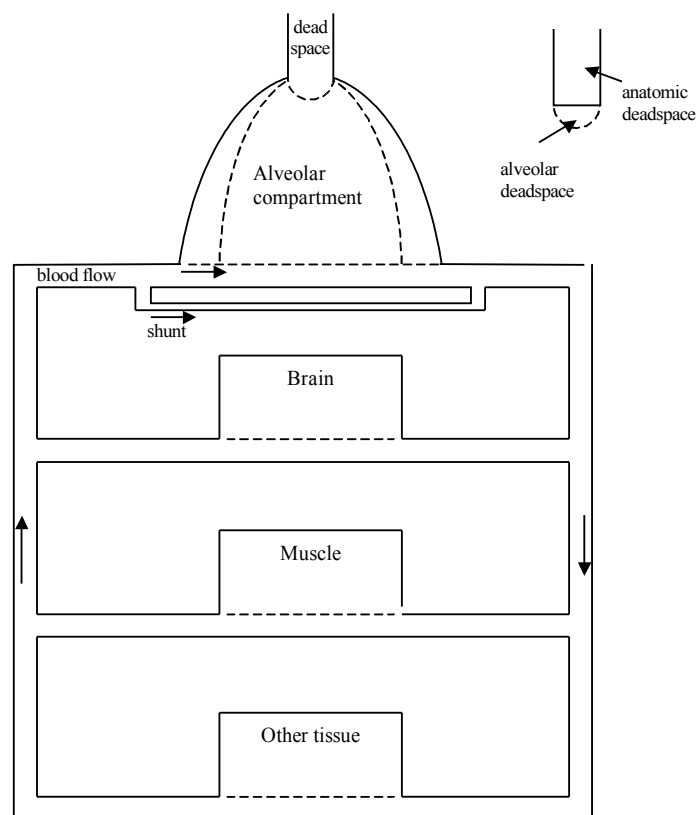


Figure 3.1. Controlled system of the Saunders, Bali and Carson model

The model includes a blood shunt across the lung to represent the part of the blood capillary that fails to participate in gas exchange process. The equations that are used to calculate the blood dissociation curve are the same as those used by Grodins et al. (1967). Saunders et al. (1980) use a controller block similar to that of Lloyd et al. (1958) (see Figure 3.2). The output of the controller depends on filtered values of arterial carbon dioxide and oxygen partial pressure.

Figure has been removed due to Copyright restrictions.

Figure 3.2. Controller used in the Saunders, Bali and Carson model. Diagram from Saunders et al. (1980)

The controller is assumed to be sensitive to both oxygen and carbon dioxide arterial partial pressures and there is a delay before the actual arterial value arrives at the controller sensory site.

Because the arterial partial pressure is oscillatory due to the cycle of respiration, the actual value of arterial partial pressure (i.e. PaO_2 and PaCO_2) contains an oscillatory element and it becomes difficult to use this variable directly as the controller input because the oscillation may cause instability. Therefore, Saunders et al. (1980) used the mean values of arterial partial pressure ($\overline{\text{PaO}_2}$ and $\overline{\text{PaCO}_2}$) which are obtained by filtering the relevant signals using a second-order filter.

The breathing frequency is generally low, in the range of 12 – 20 breaths per minute in healthy adults at rest. During peak exercise, the breathing frequency of an athlete can increase up to 60 – 70 breaths per minute. To damp the oscillation in arterial partial pressure, a low-pass filter is used which has a cut off frequency of at most 6 cycles per minute (or 0.1 Hz).

A Simulink diagram developed from the model of Saunders, Bali and Carson is depicted in Appendix A. In this figure, each interconnected subsystem involves basic blocks which have functionality similar to an identifiable element of the real system, such as the dead space, alveolar compartment, capillary, venous, tissues and the controller.

3.2. Simulation of the Saunders, Bali and Carson model under rest conditions

At rest, several disturbances were tested to evaluate the behaviour of the Simulink model (for ease, it will be referred to as “the model” later in this chapter) in comparison with results of physiological experiments of Reynolds et al. (1972) and the simulation result of the SBC model. Assessment of the model was also performed by comparing the steady state values of variables of interest with those presented in the paper of Saunders, Bali and Carson (SBC) (Table 3.2).

Table 3.2. Comparison of Simulink model parameters with those of Saunders, Bali and Carson (SBC)

	Steady state value	
	SBC value	Our model
Minute ventilation	6.85	6.66
Alveolar PO ₂	97.2	95.6
Alveolar PCO ₂	40.4	40.56

The steady state here is defined as the condition of the system three minutes after the application of a stimulus. The table shows that a slight difference exists between the SBC steady state values and the corresponding values from our model. The difference is not more than 3% for all variables shown.

All the simulation experiments presented by Saunders et al. (1980) in their paper have been repeated for the reconstructed model. They comprise CO₂ loading by increasing the inspired fraction, a step increase in CO₂ inflow in the inspired gas, a step increase in CO₂ inflow in mixed venous blood, hypoxic gas mixtures, and exercise. Among the experiments, exercise will get the most attention as it represents the most important topic for the research reported in this thesis.

3.2.1. CO₂ loading by increasing the inspired fraction

The first observation involved increasing the inspired fraction of CO₂ in a stepwise fashion from zero to 3, 5 and 7%. For each fraction of CO₂, the ventilation and the partial pressure of oxygen and carbon dioxide in the alveolar compartment were examined in terms of the steady state value, the times to reach the level of half the final value for both the on and off transients and the overshoot and undershoot percentages for the transients. The results are presented in Table 3.3. The steady state values of minute ventilation of the model were found to be very close to those published in experiments by Reynolds et al. (1972) and to those of the SBC model. The steady values of alveolar PO₂ differs slightly from Reynolds' experimental result and approach those of Saunders very closely, while the steady values of alveolar PCO₂ differ slightly from those of both the SBC model and Reynolds' experimental values.

While the steady state values of the variables of the Simulink model are quite close to those of SBC or Reynolds et al. (1972), the transient half times show varied results, some variables being close while some others differ significantly. Generally, the model shows similar trends when compared to the SBC model. In cases when the SBC model gave a higher value for a higher concentration of the CO₂ inspired fraction, the model would also give a higher value for the same variable, and vice versa.

Table 3.3. Result of examination of CO₂ loading by increasing the inspired fraction; the range shown in each entry in the upper half of the table is for different inspired fractions of CO₂, the left one being for 3% and the right for 7%

	Steady state (at the end of 25 min)			Half time on transient (s)			Half time off transient (s)		
	SBC	Reynolds	Model	SBC	Reynolds	Model	SBC	Reynolds	Model
Minute ventilation	12-44	11.25-41.4	11.35 – 41.6	42-106	64-135	56 – 172	33-42	43-12	41 – 52.4
Alveolar PO ₂	122-142	126-144	121 - 141	62-51	72-45	74 - 73	74-120	49-84	78 - 122
Alveolar PCO ₂	42-55	44.3-56.2	42.6 – 54.8	4-10	6.6-13	4 - 84	4-1	6-6	2 – 2
				Overshoot (3% stimulus)			Undershoot		
				SBC	Reynolds	Model	SBC	Reynolds	Model
Minute ventilation									
Alveolar PO ₂									
Alveolar PCO ₂				47	24	25	140 - 50	27 - 72	102 - 54

Like the SBC model, the model demonstrates that most variables agree with experimental results of Reynolds et al. (1972), except for the value of the half time for the off-transient for minute ventilation and alveolar PO₂. The half time for the off-transient of the alveolar PCO₂ was difficult to estimate because it was a very short event within the large oscillatory signal. Also, the estimate of the PCO₂ undershoot does not agree with that of Reynolds, with the model showing a decrease for higher inspired CO₂ concentration while the results of Reynolds' experiment gave an increase.

Figure 3.3 shows how the respiratory system model responds to an abrupt increase in the inspired CO₂ concentration to 7%. In general, we can see that the alveolar CO₂ partial pressure increased more rapidly than the ventilation and tidal volume, a fact that Saunders et al. (1980) stated was in agreement with results from a previous laboratory experiment by Fenn and Craig (Fenn and Craig, Jr., 1963).

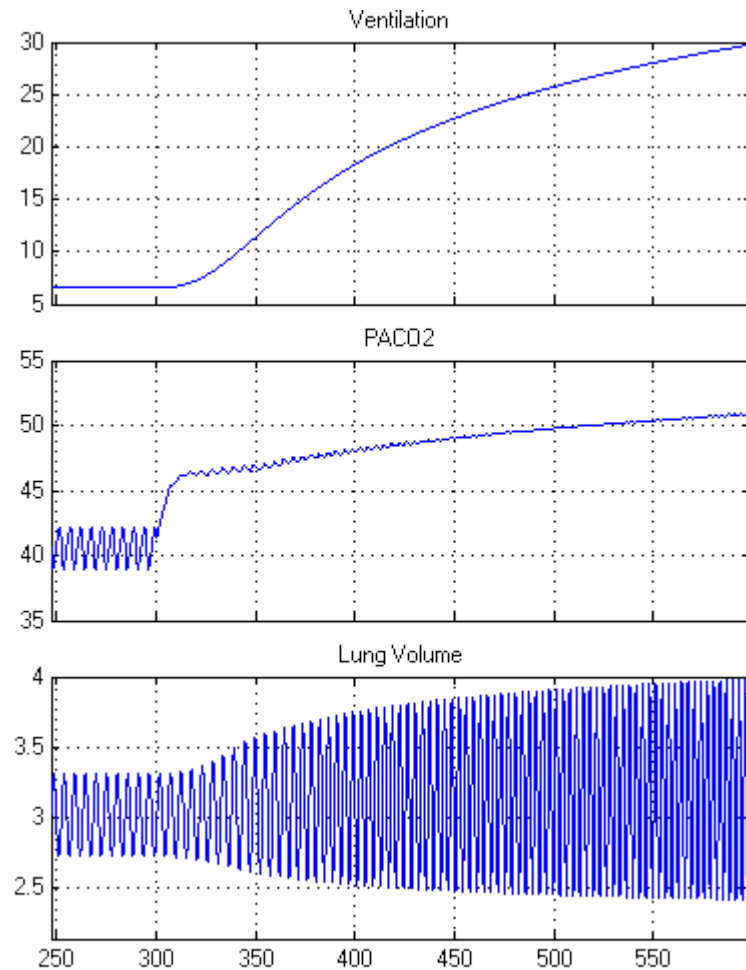


Figure 3.3. Simulation result from the Simulink model for an abrupt increase in the fraction of inspired CO_2 ($F_{\text{I}\text{CO}_2}$) at time 300 sec. from 0-7%

3.2.2. Step increase in CO_2 inflow in inspired gas

By increasing the inspired fraction of CO_2 in the previous observation, the CO_2 inflow in terms of liter/minute increases when ventilation rises. In this observation the CO_2 inflow is kept constant after the initial step. An input with a step of $F_{\text{I}\text{CO}_2}$ to 3% gives a sharp increase in PACO_2 with an associated overshoot but has a slower rise in ventilation with only a small overshoot. This is similar the result obtained from SBC model where ventilation reaches a steady state level in 3-4 minutes (Figure 3.4)

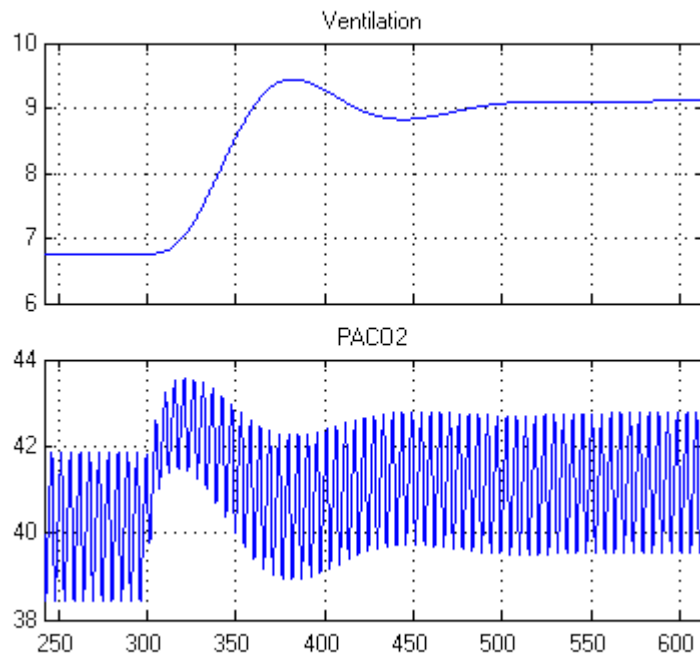


Figure 3.4. Response to step increase in CO₂ inflow in inspired gas

3.2.3. Step increase in CO₂ inflow in mixed venous blood

This observation, involving a step increase in CO₂ inflow in mixed venous blood, is similar to the previous observation and gives a similar shape of on-transient response but this has a larger magnitude. While in the previous observation the ventilation remains steady at a value of 9 l/min, this observation results in a steady value of ventilation at 10 l/min (see Figure 3.5) similar to the result obtained by Saunders et al. (1980).

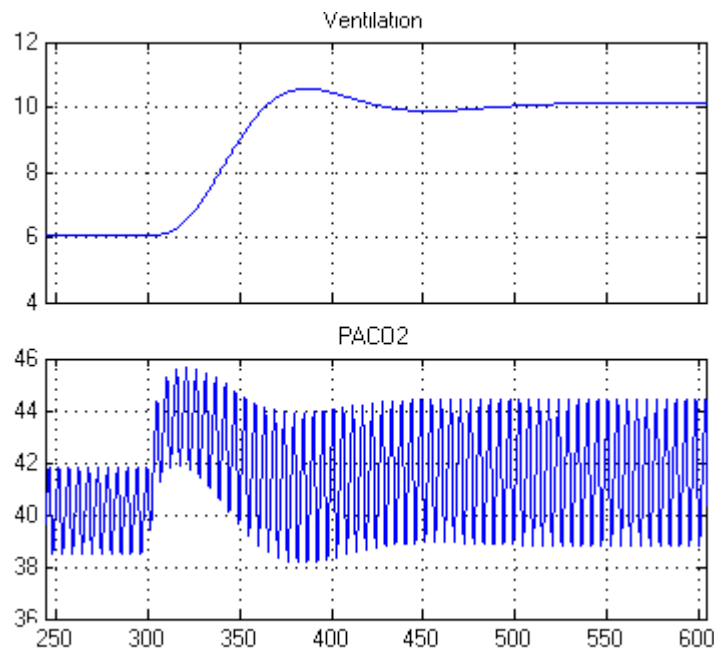


Figure 3.5. Response to step increase in CO₂ inflow in mixed venous blood

3.2.4. Hypoxic gas mixtures

In this observation, a step decrease is applied to the inspired oxygen concentration. The SBC model result for this experiment showed adverse behaviour compared to the corresponding experimental result obtained by Reynolds et al. (1972). On-transient half times for ventilation were more than 3 times too slow and there were large overshoots not seen in man. The reconstructed model performs similarly and it shows worse performance for PACO_2 . Though steady state values of PAO_2 appear close to the corresponding results from SBC model, the transient values show significant discrepancies.

Table 3.4. Result of experiment using hypoxic gas mixtures. Entries where two values are shown are for 7% and 9% of F_1O_2

	Steady state			Half time on transient			Overshoot (%)		
	SBC	Reynolds	Model	SBC	Reynolds	Model	SBC	Reynolds	Model
Ventilation	18-12	15-10	17.7 – 11.5	174-167	54-33	170 - 136	97-36	0	130 - 48
PACO_2	32-36	39-45	24 – 29	17-18	15-29	220 - 50	0	0	0
PAO_2	24-31	31-35	31 – 38	195-200	105-69	16 - 16	0	0	0
	Half time off transient			Undershoot (%)					
	SBC	Reynolds	Model	SBC	Reynolds	Model			
Ventilation	13-24	21-27	17 - 32	0	0	0			
PACO_2	-----	168-63	>600 - 130	0	0	0			
PAO_2	120-70	120-80	7 - 17	0	0	0			

3.3. Simulation of the model under exercise conditions

Saunders et al. (1980) simulated exercise conditions by increasing abruptly the O_2 consumption and CO_2 production of the muscle compartment together with an appropriate increase in cardiac output. Such increase results in the whole body O_2 uptake and CO_2 output as presented in Table 3.5.

Table 3.5. Values of cardiac output and metabolic rates for the simulation of exercise

Exercise load (W)	Cardiac output (l/min)	Whole body	
		O_2 uptake	CO_2 output
		(l BTPS/min)	
25	8.4	1.05	0.84
50	10.0	1.35	1.08
75	11.4	1.60	1.28
100	13.0	1.86	1.49

The SBC model performs better than Grodins' model in this case. The latter failed under exercise conditions. This is because the SBC model has a muscle compartment which is able to store oxygen by employing the myoglobin dissociation equation. However, at the exercise load of 100 W, the SBC model also failed and showed negative values of muscle PO_2 unless some reasonable adaptations were made. Saunders et al. (1980) introduced the following modifications during exercise at 100 W:

- (i) The CO_2 gain within the controller equation was increased rapidly at the onset of exercise to levels that would achieve isocapnia,
- (ii) Blood shunt is decreased so that QS/QT drops to 1% from the previous 5%,
- (iii) An algorithm was implemented to divert blood from other tissue to the muscle compartment if the muscle PO_2 fell to 5 mmHg.

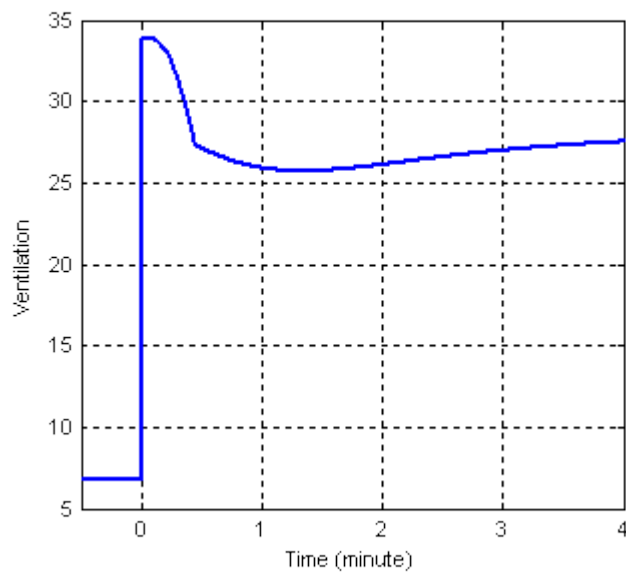


Figure 3.6. Profile of ventilation for 100 W exercise

The reconstructed model behaves similarly and needs those adaptations to make it stable for conditions involving the 100W exercise load. As Saunders et al. (1980) admitted, however, the resulting on-transients for $PaCO_2$ and ventilation are far from realistic with a high overshoot existing in the ventilation record (Figure 3.6) and there is an undershoot in $PaCO_2$. Unlike the SBC model, the Simulink model does not show a lag in $PaCO_2$ (Figure 3.7).

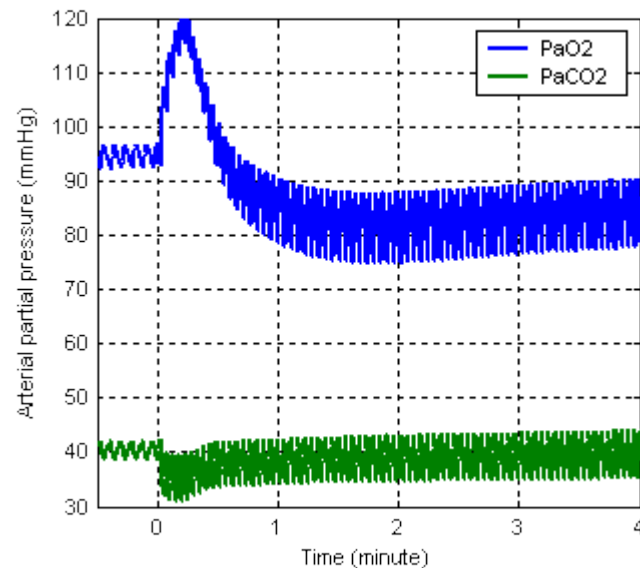


Figure 3.7. Changes in arterial gas partial pressures during 100 W exercise

Modifications have been made so that muscle CO₂ production, ventilation and cardiac output do not increase abruptly but exponentially with time constants 45, 75 and 25 seconds respectively. The muscle O₂ consumption increases exponentially with time constant 30 seconds so that the muscle venous O₂ content does not drop too rapidly. These values are within the range observed in various experiments (Grassi et al., 1996; Yoshida and Whipp, 1994; Casaburi et al., 1989a). The ventilatory controller gain is not increased as was done previously in the SBC model. Instead, a controller component is added so that during the steady-state, the value of ventilation would result in isocapnia. The simulation result is shown in Figure 3.8 and Figure 3.9.

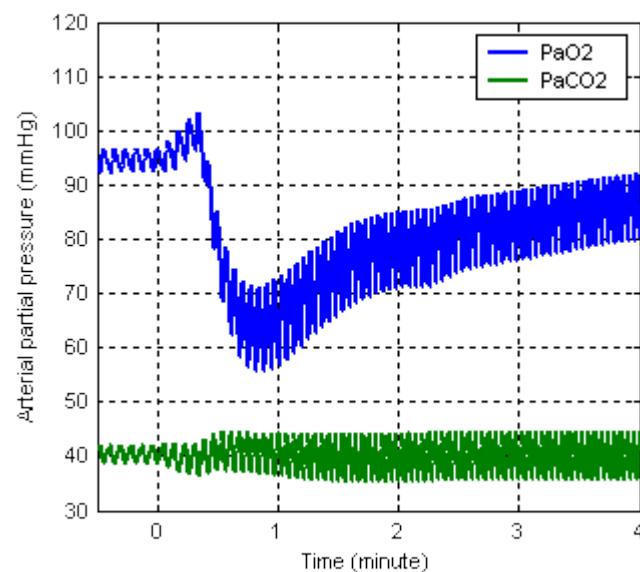


Figure 3.8. Response of the modified model for PaCO₂ and PvCO₂ during transition from rest to 100 W exercise.

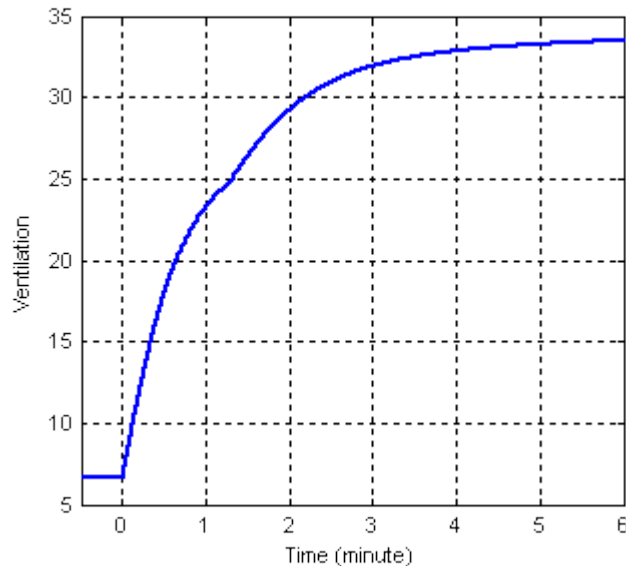


Figure 3.9. Response of the modified model for ventilation during transition from rest to 100 W exercise.

3.4. Discussion

The SBC model appears to perform well for rest conditions and has behaviour that is sufficiently close to the real system in that condition. Some disturbances have been tested with the SBC model and it is able to reproduce characteristics similar to those observed in several experiments. The Simulink model shows characteristics that are close to the SBC model and to the experimental result in most cases, although the transient value obtained in the hypoxic gas mixture test is significantly different.

The cyclical ventilation that is an essential feature of the SBC model is particularly useful in allowing observation of the system behaviour on a breath by breath basis. Data from measurements of pulmonary gas exchange is best obtained on a breath by breath basis. In this way, it becomes possible to conduct a direct comparison and assessment between the experimental and simulation results.

Responses of the SBC model during exercise show discrepancies with experiments, or are unrealistic, as Saunders et al. (1980) remarked. This is understandable for several reasons. The SBC model uses a step function to simulate the increase of muscle O_2 consumption and CO_2 production, which is not natural since the time course of muscle oxygen consumption has been observed to be exponential (Grassi et al., 1996; Hill, 1940). The time course of muscle CO_2 production can be predicted to have an exponential form similar to muscle O_2 consumption but probably with a different time constant. The cardiac output and ventilation do not increase abruptly either and these quantities are best described as having an exponential form with a short period of initial fast increase (Hughson and Tschakovsky, 1999; Hughson and Morrissey, 1982).

Modification has been made so that the time course of cardiac output is exponential. The term “exponential” in this thesis refers to the response of a first-order system, also known as first-order lag, which in many cases is a good approximation for the response of physiological system against a step input. The gain of the ventilation controller is not increased five fold as was previously done in the SBC model but an additional component is introduced that would increase ventilation against exercise work rate to the level that would attain isocapnia. Better simulation results are obtained. Ventilation does not show an overshoot, just as expected. PaCO_2 does not show undershoot any more and PaO_2 shows a temporary decrease but after a slight overshoot. The temporal patterns of PaCO_2 and PaO_2 agree with results experimentally observed in humans, (see for example Forster et al., (1986)).

The modified version of the SBC model, although it gives improved results, is still inadequate to describe experiments for exercise conditions and further examination suggests that a new model needs to be established. The current model has several points of objection as described below.

During moderate exercise at the steady state condition, ventilation is much higher than it is at rest, yet PaCO_2 and PaO_2 are still at their resting value or change only slightly. Hence it is clear that the change of ventilation during exercise does not depend (only) on PaCO_2 and PaO_2 and, this leads to a conclusion that if the current model is to be used to observe exercise conditions, the controller equations have to be modified. Changing the controller gain is not sufficient either because it means that the ventilation is still supposed to depend fully on arterial gas partial pressure. A new additional controller component (besides the current one) has to be incorporated and the role of this new component needs to be established. It is necessary to keep in mind the fact that, with the existence of another controller component, the dependency on PaCO_2 and PaO_2 may increase or be reduced.

The current model calculates the tidal volume based on a relationship developed from an experimental result obtained by Reynolds et al. (1972), where the respiratory system is exposed to different levels of inspire at rest. They obtained the maximum value of ventilation as 40 l/min for the conditions of the experiment, suggesting that the relationship may be adequate for ventilation up to 40 l/min. However, for exercise conditions, ventilation can rise far beyond that level depending on the intensity and the fitness of the subject. Athletes, for instance, can ventilate to levels of more than 100 l/min during very heavy exercise (see e.g. Wassermann et al. (1967)). Therefore, a study needs to be conducted to establish a relationship between ventilation and tidal volume that is applicable to a wider range of ventilation.

The tissue compartments of the model calculate partial pressures of respiratory gases based on the assumption that the tissue volume is constant. This assumption is

sufficient for the brain and the other tissue compartment but it may not be adequate for the muscle compartment because oxidation of metabolic fuel produces CO_2 and water, which increases the muscle fluid volume. Furthermore, the calculation of gas partial pressure inside tissue is hard to verify.

3.5. Summary

The SBC model is a general model of respiratory control system. It features cyclic ventilation and has a separate muscle compartment. The SBC model performs well in rest condition, i.e. when it simulates several test situations. The SBC model performs poorly in exercise condition because it uses only O_2 and CO_2 partial pressures to calculate ventilation.

Chapter 4

A Model of the Respiratory System for Conditions of Moderate Exercise

This chapter describes the development of a model of the respiratory control system that is applicable for exercise in the moderate intensity domain. The structure of the model is provided, along with the major variables involved, i.e. cardiac output and muscle blood flow, ventilation, pulmonary oxygen uptake, muscle oxygen consumption, carbon dioxide production, and arterial partial pressure. Simulation results are also presented and analysed.

4.1. Model structure

The structure of the model is described in Figure 4.1 where blocks represent body compartments, thick lines represent blood flow, thin lines represent controller stimuli to the corresponding compartments, and dashed lines indicate which compartments are directly influenced by the changes in work rates. Gas flows between lung and the air are depicted using block arrows, where O_2 has a net flow into the lung and CO_2 has a net flow out of the lung. It may need to be noted that within this structure the representation for the blood flow between the lung and the heart has been simplified with blood being shown as flowing from the mixed venous compartment to the lung and the heart.

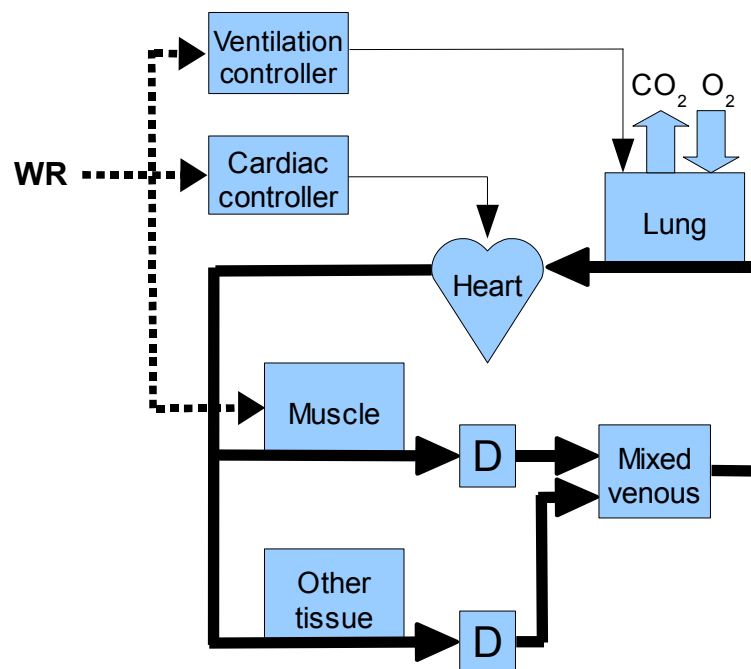


Figure 4.1 Structure of the Respiratory System Model; see text for description.

Blocks with the letter D represents time delay elements. Venous blood is assumed to have delay elements but arterial blood is not. The reason is that the volume of venous blood constitutes more than 60% of the total blood volume and venous blood flow is slower than arterial blood flow.

The muscle compartment represents the muscles that perform the exercise. Hence muscles that do not participate in the exercise, and all body tissues other than muscle, are lumped together in the compartment labelled other tissues.

A change in exercise work rate will directly affect the muscle, other tissues, cardiac controller and ventilation controller. An increase in work rate will increase the muscle O_2 extraction and its lactate production. At the onset of exercise by the time O_2 extraction reaches a steady state level, the energetic (or ATP) requirement is fulfilled anaerobically so lactate production at this period is high. The work rate increase, as well as the increase in blood lactate concentration, increases the lactate consumption of other tissues. The work rate also has a positive impact on ventilation and on the cardiac controller, whereby the lung will increase ventilation and the heart will increase cardiac output.

As illustrated in Figure 4.1, work rate is the only stimulus included within this representation of the human respiratory system during exercise. In order that the simulation may run, the behaviour of certain variables from compartments that are directly affected by work rate has to be pre-defined. Those variables include the cardiac output, ventilation and muscle oxygen consumption, each of which will be described in Sections 4.2, 4.3 and 4.5, respectively. The net flow of oxygen (pulmonary O_2 uptake) and carbon dioxide (pulmonary CO_2 production) increase with exercise and these variables will be described in Sections 4.4 and 4.6, respectively. Among the target of control of ventilation is to achieve homeostasis for oxygen and carbon dioxide partial pressure in artery, which will be described in Section 4.7. To widen the scope of the model so that it includes early acidosis, the behaviour of another variable needs to be defined, i.e. the ATP turn over rate, which is described in Section 6.

Our model of the respiratory system is for a situation where the subjects perform cycle ergometer exercise. This chapter discusses the model for experimental situations where the exercise load is limited to levels below the lactate threshold. The limit for aerobic cycle ergometer exercise for an average male person in good physical condition lies between 110 and 130 watt and we perform the simulation for conditions of exercise at the level of 100 watt. The Simulink diagram of the model is presented in appendix B.

4.2. Cardiac output and muscle blood flow

The cardiac output is the amount of blood flowing out of the heart per unit time. It is usually measured in litres per minute (l/min). The cardiac output is determined by the frequency of heart beat and the stroke volume, i.e. the volume of blood pumped by the heart for each beat. Thus

$$\dot{Q} = HR \cdot SV \quad (4.1)$$

where Q' is the cardiac output, HR is the heart rate (beats per minute) and SV is the stroke volume (litres per beat). While the heart rate can be measured easily and at times is used for the preliminary detection of cardiac output changes, stroke volume is hard to measure. In fact, methods have been developed to measure cardiac output including

invasive methods such as the dye dilution technique and the non-invasive Doppler ultrasound method (Radegran, 1997).

Because of exercise stress, the muscle needs to consume more oxygen and fuel and has to get rid of carbon dioxide and other by-products. The increased requirements are fulfilled by the increase of muscle blood flow and cardiac output. The increase of cardiac output goes mostly to the exercising muscles. Some portion of the increased cardiac output may go to other tissues, for instance to the skin when the body needs to get its temperature down by sweating.

The cardiac output is the primary determinant of oxygen delivery. Therefore it is not surprising that cardiac output will increase during exercise when the oxygen requirement of the working muscles increases significantly. Many investigations have suggested a close relationship between the cardiac output and oxygen delivery or oxygen consumption. The cardiac output rises nearly linearly with oxygen uptake and body arrives at its maximum oxygen uptake when the maximum cardiac output is reached (Lewis et al., 1983). For normal active subjects and endurance athletes, the quantitative relationship between cardiac output and oxygen uptake is approximately 5 l/min cardiac output per l/min increase in oxygen uptake.

Despite this steady state linear relationship, the transient response of cardiac output during exercise shows a different shape from that of the oxygen uptake. De Cort et al. (1991) investigated six subjects and for each individual they suggested that the kinetics of cardiac output may be described by a single exponential. They found that the time course of adjustment of cardiac output for an exercise transient from unloaded pedalling to 70 or 80 W work rate is always faster than that of oxygen uptake, with mean time constants of 27.7 ± 6 s and 55 ± 21 s for Q' and $V'O_2$ respectively. The cardiac output increases without delay while oxygen uptake shows a 5 s lag. Assuming that the oxygen uptake is determined entirely by the cardiac output and arteriovenous oxygen difference, they suggested that cardiac output is not the only determinant but plays a more dominant role in the early rise of oxygen uptake.

Yoshida and Whipp (1994) have made a similar suggestion. If it is characterized in terms of first order kinetics (a simple exponential), the time constant of cardiac output during the on-transient is consistently shorter than the time constant of oxygen uptake.. Data from their experiments suggest that Q' has a time constant of 29.4 ± 3.2 s during a transient from rest to 50 W exercise (the on-transient) and a time constant of 44.3 ± 3.6 s for the corresponding off-transient (or recovery) from 50 W exercise to rest. The oxygen uptake $V'O_2$ has time constants of 33.9 ± 3.5 s and 37.2 ± 2.9 s during on-transient and recovery respectively for this level of exercise. Thus the oxygen uptake exhibits more or less symmetrical responses during the on and off transients but the cardiac output has asymmetry in its transient kinetics. The asymmetry serves to maintain a sufficiently high

blood flow to the muscle during recovery at a time when the muscle oxygen uptake remains high.

A more recent experimental result shows similar characteristics of Q' and $V'O_2$ but faster kinetics. Lador et al. (2006) suggest that the kinetics of cardiac output can be as fast as 12.81 ± 1.67 s with the corresponding O_2 uptake kinetics being 18.75 ± 2.50 for 100 watt exercise.

MacDonald et al. (1998) suggested that both the muscle blood flow and the oxygen uptake slow down during an exercise transient in the supine position compared with an exercise transient in the upright position. This finding supports the idea that the cardiac output, as represented by the muscle blood flow, and the oxygen uptake have a close correlation even during transients.

Body position certainly has an effect in terms of changing the kinetics of cardiac output. The time constant of exercise in the upright position is smaller (i.e. faster) than the time constant in the supine exercise. However, in the steady state condition, the cardiac outputs for exercise in both positions are not significantly different. Such a conclusion has been reported for conditions from rest to 40 W exercise (MacDonald et al., 1998).

Many observers suggest that the response of the cardiac output to exercise has two phases (Lador et al., 2006; MacDonald et al., 1998; Hughson et al., 1993; Hughson and Morrissey, 1982). Phase 2 is believed to be the cardiovascular feedback response to the increasing work rate and the shape is largely agreed to be of a single exponential form. Phase 1, which is also called immediate exercise hyperaemia, is caused by local vasodilation which increases the vascular conductance of the exercising muscle (Saunders and Tschakovsky, 2004) and also by a muscle pump effect where contraction and relaxation, especially during the first few contractions, allows additional blood to pass through the muscle (Radegran and Saltin, 1998). Phase 1 is usually assumed to be exponential. The two phase response is depicted in Figure 4.2.

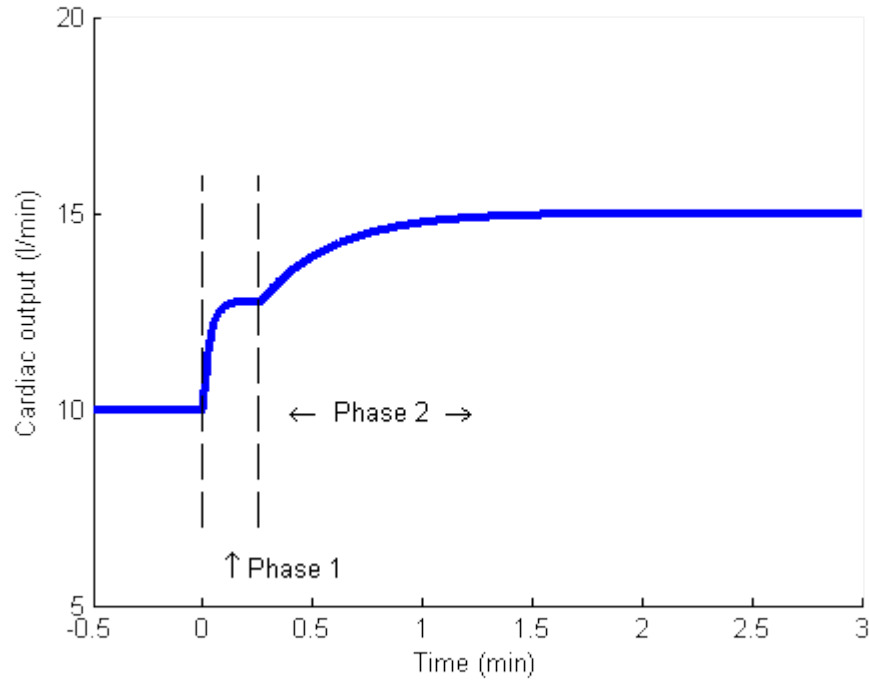


Figure 4.2. The two phase response of cardiac output as suggested by some investigators.

Based on the above information, the cardiac output has been modelled as a system with a two-exponential response so it has two time constants of the exponentials representing phase 1 (or initial) and phase 2 (or fundamental) components, which is mathematically described as:

$$\dot{Q}(t) = \dot{Q}_{bl} + 0.05 \cdot WR \cdot \{ \mu \cdot (1 - e^{-t/\tau_i}) + (1 - \mu) \cdot (1 - e^{-(t-TD_f)/\tau_f}) \} \quad (4.2)$$

or if expressed in terms of differential equation:

$$\begin{aligned} \tau_i \frac{d\dot{Q}_i(t)}{dt} &= 0.05 \cdot \mu \cdot WR \\ \tau_f \frac{d\dot{Q}_f(t)}{dt} &= 0.05 \cdot (1 - \mu) \cdot WR \\ \dot{Q}(t) &= \dot{Q}_{bl} + \dot{Q}_i(t) + \dot{Q}_f(t) \end{aligned} \quad (4.3)$$

where \dot{Q}'_{bl} is the base line cardiac output, i.e. the cardiac output before the exercise work load is applied, WR is the work rate in watts, TD and τ are the time delay (s) and time constant (s) of the response components respectively, and subscripts i and f represent variables for initial and fundamental components respectively. The constant μ represents the relative magnitude of initial component compared to the fundamental component. In our model, fundamental time constant is set at 15s, and initial time constant is assumed to be 4 s with magnitude 66% of steady state increase. The initial component values are estimated from the experimental result presented by Lador et al. (2006). Using the assumption that all of the increase in cardiac output goes to muscle, a similar equation is applicable for the muscle blood flow. The difference is only in terms of the base line value

where muscle blood flow is certainly smaller because blood also flows to the brain and to other tissues.

4.3. Ventilation

Ventilation is the process of exchange of gases between the lungs and the ambient air. Ventilation, or more precisely pulmonary ventilation, refers to the amount of air flowing in or out of the lung through the ventilatory airways and is measured in litre per unit of time. Alveolar ventilation refers to the effective ventilation of the alveoli, in which gas exchange with the blood takes place.

There are two ways to express gas volume measurement. One uses litre BTPS which stands for body temperature and pressure saturated. The volume is measured at body temperature (37°C), at ambient barometric pressure and for the condition under which the gas is saturated with water vapour. Barometric pressure varies with weather and altitude and is approximately 760 mmHg at sea level. Water vapour in saturated air contributes about 47 mmHg to the overall gas pressure. Another form of measurement uses litre STPD, which stands for standard temperature and pressure dry. Standard temperature is at 0°C (or 273K) and standard pressure is 1 atmosphere (atm) which corresponds to 760 mmHg.

The main determinant of ventilation in the context of exercise is the regulation of arterial blood gas (P_{aO_2} and P_{aCO_2}) and arterial blood acidity (pHa). It is widely agreed that the ventilation response for normal subjects during moderate exercise involves maintaining P_{aCO_2} and pHa relatively constant (Whipp, 1990).

In the ideal lung (a lung with no ventilation-perfusion inequalities, no diffusion limitation and no right-to-left shunt), alveolar and arterial PCO_2 are equal and have a value which is determined by the equation:

$$P_{aCO_2} = P_{ACO_2} = 863 \cdot \frac{\dot{V}CO_2 [STPD]}{\dot{V}A [BTPS]} \quad (4.4)$$

where P_{aCO_2} and P_{ACO_2} are the carbon dioxide partial pressure in the artery and alveoli respectively, and 863 is the constant which derives from the temperature, pressure and water vapour corrections:

$$1 \text{ BTPS} = 863 \text{ STPD} = (273 + 37)/273 \times [760/(760-47)] \times (PB - 47) \text{ STPD}$$

The equation (4.4) can be expressed as:

$$P_{aCO_2} = 863 \cdot \frac{\dot{V}CO_2}{\dot{V}A} \quad (4.5)$$

$$\dot{V}A = 863 \cdot \dot{V}CO_2 / P_{aCO_2}$$

which implies that the relationship between $\dot{V}CO_2$ and $\dot{V}A$ is linear with the slope 863/ P_{aCO_2} . During moderate exercise where P_{aCO_2} is relatively constant except for a

transient period, the increase of alveolar ventilation resembles the increase of carbon dioxide flow out of the lung. Non simultaneous increase of both variables will yield a value of PaCO₂ which deviates from the regulation level, which is the case for patients having pulmonary hypertension or restrictive lung disease (Habedank et al., 1998).

The total ventilation at the mouth differs from the alveolar ventilation due to the presence of dead space in the lung. Dead space is the part of the lung that does not contribute to the exchange of gases between the lung and the blood. While the value of the dead space is considered constant at rest, its value during exercise increases with ventilation and this is usually expressed in terms of the ratio of the dead space volume and tidal volume VD/VT. At rest VD/VT is approximately 0.35 and during unloaded exercise it drops to 0.20. When the exercise work load increases, the value of VD/VT decreases and can reach a value of around 0.15 for 75 watt exercise (Davis et al., 1980).

Taking into account the presence of dead space, the total ventilation is given by:

$$\dot{V}E = \frac{863 \cdot \dot{V}CO_2}{PaCO_2(1 - VD/VT)} \quad (4.6)$$

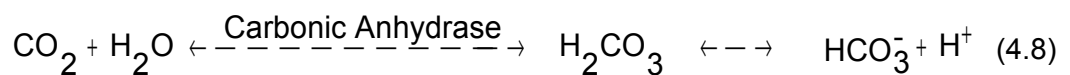
Empirical investigation has shown that the relationship between V'E and V'CO₂ is linear. However, equation (4.6) does not at first glance show the linearity because VD/VT changes with ventilation. In order that the V'E – V'CO₂ relationship is linear, it has been suggested that VD/VT should be a hyperbolic function of the increasing V'E (Whipp and Ward, 1982):

$$VD/VT = 1 - \frac{863 \cdot m}{PaCO_2} + \frac{C}{\dot{V}CO_2} \quad (4.7)$$

where m is the slope of V'E – V'CO₂ relationship and c is its positive intercept.

4.3.1. Ventilatory efficiency

The ability to clear carbon dioxide out of the body in sufficient quantities is very important in order to keep the body within the normal metabolic condition. The amount of CO₂ in the blood is given by:



A high concentration of CO₂, which could arise, for example, if the lung does not clear CO₂ sufficiently, means a high proton concentration and the blood becomes acidic. Severe acidosis reduces the ability of our body to function and cellular metabolism can fail.

Ventilation is the main way in which carbon dioxide is washed out of the body and the ratio between ventilation and carbon dioxide wash-out is called the ventilatory efficiency. Normally, the higher the ventilation the greater is the amount of carbon dioxide

washout. However, some diseases and deficiencies in the lung and heart can alter the ventilatory efficiency. In fact it is one of the tools used by cardiologists and pulmonary clinicians to assess the severity of heart and lung failure.

For normal healthy subjects, ventilatory efficiency ranges from 23 to 29 depending on age. Older subjects tend to have a higher ventilatory efficiency and males tend to have a lower ventilatory efficiency than females (Sun et al., 2002; Neder et al., 2001).

During exercise, the ratio $\dot{V}'E/\dot{V}'CO_2$ shows a slight change with the work rate.

$$\dot{V}'_E = m \cdot \dot{V}'CO_2 + c \quad (4.9)$$

where m is the gradient and c is the intercept. Again, the values of m and c are within a range that depends on gender and age. The average values are $m = 25$ and $c = 2.4$ l/min (Sun et al., 2002). Other investigators have suggested similar values where $m = 24.6$ and $c = 3.2$ l/min (Davis et al., 1980). This regression relationship has an unusually small level of uncertainty because the values of the parameters have been obtained from analysis of hundreds of subjects. The relationship is also stable and uniform for conditions of rest and higher intensity exercise before ventilatory compensation occurs.

4.3.2. Ventilation profile in the model

The previous section suggests the possibility of deriving the ventilation profile if $\dot{V}'CO_2$ is known because the relationship between the ventilation and carbon dioxide wash-out is applicable over a wide range of conditions of exercise. However, the above descriptions have been obtained from analysis in steady-state conditions and below the point of compensatory ventilation. Thus only the steady state value of ventilation can be estimated from the expected

$$\Delta \dot{V}'_E(ss) = m \cdot \Delta \dot{V}'CO_2(ss) + c \quad (4.10)$$

where $\Delta \dot{V}'E(ss)$ and $\Delta \dot{V}'CO_2(ss)$ are the steady state increases of ventilation and carbon dioxide washout respectively.

During moderate intensity exercise, the expected steady-state values of oxygen uptake and carbon dioxide washout can be estimated if the work rate is known (see sections 4.4 and 4.6 for further details). For the oxygen uptake, we have

$$\Delta \dot{V}'O_2(ss) = 10 \cdot WR \quad (4.11)$$

where $\Delta \dot{V}'O_2(ss)$ in ml/min is the steady state increase of oxygen uptake calculated from the baseline of unloaded exercise and WR is work rate in watt. It should be noted that the equation (4.11) holds for upright cycle ergometry exercise; other types of exercise may generate a different profile of oxygen uptake. Then for carbon dioxide wash-out:

$$\Delta \dot{V}'CO_2(ss) = RQ \cdot \Delta \dot{V}'O_2(ss) \quad (4.12)$$

where $\Delta V'CO_2(ss)$ is the steady state increase of carbon dioxide washout and RQ is the muscle respiratory quotient which resembles the ratio of muscle CO₂ production to muscle O₂ consumption.

A typical baseline value for ventilation is approximately 11 litres/minute which is calculated to set the PaCO₂ level at 40 mmHg. This is higher than the value for ventilation at the rest condition which is 6 l/min.

At the onset of exercise, ventilation increases from a baseline value to a new steady-state value showing a two-phase characteristic in the transient, i.e. phase 1 and phase 2. Phase 1 is an obvious feature of the response if the exercise increases from a baseline at rest. It is step-like and has significant amplitude and it lasts for about 15s (Whipp et al., 1982). The amplitude of phase 1 increases for larger increases in exercise but is smaller in percentage terms compared to the magnitude of the steady state increase ($\Delta V'E(ss)$). However, from the baseline of unloaded exercise, phase 1 is less noticeable both in amplitude and shape. In our model, it is assumed to be exponential with time constant 4s and its amplitude is 15% of $\Delta V'E(ss)$.

The phase 2 component of ventilation has been largely modelled as a simple exponential. This is particularly applicable for moderate exercise conditions. During heavy exercise with sustained lactic acidosis, additional CO₂ (which is the outcome of acid buffering by blood bicarbonate) will affect the shape of the V'CO₂ transient. The kinetics may be illustrated using a two phase characteristic, similar in shape to that for cardiac output shown in Figure 4.2, but with phase 1 having a much smaller amplitude.

The kinetics of ventilation following the start of moderate exercise vary among subjects and range from 50 to 100 seconds if ventilation is assumed to involve a single exponential. The fundamental, or phase 2 component, certainly has a smaller time constant considering the existence of the phase 1 (or initial) component which delays the occurrence of the fundamental component by values ranging from 12 to 29 seconds (Casaburi et al., 1989a; Hughson and Morrissey, 1982).

In the model, ventilation has, therefore, been expressed as

$$\dot{V}E(t) = \dot{V}E_{bl} + G_i \cdot (1 - e^{-(t-TD_i)/\tau_i}) \cdot \mu_i + G_f \cdot (1 - e^{-(t-TD_f)/\tau_f}) \cdot \mu_f \quad (4.13)$$

or in differential equation:

$$\begin{aligned} \tau_i \frac{d\dot{V}E_i(t)}{dt} &= G_i \cdot e^{-t/TD_i} \\ \tau_f \frac{d\dot{V}E_f(t)}{dt} &= G_f \cdot e^{-t/TD_f} \\ \dot{V}E(t) &= \dot{V}E_{bl} + \dot{V}E_i(t) + \dot{V}E_f(t) \end{aligned} \quad (4.14)$$

where $V'E_{bl}$ is the base line value of ventilation, G , TD and τ are the gain, time delay and time constant of the response components respectively, and subscript i and f represent variables for initial and fundamental components respectively and

$$\mu_i = 0 \text{ for } t < TD_i \text{ and } \mu_i = 1 \text{ for } t \geq TD_i$$

$$\mu_f = 0 \text{ for } t < TD_f \text{ and } \mu_f = 1 \text{ for } t \geq TD_f$$

Note that initial component can be assumed to start immediately without delay so TD_i may be assigned zero.

4.4. Pulmonary oxygen uptake

The pulmonary oxygen uptake ($V'O_2$) increases, predominantly in an exponential fashion, towards a new steady-state value in response to a step increase in work rate involving moderate intensity exercise (Whipp et al., 1982). Basically, for constant-load exercise, the oxygen uptake response may be described as:

$$\dot{V}O_2(t) = VO_{2,bl} + \Delta \dot{V}O_2(ss)(1 - e^{-(t-TD)/\tau}) \quad (4.15)$$

where $V'O_{2,bl}$ is the base line value of oxygen uptake prior to the increase of work rate, $\Delta V'O_2(ss)$ is the magnitude which reflects the increase from base line to the steady state value, τ is the time constant describing the time taken for the response to reach 63% of its magnitude and TD is the time delay after exercise starts until the response actually increases.

During the time delay period, a small rapid initial component emerges in the response and this is known as the phase 1 component. The phase 1 component can last for 15-20s reflecting the dynamics of cardiac activity at the onset of exercise. The rapid increase in cardiac output which also increases the pulmonary blood flow pulls venous blood with a relatively low O_2 concentration through the lung, thus attracting more oxygen into the blood stream.

The fundamental component, which is also known as the phase 2 component, reflects the changes in body oxygen consumption during exercise. It mainly comes from the increase in muscle oxygen extraction required to maintain the exercise. Additional oxygen consumption also results from the increase in cardiac work to increase the blood flow, the increase in ventilatory mechanical work and other work relating to maintaining the body posture. The phase 2 time constant varies between different subjects and is approximately 30 seconds. It is smaller in trained athletes and much larger for unhealthy subjects. $V'O_2$ does not change much for different work rates within the moderate intensity domain. Oxygen uptake, however, depends not only on the level of exercise being applied but also on the muscle mass and on the body position, e.g. supine or upright (Cerretelli et al., 1977).

The $\dot{V}O_2$ steady state level (phase 3) increases as a relatively linear function of work rate for moderate-intensity cycle ergometry exercise at a constant pedalling frequency. The slope of this relationship ($\Delta\dot{V}O_2/\Delta WR$) is approximately 10 ml $\dot{V}O_2/W$. Thus, an increase in power output from unloaded cycling (“zero” watts) to 100 W results in an increase in $\dot{V}O_2$ from a baseline of approximately 500 ml/min (i.e. 250 ml/min resting $\dot{V}O_2$ plus 250 ml/min additional $\dot{V}O_2$ required by the “standard” 70 kg adult to pedal a well-designed ergometer at 60 to 70 rpm with no braking force applied to the flywheel) to approximately 1500 ml/min in the steady state.

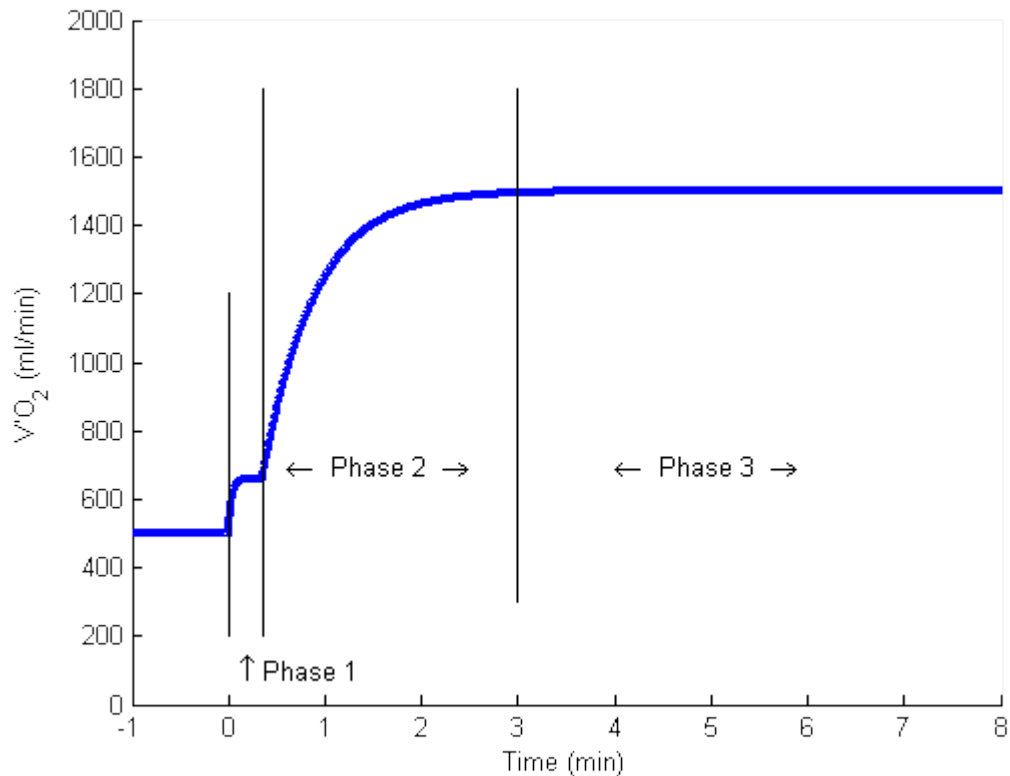


Figure 4.3. Kinetics of pulmonary oxygen uptake ($\dot{V}O_2$) at the onset of a step increase in moderate intensity exercise

The baseline value may be higher for subjects with “heavy legs”, for example because of obesity. This increases the $\dot{V}O_2$ cost of unloaded cycling, but the $\Delta\dot{V}O_2/\Delta WR$ slope is usually unaltered (Whipp et al., 1982).

When a group of subjects were tested performing different types of exercise, they appeared to show different pulmonary kinetics. For example, during knee extension exercise, the ratio of $\dot{V}O_2$ to work rate during the steady state (phase 3) is 12 ml/min/W which is higher than the ratio for cycle ergometer exercise but both types of exercise yield the same time constant (Koga et al., 2005). Knee extension exercise is believed to involve a different pattern of muscle fibre recruitment and involves a different pattern of blood flow to muscle.

Subject posture also influences the response in terms of oxygen uptake. Hughson et al. (1993) observed kinetics of oxygen uptake at the onset of submaximal cycling exercise in seven men and one woman [mean age 22.6 ± 0.9 (SE) yr] in the upright and supine positions. They found significant differences in terms of the peak $\dot{V}O_2$ and the ventilatory threshold when results for the supine situation ($3,081 \pm 133$ and $1,95 \pm 138$ ml/min, respectively) were compared with corresponding results for upright exercise conditions ($3,483 \pm 200$ and $2,353 \pm 125$ ml/min). Hughson et al. also suggested that kinetic analysis applied to six repetitions by each subject indicates a slowing from a time constant of 36.3 ± 2.7 s in the case of upright exercise to 44.1 ± 3.5 s in the supine position (Hughson et al., 1993).

4.5. Muscle oxygen consumption

Muscle is the organ that performs exercise so it is not surprising that its oxygen consumption increases considerably during the activity. Some other tissues such as heart and lung muscles also increase their oxygen consumption because they get more work stress which is indicated by the increase in heart rate and breathing frequency. However, the increase of other tissue O_2 consumption is relatively small compared to that consumed by the exercising muscle. It is generally acceptable to assume that all the increase in pulmonary oxygen uptake relates to the increase of muscle oxygen consumption ($\dot{Q}'O_2$), as has been predicted using a computer model (Barstow and Mole, 1987).

The transient behaviour of muscle oxygen consumption is in some ways similar to that of pulmonary oxygen uptake. At the onset of exercise the kinetics of alveolar oxygen uptake and oxygen flow to the exercising leg are similar (Grassi et al., 1996). This means that the alveolar oxygen uptake reflects the oxygen consumption of the exercising muscle.

The kinetics of muscle oxygen consumption resemble the response of a first order system. Hill (1940) is recognized as being the first to suggest that the time course of muscle oxygen consumption is exponential following the onset of tetanus. This finding related to experiments involving frog muscle at 0°C . In Hill's experiment, applying tetanus to a muscle fibre is equivalent to giving a repeated impulsive stimulus to the muscle. Another experiment with frog muscle was conducted later using more recent technology but with different method. Results, however, were consistent with what had been found previously (Mahler, 1985).

As inferred from the kinetics, muscle does not immediately take from blood an equivalent amount of oxygen needed for a given the exercise load. For example, a step increase in exercise load is followed by an exponential increase in $\dot{Q}'O_2$. This is because muscle stores ATP (adenosine tri phosphate) and PCr (Phosphocreatine) as the immediate sources of high energy phosphate needed in muscle contraction. Muscle has

also an ability to store oxygen by binding O₂ molecules with its myoglobin. Therefore, at the time when the O₂ requirement suddenly increases the stored O₂ is available to use.

The role of ATP, PCr and myoglobin in terms of energy storage is significant. Although muscle fibres can utilize ATP and PCr within seconds during intense exercise, both species (together with stored O₂) have sufficiently large capacitance to shape the transient behaviour of muscle oxygen consumption. At the onset of exercise, the utilization of stored energy sources slows the muscle consumption of oxygen and during recovery from exercise muscle still consumes oxygen to restore the energy storage to the level prior to exercise. This slow increase in O₂ consumption at the onset of exercise is often called the "oxygen debt", which is paid during recovery from exercise.

It needs to be noted that during recovery, pulmonary oxygen consumption drops exponentially with the same time constant observed during the increase in pulmonary oxygen consumption at the onset of exercise.. However, muscle blood flow does not decrease as rapidly as the increase that occurs at the onset of exercise because the muscle requirement for oxygen needs support in terms of the blood flow required to transport oxygen from the lung to muscle (Yoshida and Whipp, 1994).

Based on the description in this section and Section 4.5, the gain of muscle O₂ consumption is set to be 10 ml/min/watt and the time constant is 32 s.

4.6. Carbon dioxide production

The provision of energy for exercise from the burning of fuel with oxygen involves complicated chains of reactions in the muscle. Among the end products of the reactions is the carbon dioxide which is formed by oxidative metabolism. In a short form, the oxidative metabolism may be represented through the following chemical equations:



The first of the above two equations involves glycogen (C₆H₁₂O₆) as the substrate whereas the second one involves lipid (C₁₆H₃₂O₂).

The relative amount of carbon dioxide produced in muscle during exercise depends on the substrate used in the metabolism. The burning of each mole of glucose will need 6 moles of O₂ and produce 6 moles of CO₂. When lipid is used as the fuel, the burning of each mole needs 23 moles of O₂ and releases 16 moles of CO₂.

It is customary to express the amount of CO₂ produced in relation to the amount of O₂ consumed by a tissue in terms of a quantity known as the respiratory quotient (RQ) which is defined as:

$$\text{RQ} = \dot{Q}\text{O}_2 / \dot{Q}\text{CO}_2 \quad (4.18)$$

where $\dot{Q}'O_2$ and $\dot{Q}'CO_2$ are the tissue O_2 consumption and CO_2 production respectively. In this respect, the RQ of burning glucose is 1 and the RQ of burning lipid is 0.7.

4.6.1. Carbon dioxide storage in muscle

Muscle has a capability to store oxygen primarily by binding O_2 to a type of muscle protein called myoglobin. The question is: does muscle have a capability to store carbon dioxide? The existence of carbonic anhydrase in muscle (Geers and Gros, 2000) implies that the carbon dioxide produced during exercise will be quickly converted into carbonic acid (H_2CO_3) which ionizes immediately into proton and bicarbonate (HCO_3^-). Both CO_2 and bicarbonate can diffuse out of the muscle but of course it needs time to move between the muscle cells and the artery. Myoglobin might not be capable of binding CO_2 , but the temporary containment of bicarbonate or dissolved CO_2 in muscle cytoplasm may be regarded as a kind of storage and the total muscle CO_2 concentration in all of its forms will increase during exercise.

The kinetics of CO_2 production at the mouth ($\dot{V}'CO_2$) suggests that there has to be a significant capacity in terms of CO_2 storage in the human body to produce the slower $\dot{V}'CO_2$ kinetics compared to the kinetics of $\dot{V}'O_2$. The CO_2 concentration of the blood increases significantly during exercise, mainly due to its role in transporting the CO_2 from muscle to the lung and some other factors including the increase of PCO_2 and the decrease of venous PO_2 . On passing the lung, arterial blood CO_2 content falls significantly which is reflected in the low value of $PaCO_2$ compared to that of venous PCO_2 .

4.6.2. Calculation of pH

Metabolism in the human body runs well within "normal" conditions. Conditions outside the range of normal values may prevent metabolism from functioning well and may lead to severe illness or, possibly, death. Normal arterial and venous blood pH is about 7.4 and 7.35, respectively. A much lower pH value, which corresponds to a higher hydrogen concentration, is called acidosis (too acidic) and a much higher pH value is called alkalosis.

There are three important independent variables that influence pH in blood: carbon dioxide content, relative electrolyte concentrations, and total weak acid concentrations. Exercise increases the production of CO_2 which drains the venous blood compartment so that during exercise, venous blood pH decreases significantly. Arterial pH, on the other hand, may decrease unless all the produced CO_2 during exercise is washed out after passing the lung.

In our model, blood pH is calculated using a model developed by researchers at the University of Prague (Kofranek et al., 2007). The calculation can be regarded as a computer implementation of the Siggaard-Andersen nomogram which was explained in

Andersen and Engel (1960). The Siggaard-Andersen nomogram describes the relationship among variables in blood which include PCO_2 , pH, base excess and buffer base with a precondition that the concentration of blood haemoglobin is known (see Figure 4.4).

The concept of the buffer base (BB) is introduced to express quantitatively the surplus amount of fixed acid or base in blood (Singer and Hastings, 1948). Buffer base is defined as the sum of concentration of all buffer anions in blood (usually expressed in mEq/l). The value of buffer base is independent of PCO_2 but it is dependent on haemoglobin concentration. At normal pH = 7.4 and $\text{PCO}_2 = 40$ mmHg, normal buffer base can be expressed as:

$$\text{NBB} = 40.8 + 0.36 \times [\text{Hb}] \quad (4.19)$$

where [Hb] is haemoglobin concentration in g/dl blood. Disturbance of the acid base balance results in buffer base values deviating from NBB.

Base excess (BE) refers to the amount of strong acid or alkali required to return the fully saturated blood pH of an individual to the normal value of 7.4 when $\text{PCO}_2 = 40$ mmHg and temperature is 37°C (Andersen et al., 1960). The value is usually reported in the unit of (mEq/l). The normal value of base excess is zero. A positive value indicates a positive amount of acid needed to return pH to 7.4 which means a condition of alkalosis and a negative value indicates acidosis. Numerically, the deviation of buffer base from its normal value (NBB) is equal to the base excess.

The Siggaard Andersen nomogram is built on a coordinate system where pH is put on the horizontal axis and PCO_2 on the vertical axis with a logarithmic scale. Logarithmic scaling for PCO_2 has the advantage that the graphical relationship between pH and PCO_2 can be drawn using an approximately straight line within the physiological range. An example of such a line is depicted as the dashed line on Figure 4.4.

The slope of the line relating PCO_2 -pH in the nomogram is dependent on haemoglobin concentration where the steepness increases with increasing haemoglobin concentration. If several lines are drawn on the nomogram for different haemoglobin concentration levels, they will intersect on the same point. When the acid-base content of the blood is changed by adding fixed acid or base, the lines and the point are displaced. The collection of intersection points for different acid base content can be connected together to form what is called the base excess curve. Recalling Figure 4.4, the base excess (BE) of normal blood is 0 so for the normal $\text{PCO}_2 = 40$ mmHg it gives the normal pH = 7.4. If BE = -12 mEq/l, regardless of haemoglobin concentration, at $\text{PCO}_2 = 29$ mmHg, the nomogram gives pH = 7.28.

A curve for the determination of buffer base (BB) is shown in the upper left side of Figure 4.4. This is buffer base curve. A point in the curve can tell the value of pH and PCO_2 at a certain BB for BE = 0. If [Hb] = 14 g/dl, the normal buffer base according to

equation (4.19) is 45.84 mEq/l. For $[Hb] = 14$ g/dl and $BE = -12$ mEq/l, the buffer base (BB) will reside at $45.84 - 12 = 33.84$ mEq/l. The line connecting the BE at BE curve and BB at BB curve defines the relationship between PCO_2 and pH for the associated CO_2 content and $[Hb]$. Hence for $[Hb] = 14$ g/dl and $BE = -12$ mEq/l, the relationship between PCO_2 and pH follows the dashed line so at $PCO_2 = 50$ mmHg, $pH = 7.14$.

Figure has been removed
due to Copyright restrictions.

Figure 4.4. Siggaard Andersen nomogram; red curve with dots is the base excess curve, blue curve with dots is the buffer base curve; dashed line is an example of PCO_2 -pH relationship for base excess equals to -12 mEq/l and haemoglobin concentration of 14 g/dl (Adapted from Andersen, 1962)

Within the physiological range of blood pH, lactic acid belongs to the strong acid group. The release of lactic acid during early acidosis or metabolic acidosis of high exercise is equivalent to addition of fixed acid into the blood stream so that it can be regarded as changing the buffer base and base excess (Siggaard-Andersen and Fogh-Andersen, 1995), which displace the PCO_2 -pH relationship line to the left. Therefore, the Siggaard Andersen nomogram is very suitable for the calculation of pH for situations where the lactic acid needs to be taken into consideration. Simpler methods such as the use of the Henderson-Hasselbach equation for calculating pH is not sufficient for this situation.

4.7. Arterial partial pressure

Arterial partial pressure for oxygen and carbon dioxide can be calculated using the following equations:

$$PaCO_2 = \frac{863 \cdot \dot{V}CO_2}{\dot{V}_E(1 - VD/VT)} \quad (4.20)$$

$$PaO_2 = 147 - \frac{863 \cdot \dot{V}O_2}{\dot{V}_E(1 - VD/VT)} \quad (4.21)$$

which were described in Section 2.1. These equations are derived with an assumption that the ventilation-perfusion ratio is uniformly normal; the lung has no diffusion limitation and no right to left shunt. The assumptions ensure that alveolar partial pressure is equal to arterial partial pressure which leads to applicability of the equations. Practically, however, there is always a difference between the alveolar and arterial partial pressures for both oxygen and carbon dioxide, as suggested by many previous observations (Sylvester et al., 1981; Whipp and Wasserman, 1969; Wasserman et al., 1967) with diffusion constraint and exercise contributing to this difference (Rice et al., 1999; Sylvester et al., 1981; Cohen et al., 1971).

Despite the arterial alveolar differences, the arterial partial pressures of O₂ and CO₂ do not change much during steady state conditions of exercise and the value is very close to the rest value. This fact has been widely reported in literatures, e.g. in Wasserman et al. (2005), Stringer et al. (1992), Brice et al. (1988). Only at a very high level of exercise does PaCO₂ drop to a value lower than the rest value because the lung hyperventilates in order to reduce the reduction in blood acidity. Because the levels of PaO₂ and PaCO₂ are relatively constant at rest and during exercise at most conditions, these two variables have been suggested as being the primary variables involved in “homeostasis” or the regulatory target of the respiratory control system.

The developed model has strictly accommodated the homeostasis of arterial gas partial pressures during moderate exercise. In order that the levels of PaCO₂ and PaO₂ in equations (4.20) and (4.21) remain constant, the ratio of dead space to tidal volume (VD/VT) needs to vary from 0.2 at unloaded exercise to 0.16 at 100 W of exercise and it may go down to as low as 0.15 for higher exercise levels (Davis et al., 1980; Wasserman et al., 1967). The ratio of VD/VT over exercise has been observed to decrease hyperbolically with ventilation where the decrease is steep for the transition from unloaded or low levels of ventilation and gentler at higher levels. Therefore, VD/VT will be estimated to depend hyperbolically on ventilation using the following approximation:

$$VD/VT = \frac{0.5578}{V_E} + 0.1482 \quad (4.22)$$

This approximation ensures that $VD/VT \approx 0.2$ at unloaded exercise (baseline $V'E \approx 11$ l/min) and $VD/VT \approx 0.16$ at 100 W exercise ($V'E \approx 35$ l/min). Graphically, the relationship of VD/VT and ventilation as defined in equation (4.22) is depicted in Figure 4.5 below.

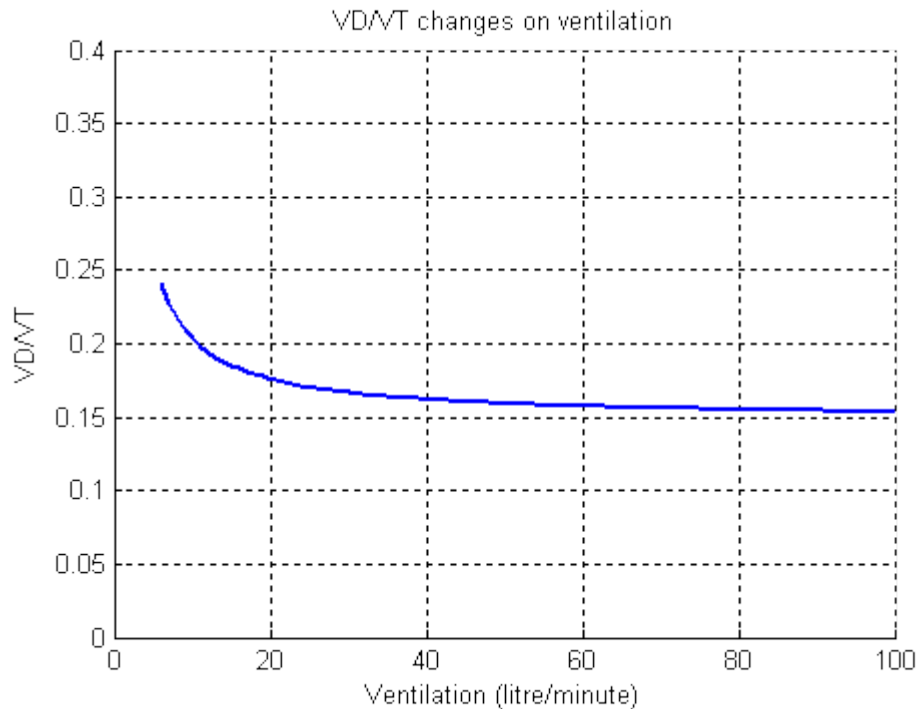


Figure 4.5. Changes of the ratio of dead space volume to tidal volume (VD/VT) over the range of ventilation considered

4.8. Simulation Results

4.8.1. Parameter Values

Important parameter values that is used in this model is listed in appendix C. Fundamental time constants for oxygen uptake, carbon dioxide output and ventilation are selected considering that τ_{VO_2} is smaller than τ_{VCO_2} and τ_{VE} , τ_{VCO_2} is usually slightly smaller than τ_{VE} , and τ_Q is much smaller than τ_{VO_2} . This fact can be found in many investigations such as in Lador et al. (2006), De Cort et al. (1991), Whipp et al. (1982), and Whipp and Ward (1982).

In the steady state condition of moderate exercise, the increase of ATP turn over rate has a magnitude that is equivalent to the increase of $Q'O_2$, although that ATP requirement is fulfilled completely by the aerobic catabolism. However, the kinetics of the ATP turnover rate is faster than the kinetics of $Q'O_2$ which implies that during transients, the ATP turn over rate is higher than that is provided by aerobic catabolism. The discrepancy is fulfilled with anaerobic catabolism which causes production of lactic acid. In

the model, the kinetics of ATP turn over rate is set to have fundamental time constant of 28 s (see Section 6.2 for more detail).

In the muscle compartment, lactate production rate is dependent on the work rate. In muscle and the other tissues compartment, lactate utilization is dependent on work rate and lactate concentration in the corresponding compartment. More information about lactate production and utilization is provided in Chapter 5.

4.8.2. General Model Behaviour

Running the simulation, the model is able to produce and show the behaviour of many output variables, most of which are calculated and a few are assumed to have a certain relation to the pre-defined variables. These output variables include the pulmonary oxygen uptake ($V'O_2$), pulmonary CO_2 output ($V'CO_2$), blood O_2 and CO_2 partial pressures, bicarbonate concentration and pH. Assessment of the model, through consideration of whether the model reproduces the behaviour of the real system, is carried out by comparing the system response in terms of output variables generated by simulation with the corresponding profile presented in published literature.

Some of the output variables are regulated during exercise. For moderate intensity exercise, these variables are the arterial carbon dioxide partial pressure ($PaCO_2$) and the arterial oxygen partial pressure (PaO_2). Actually, ventilation is physiologically sensitive to O_2 and CO_2 partial pressure in the artery and blood pH but the response to changes in pH is not obvious until pH is very low (i.e. when acidosis is severe) which is the case during a very high level of exercise.

Simulation was performed by applying a 100 W step increase of work rate, which is assumed to be in the moderate exercise intensity domain. This means that no lactate accumulation is expected. The time origin is the moment at which the work rate increase is applied.

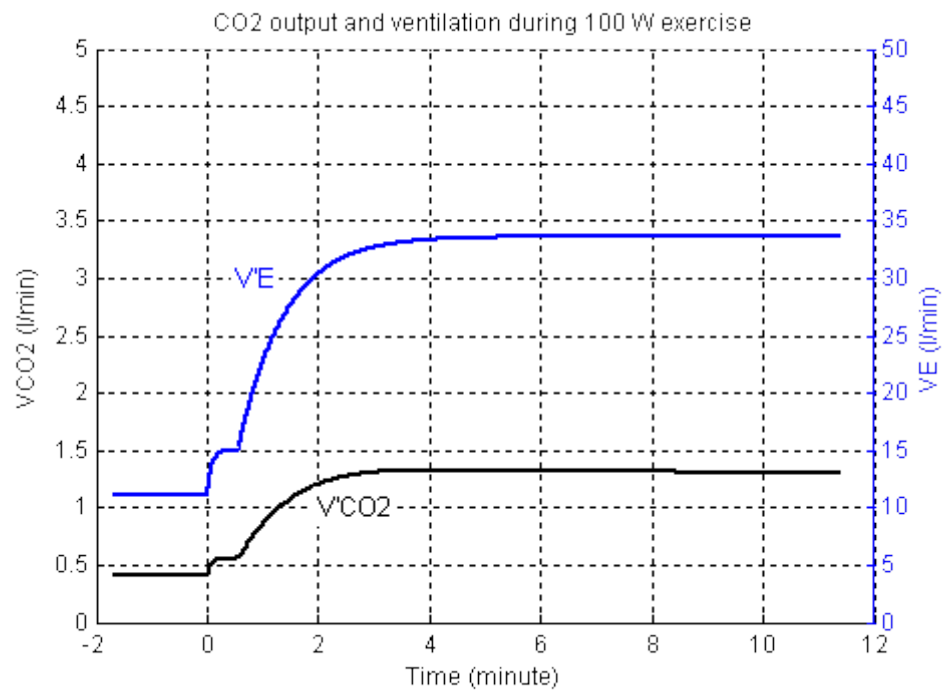


Figure 4.6 Response for exercise in moderate intensity domain: Ventilation ($V'E$) and CO2 output ($V'CO_2$) from simulation

Figure 4.6 shows the response in terms of ventilation ($V'E$) as pre-defined for the corresponding work rate. The figure also shows the simulation result for carbon dioxide output ($V'CO_2$) which demonstrates that the kinetic of $V'CO_2$ is biphasic. By considering the detail of the simulated response, it can be estimated that the phase 1 component of $V'CO_2$ has an amplitude of about 20% of the steady state increase. If phase 1 is assumed to be exponential, it has a time constant of approximately 3 s. The fundamental component has a time constant of approximately 44 s and amplitude 1 l/min.

Figure 4.7 depicts the graphical representation of cardiac output (Q') and oxygen uptake ($V'O_2$). The profile of cardiac output is a pre-defined as biphasic. The profile of oxygen uptake is a result of the simulation and it is estimated that the phase 1 component of $V'O_2$ has a magnitude of about 16% of the steady state increase. If assumed to be exponential, the phase 1 has a time constant of approximately 3 s. The fundamental time constant is approximately 36 s.

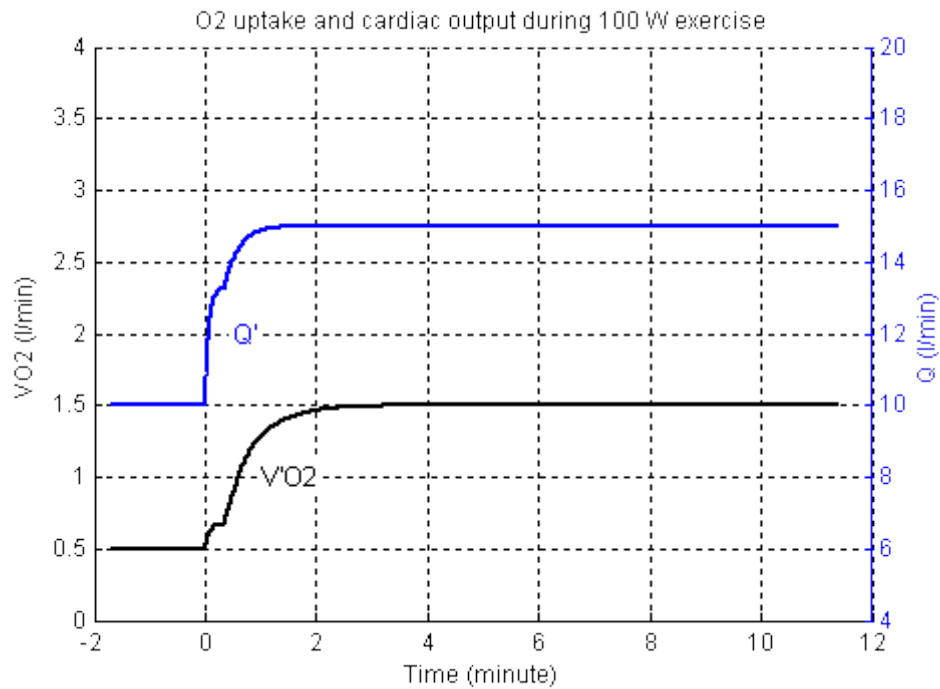


Figure 4.7 Response for cardiac output (Q') and pulmonary oxygen uptake ($V'O_2$) from simulation

Figure 4.8 shows the response in terms of the arterial and venous CO_2 partial pressures. Venous PCO_2 increases from its base line value of 47.5 mmHg towards a new steady-state value of approximately 57 mmHg. The increase is delayed by about 30 seconds after the onset of exercise and during this delay time a small negative-going fluctuation is observable which is fairly typical of systems with non-minimum-phase characteristics.

Arterial PCO_2 on the other hand does not change much throughout the whole period of exercise. It has some fluctuations at the onset of exercise, and then increases slightly approaching 41 mmHg and declines towards a steady state value which is similar to the initial value before exercise is applied.

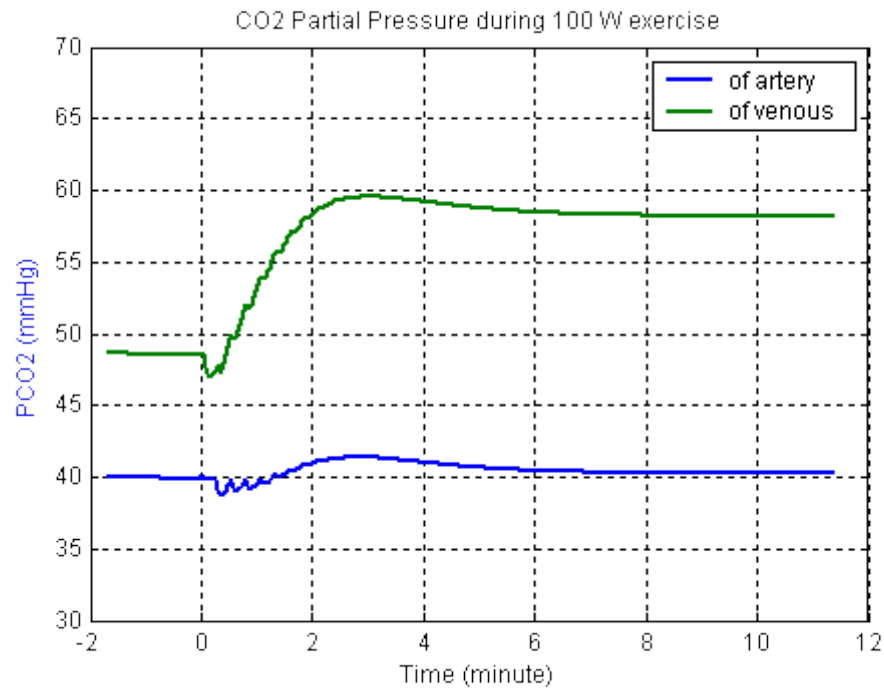


Figure 4.8 Arterial and venous CO₂ partial pressures from simulation.

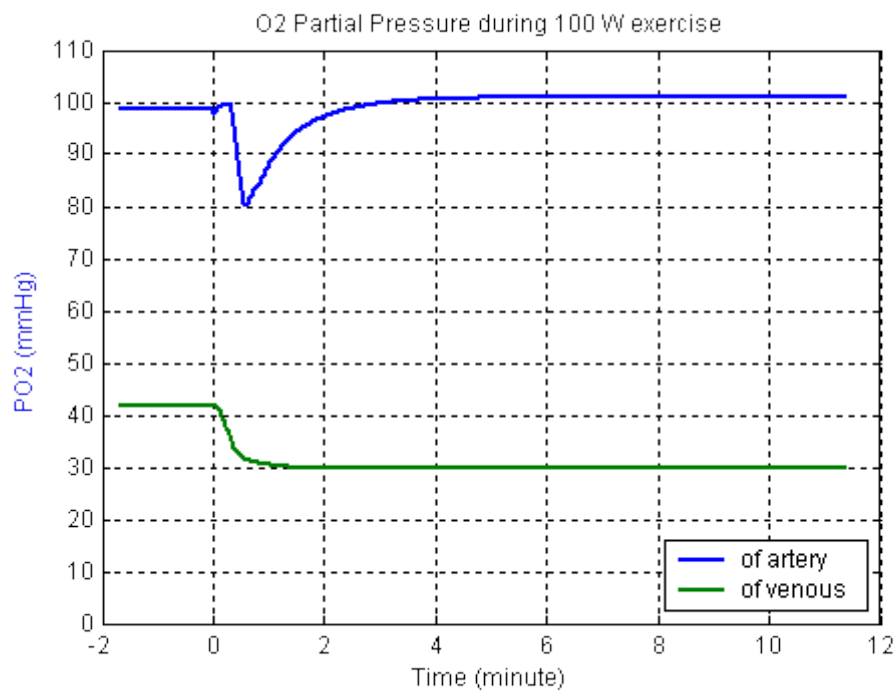


Figure 4.9 Arterial and venous O₂ partial pressures from simulation

Figure 4.9 displays the simulation result for venous (PvO₂) and arterial (PaO₂) oxygen partial pressure. The venous PO₂ decreases significantly from the base line value of 43 mmHg to a steady state value of 30 mmHg during exercise. At the onset of exercise, however, the base line value of arterial PO₂ exhibits different dynamics. For approximately 15 s after the onset of exercise, the PaO₂ value does not change significantly and stays close on the base line value of 100 mmHg. It then quickly drops to 80 mmHg and it gradually moves up and settles at the final value which is similar to the baseline.

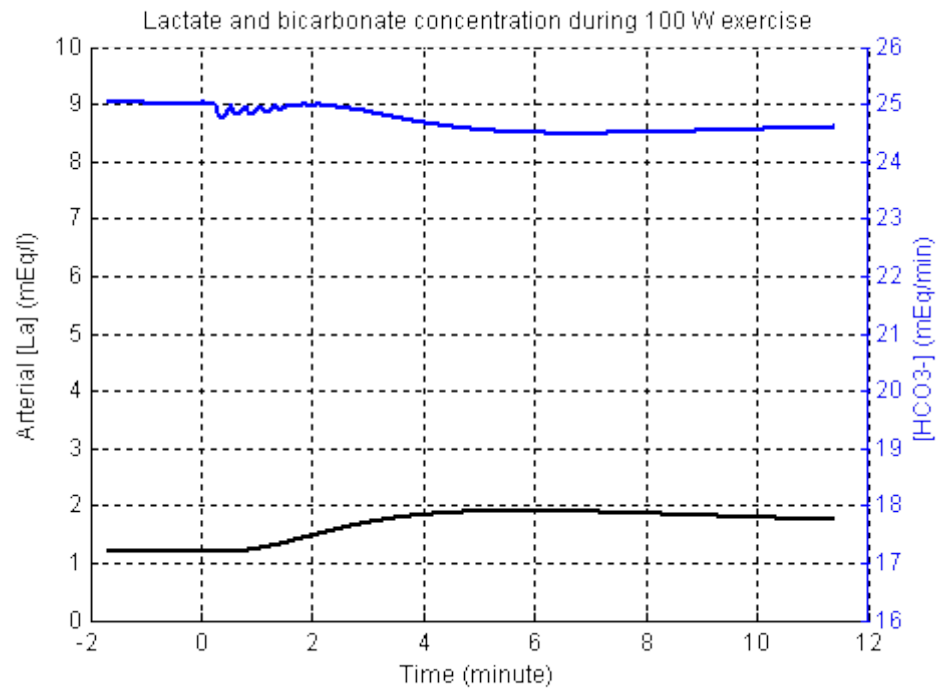


Figure 4.10 Simulation result for bicarbonate concentration and arterial lactate concentration

Figure 4.10 provides a picture of the kinetics of arterial lactate concentration [La] and arterial bicarbonate concentration [HCO₃⁻]. Bicarbonate concentration shows a decrease just after the onset of exercise but it then increases to a steady state value which is lower than the baseline value by approximately 0.3 mEq/l. Arterial lactate concentration [La] increases at the onset of exercise. Subsequently arterial [La] decreases towards a steady state value which is higher compared to the base line value before exercise.

Metabolic acidosis increases during exercise. This is shown by the reduced value of arterial and venous pH (see Figure 4.11). At the base line condition for unloaded exercise, arterial and venous pH levels are steady at 7.4 and 7.35 respectively. The arterial pH decreases at the exercise onset, showing some fluctuations, and then rises towards a steady state value slightly below the base line. Venous pH decreases significantly and reaches a steady state at approximately 7.29.

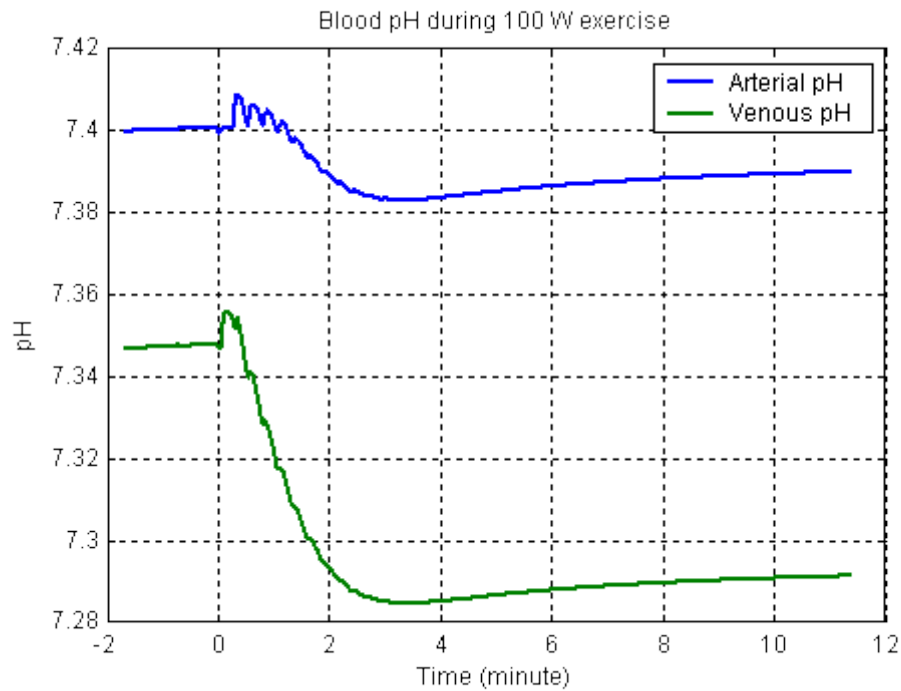


Figure 4.11 Arterial and venous pH during 100 W exercise

4.8.3. Relationship between the $V'CO_2$, $V'O_2$, $V'E$ and Q' variables during phase 1

Figures 4.12 – 4.15 depict simulation tests to assess the changes of the initial phase-1 component of $V'CO_2$ and $V'O_2$ for different magnitudes of phase-1 component of ventilation or cardiac output. Figure 4.12 and 4.13 show the changes of $V'CO_2$ and $V'O_2$ respectively against the changes in phase 1 component of cardiac output. Figure 4.14 and 4.15 show the changes of $V'CO_2$ and $V'O_2$ respectively against the changes in phase 1 component of ventilation. These results are discussed in Section 4.9.2.

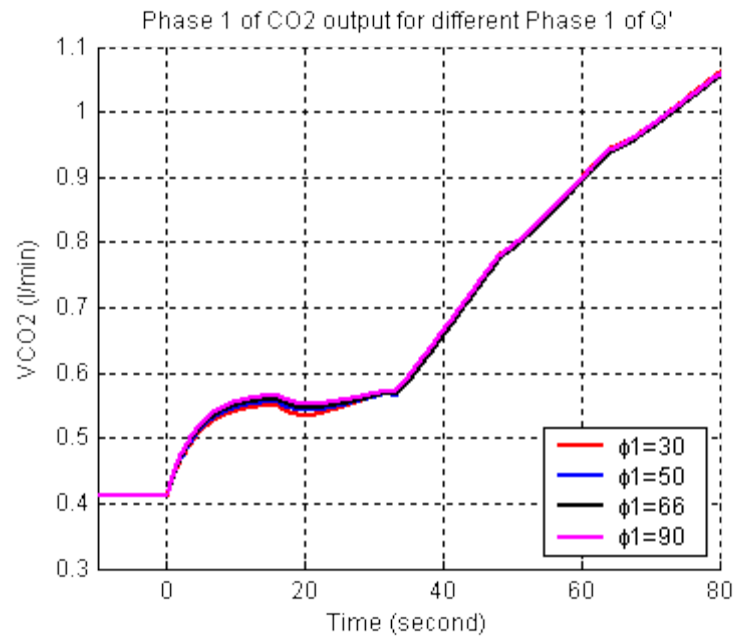


Figure 4.12. Kinetics of $V'CO_2$ for different phase-1 kinetics of Q' . Numbers in the legend represent the percent magnitude of phase-1 compared to the steady state increase of Q' .

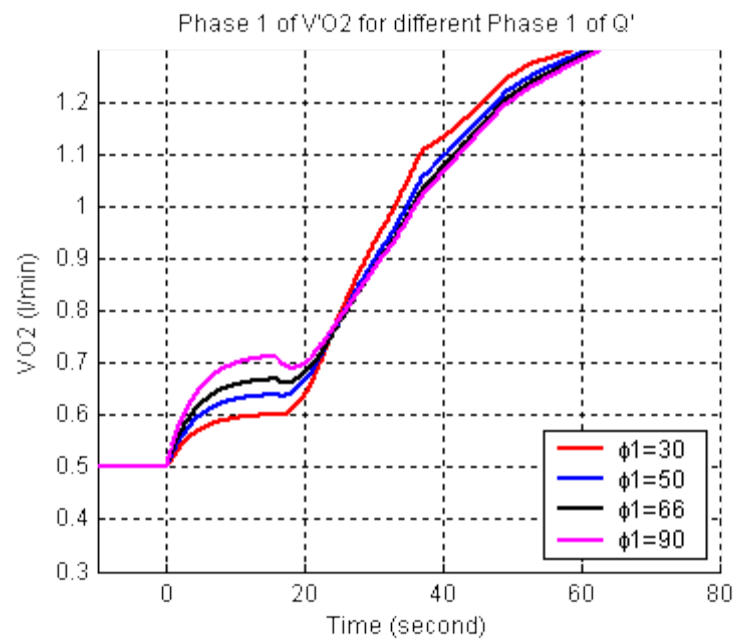


Figure 4.13. Kinetics of $V'O_2$ for different phase-1 kinetics of Q' . Numbers in the legend represent the percent magnitude of phase-1 compared to the steady state increase of Q' .

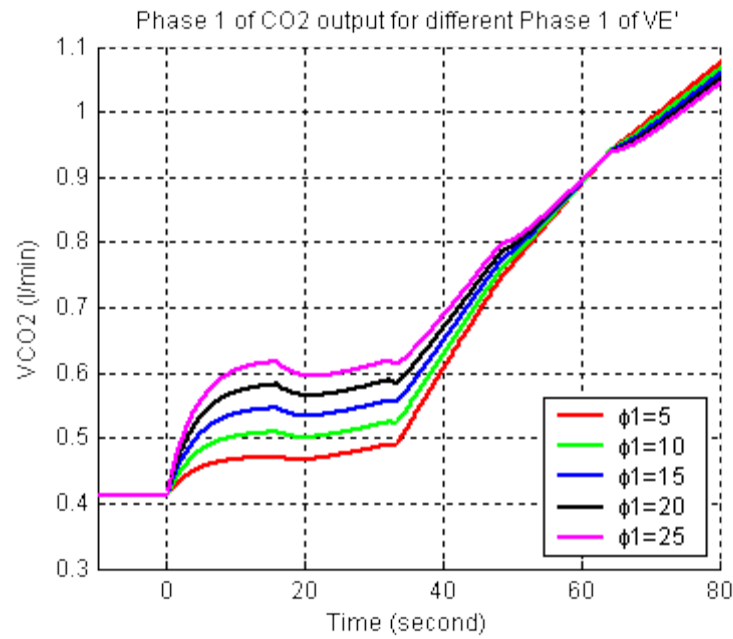


Figure 4.14. Kinetics of $V'\text{CO}_2$ for different phase-1 magnitudes of VE' . Numbers in the legend represent the percent magnitude of phase-1 compared to the steady state increase of VE' .

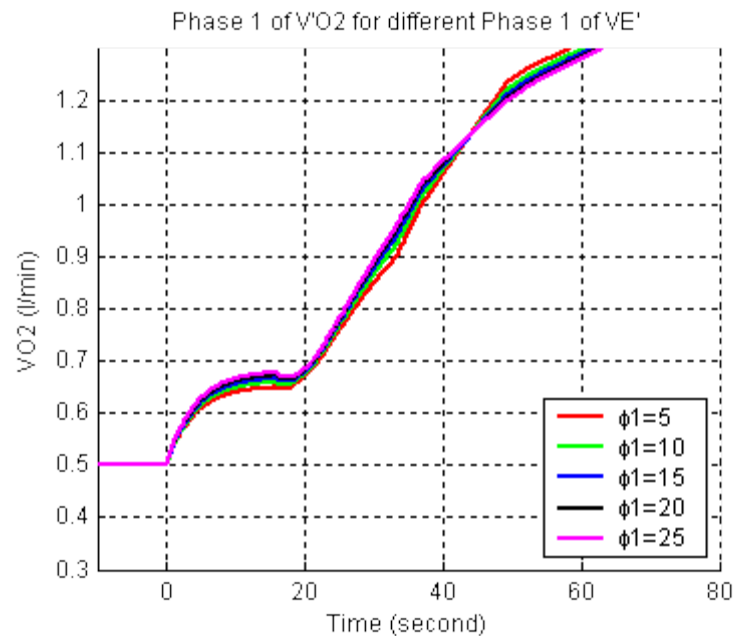


Figure 4.15 Kinetics of $V'\text{O}_2$ for different phase-1 magnitudes of VE' . Numbers in the legend represent the percent magnitude of phase-1 compared to the steady state increase of VE' .

4.8.4. Kinetics of blood gas variables during phase 2

Figure 4.16 shows an experimental result for the arterial oxygen content (CaO_2) and the mixed venous oxygen content (CvO_2) in ml/100 ml which was obtained from (Raynaud et al., 1973). These results suggest that CaO_2 decreases transiently during the first minute of exercise and CvO_2 keeps decreasing until it reaches a steady state.

Figure has been removed
due to Copyright restrictions.

Figure 4.16. Concentration of blood oxygen at the onset of exercise. This figure is from (Raynaud et al., 1973) with adaptation.

Another experiment by Grassi et al. (1996) investigated the blood gas variables in the muscle. The kinetics of oxygen concentration in the muscle venous ($CvMO_2$) (Figure 4.17) show a trend similar to that for the kinetics in arterial blood (Figure 4.16) but the value for the muscle vein is lower than that for mixed venous blood.

Figure has been removed
due to Copyright restrictions.

Figure 4.17 Muscle vascular gas content at the onset of exercise (Grassi et al., 1996).

Figure 4.18 depicts the simulation result for O_2 concentration in the artery, muscle venous and mixed venous blood. The figure shows that the values of the three variables are within the range that is set in Figure 4.16 and 17.

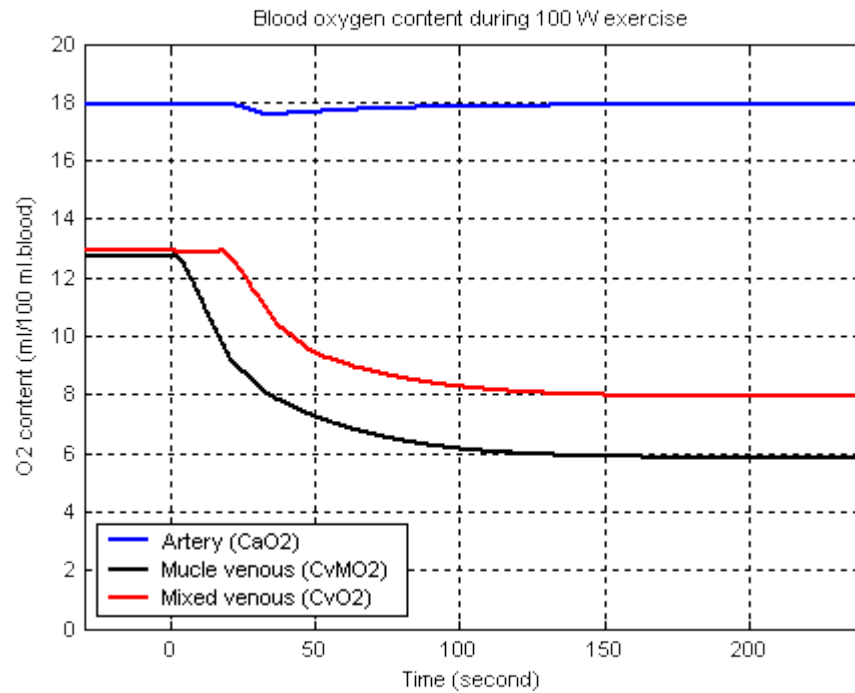


Figure 4.18 Simulation result for blood oxygen concentration in artery, muscle venous and mixed venous blood. Note that O₂ content is in ml/100 ml of blood.

4.8.5. Does muscle have capacity to store CO₂?

Figure 4.19 – 4.21 depict CO₂ output, RER and arterial PCO₂ for two simulation conditions: with and without muscle CO₂ storage. For the model without muscle CO₂ storage, the transient magnitudes of V'CO₂ and RER are slightly higher than the simulation result of the model with muscle CO₂ storage. Arterial PCO₂ for model without muscle CO₂ storage shows a significantly higher peak value than the result for the model with muscle CO₂ storage. These results are discussed in Section 4.9.4.

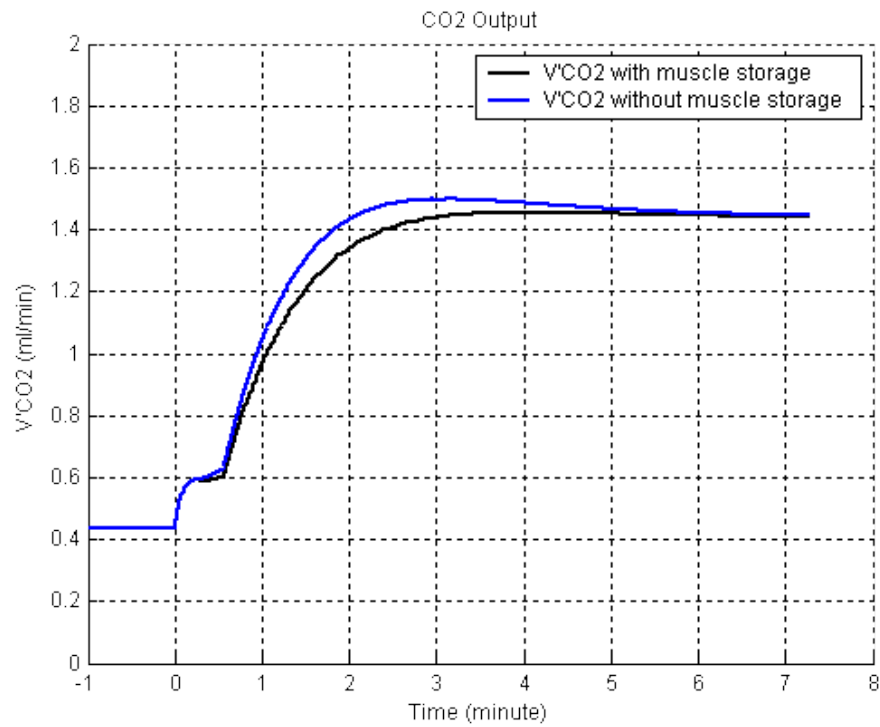


Figure 4.19. CO₂ output for two simulation conditions: with and without muscle CO₂ storage. Model without muscle CO₂ storage has a slightly faster kinetics in terms of $\dot{V}CO_2$ with a small overshoot.

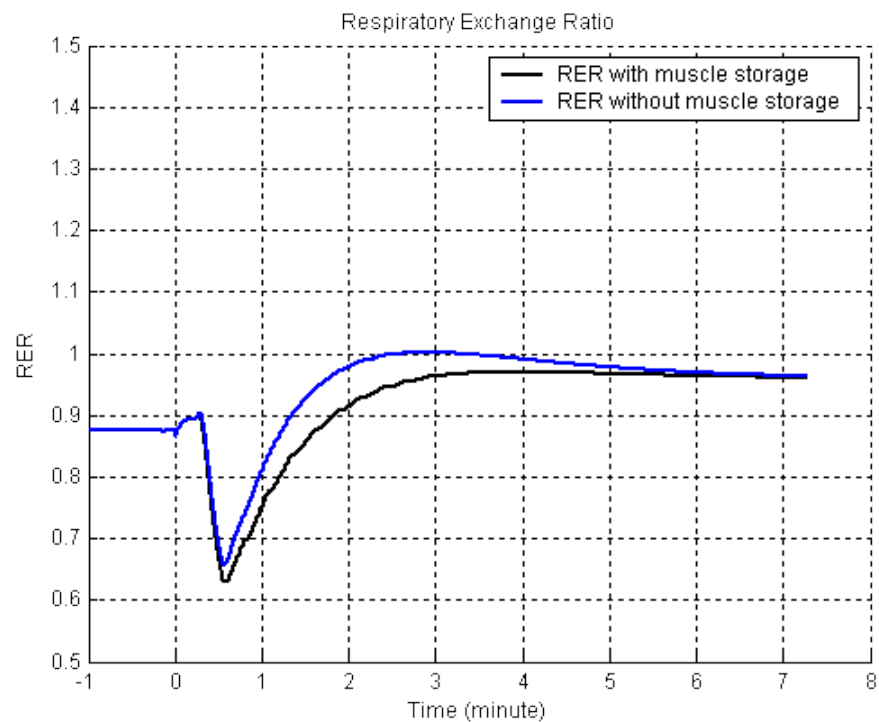


Figure 4.20. RER for two simulation conditions: with and without muscle CO₂ storage. The model without muscle CO₂ storage has a slightly higher RER during phase 2.

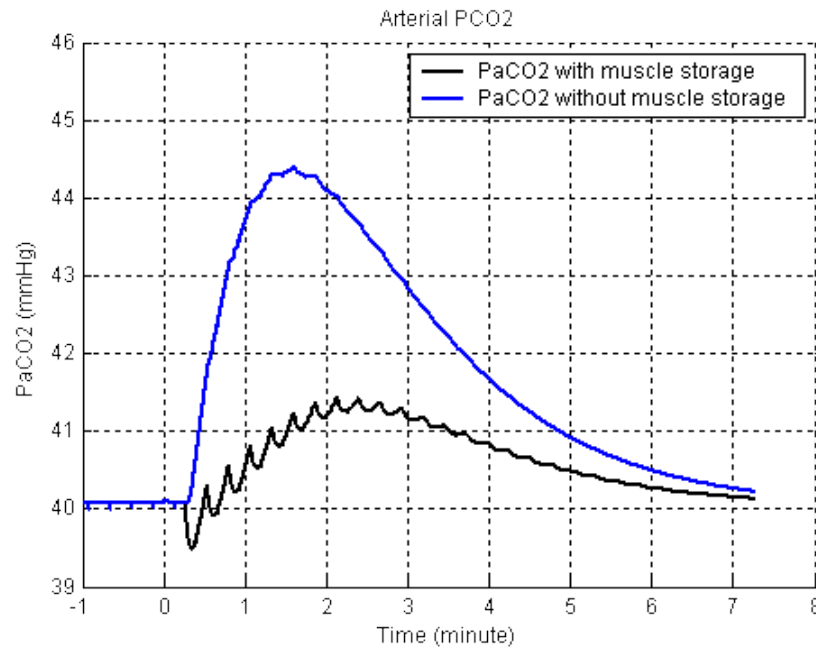


Figure 4.21. Arterial PCO₂ for two simulation conditions: with and without muscle CO₂ storage. In the model without muscle storage capacity, PaCO₂ level increases considerably during phase 2.

4.9. Model Assessment and Discussion

Much experimentation has been carried out over a long period of time on human subjects doing exercise so there is much information available in the physiological and sports science literature that can be used to validate a model. However, validation of a physiological model which comprises many equations, variables and parameters such as the one being developed in the course of this work is never straightforward. Most of the experimental results are presented in graphical form which limits the interpretation and types of comparison possible. In most cases, comparisons of the model behaviour and the measured results are best established in terms of similarities or otherwise in terms of the trends of selected variables during exercise. A few experimental results may be presented in the form of numbers but usually these have a wide range of values so that when such results are included as model parameters, for example, care must be taken so that the selected values agree with other parameter values which might have some correlation with the quantity in question. For example, there is a quote in Section 4.4 that $\dot{V}O_2$ has a fundamental time constant of 55 ± 21 s and another quote relating to $\dot{V}E$ in subsection 4.3.2 suggests that it has a value of 50 - 100 seconds. Choosing $\tau_{VO_2} = 60$ s. and $\tau_{VE} = 50$ s. seems appropriate because they fall within the quoted ranges but this choice ignores the fact that there is a widely observed pattern that shows that the kinetics of $\dot{V}O_2$ is always faster than the kinetics of $\dot{V}E$ (Whipp et al., 1982).

There is not a single experiment which probes the whole set of variables and parameters that are present in the model, and probably there will be no such experiment

in the foreseeable future. An experiment with hundreds of measurements is possible with engineering systems, but an experiment with tens of physiological variables *in vivo* can be hard to carry out and may never be possible in some situations. In many cases, at a certain level of complexity, a physiological model can only be developed using assumed relationships and assessment of model quality and fitness for the intended purpose can only be approached using a limited number of measurements. It must always be recognised that unmeasured variables in the real system may differ significantly from those in the simulation and that any form of “validation” in terms of a specific chosen variable may lead to errors due to the fact that model uncertainties are not fully taken into account either in terms of the exactness of the value produced by the model or in terms of the experimental values. Therefore, it is often considered sufficient for validation purposes in physiological system modelling to assess whether a simulation result lies within an acceptable range of values and that the model has behaviour that is consistent with the trends and profiles of variables observed in experiments. This validation process leads to a limited form of pragmatic validation as described in Chapter 1.

4.9.1. General Impressions of the Model Behaviour

The responses of the model as presented in Section 4.8.1 show a general agreement with results found in publications.

Oxygen uptake and carbon dioxide output exhibit two-phase kinetics where the magnitude of phase 1 is small compared to the magnitude of the steady state increase, i.e. approximately 20% and 16% for $V'\text{CO}_2$ and $V'\text{O}_2$ respectively (see Figure 4.6 and 4.7). The simulation results for phase 1 magnitude of these two variables are within the range that is suggested from experiment by Whipp et al. (1982).

The kinetics of arterial PCO_2 and PO_2 are predictable from Equations (4.20) and (4.21) which are derived for an ideal lung. Arterial PCO_2 and PO_2 is generally unchanged during phase 1 and this can be achieved if the phase 1 increase of $V'E$ is proportional to the increase of $V'\text{CO}_2$ and the phase 1 increase of Q' is proportional to the increase of $V'\text{O}_2$ (see Section 4.9.2 for more details). Arterial PCO_2 increases slightly during phase 2 as a consequence of the slower kinetics of $V'E$ compared to $V'\text{CO}_2$. The arterial PO_2 , on the other hand, decreases significantly because the response in terms of $V'\text{O}_2$ is much faster than for $V'E$. Approaching steady state conditions, both PaCO_2 and PaO_2 slowly return to a level at or near the base line value. Such transient responses have been observed by many investigators (Lamarra et al., 1989; Whipp, 1983; Whipp and Ward, 1980). Some of investigators, on the other hand, have obtained different results for PaCO_2 and have observed a transient decrease (Brice et al., 1988; Forster et al., 1986), which relates to hyperventilation (Powers et al., 1987). However, if hyperventilation does occur during the phase-2 period, the $V'E$ time constant should be small, even smaller than the

time constant of $V\dot{C}O_2$, which is not the case. For the steady state condition all the investigators agree that $PaCO_2$ and PaO_2 are generally maintained near their base line values.

Experiments have shown that mixed venous PCO_2 increases and PO_2 decreases with the increase in exercise work rate (Sun et al., 2001; Raynaud et al., 1973; Cruz et al., 1969). There has been no attempt to model the kinetics of mixed venous gas so quantitative assessment cannot be made to compare the simulation and experimental result of mixed venous kinetics.

The kinetics of lactate and bicarbonate concentration shows the occurrence of early acidosis. This is discussed in more detail in Section 4.9.5.

4.9.2. Relationship between the $V\dot{C}O_2$, $V\dot{O}_2$, $V\dot{E}$ and Q' variables during phase 1

As described in Section 4.2 the cardiac output and blood flow to exercising muscle increase rapidly during the early period of exercise which is termed the phase 1 period. Ventilation also increases during phase 1 but to a less marked extent compared with the increase of blood flow during the same period. Considering the mechanisms involved, the phase 1 increases of these two variables are independent of each other and the duration is likely to be different. On the other hand, the arterial partial pressures of oxygen and carbon dioxide do not change during phase 1 because changes that take place in muscle have not by then reached the artery (see Figure 4.8 and 4.9).

Simulation results for the oxygen uptake and carbon dioxide output as depicted in Figure 4.6 and 4.7 shows that these two variables have an initial phase 1 increase. Simulation tests have been performed to check whether phase-1 kinetics of $V\dot{O}_2$ and $V\dot{C}O_2$ are correlated with the kinetics of cardiac output and ventilation during the same period. It can be observed from Figure 4.12 and 4.13 that an increase in the magnitude of cardiac output during phase 1 increases the magnitude of $V\dot{O}_2$ but does not change the magnitude of $V\dot{C}O_2$. Indeed, this has been quantitatively supported by results from an experiment showing that $V\dot{O}_2$ kinetics during phase 1 are dependent on blood flow or Q' (Lador et al., 2006; Barstow and Mole, 1987). On the other hand, Figure 4.14 and 4.15 suggest that the kinetics of $V\dot{C}O_2$ during phase 1 are dependent on the kinetics of ventilation but the response for $V\dot{O}_2$ is not.

4.9.3. Kinetics of blood gas variables during phase 2

Section 4.8.4 presents simulation results of the kinetics of oxygen content in the artery, mixed venous blood and the muscle vein (Figure 4.18). Experimental results from the published literature are also depicted for arterial and mixed venous O_2 content (Figure 4.16) and muscle venous O_2 content (Figure 4.17). Visual comparison of these graphical

results suggests that the model is able to reproduce simulated results for blood gas variables that correspond to those found in experimental investigations.

4.9.4. Does muscle have capacity to store CO₂?

During steady state conditions, the amount of carbon dioxide produced at the mouth is statically dependent on the respiratory quotient (RQ) of muscle and other tissues. During transient conditions, on the other hand, the CO₂ produced depends not only on the RQ but also on the transport delay and the storage capacity for O₂ and CO₂. The transport delay shifts the moment when V'CO₂ increases or decreases compared to the time of V'O₂ changes. Storage capacity affects the kinetics of V'O₂ and V'CO₂. A step increase in energy requirement at the onset of exercise does not increase V'O₂ stepwise. One reason for this is the availability of O₂ stored in myoglobin. The capacity of blood to store CO₂ is higher than the capacity to store O₂ so that the kinetics of V'CO₂ are slower than for V'O₂.

One question raised here is whether the slowing of the V'CO₂ kinetics is solely due to the blood CO₂ storage or whether muscle has significant capability to store CO₂. The reason for the query is because in the past there were suggestions that muscle may not have the enzyme called carbonic anhydrase (Cherniack and Longobardo, 1970; Fowle et al., 1964; Farhi and Rahn, 1960; Nichols, 1958) so that the CO₂ storage capacity is low. Simulation tests have been carried out for one case where the muscle is set to have a certain level of CO₂ storage capacity and for another case where the muscle is not capable of storing CO₂. The results are depicted in Figures 4.19 – 4.21.

The CO₂ output and the RER (see Figures 4.19 and 4.20) do not differ very much between the two simulation conditions. However, in the case of the model without muscle CO₂ storage V'CO₂ and RER are higher during phase 2 which indicate that CO₂ is more quickly driven out from the lung. Because experimental evidence suggests a wide range of kinetics of V'CO₂, the differences in the two simulation results are not sufficient to allow one to judge which condition is more likely to be true.

Figure 4.21 depicts the arterial PCO₂ for simulation conditions with and without muscle CO₂ storage. During phase 2, in the model without muscle CO₂ storage, PaCO₂ increases greatly peaking at 44 mmHg but in the model with muscle CO₂ storage it increases only slightly. Experimental results suggest that the increase of PaCO₂ during exercise transients is small which hints that the model with CO₂ storage is more acceptable.

Past experiments which led to suggestions that muscle might not have enzyme carbonic anhydrase were based on investigations showing that muscle is very slow in terms of the increase of CO₂ content after a long period of CO₂ inhalation or exposure to a high atmospheric concentration of CO₂. However, later studies proved that muscle indeed

has carbonic anhydrase (Geers and Gros, 2000) but the functionality of the enzyme is affected by muscle contraction. Furthermore, CO₂ transport in muscle depends not only on the diffusion rate but also on transport mechanism of H⁺/Ca²⁺ (during muscle relaxation), neuromuscular energetic, and facilitation (Henry, 1996). It seems that past experiments failed to reach the correct conclusion because some mechanisms might still have been unknown then.

4.9.5. Early acidosis

As will be described in Chapter 5, when the ATP turn-over rate exceeds the amount of ATP produced by aerobic catabolism, lactate is produced. At the onset of exercise, muscle oxygen extraction is still small and not sufficient to support a full aerobic catabolism so there is a significant production of lactate and hydrogen ion during a short period until oxygen extraction increases to a steady state level. Lactate production is a marker which indicates metabolic acidosis in the muscle. Acidosis that occurs during this period is known as early acidosis.

Several organs within the human body have the ability to consume lactate so that lactate accumulation is limited. When lactate production has declined, lactate concentration decreases to a level close to that before the start of exercise.

Bicarbonate is the major, but not the only, buffer in the blood system. When hydrogen ions from lactate-proton co-transport enter the blood stream, most of the protons react with bicarbonate according to Equation 2.17. The consequence is that when lactic acid increases then bicarbonate concentration decreases, and vice versa.

Figure 4.10 demonstrates that the model is able to show the behaviour of early lactic acidosis and the associated buffering. Although muscle lactate production peaks approximately 30 seconds after the onset of exercise and decreases to a level near that of the resting condition after 90 seconds (Grassi, 2003), arterial lactate concentration keeps increasing for more than four minutes because lactate-proton co-transport and blood transport involve a significant delay before lactate ions produced in the muscle reach the artery. This is consistent with experimental evidence which shows that after heavy exercise ceases the blood lactate concentration is still high and is still increasing while other variables are on the way to recovery (Kowalchuk et al., 1988). The kinetics of lactic acid are slow compared to the kinetics of respiratory gases, due to the limited speed of release and consumption of lactate. However, the peak time of arterial lactate kinetics differs widely among subjects (see e.g. Figure 5.1) which ranges from 3 – 10 minutes (Freund and Zouloumian, 1981; Hubbard, 1973).

The decrease of bicarbonate concentration is less than the increase of lactic acid concentration because a portion of the hydrogen ions from lactic acid is buffered by other buffering systems, i.e. phosphate and haemoglobin.

Figure 4.11 shows the kinetics of pH during early exercise. For the first few seconds (approx. 20s) the arterial and mixed venous pH values do not show an obvious change from the base line levels. Thereafter, pH shows a temporary increase followed by a steady decrease towards a steady state level. This behaviour is clearly observable in various experimental results, e.g. at (Wasserman et al., 1997; Stringer et al., 1992; Casaburi et al., 1989b), especially when the data collection involves taking samples at short intervals during the transient period (phase 1 and phase 2).

4.10. Summary

The development of a model for condition below lactate threshold has been described. The structure is simpler than the SBC model described in chapter 3 but many formulations change. Cardiac output and ventilation are modelled as biphasic and have a first-order exponential fundamental component. Blood pH is calculated using Siggaard-Andersen nomogram. The simulation result shows a general agreement with results found in publication.

Chapter 5

Model for Lactate Metabolism

This chapter describes lactate metabolism. A model for lactate metabolism is developed which is suitable in form to incorporate as an integral part of the general model. The lactate model focuses on the reproduction of the kinetics of arterial lactate concentration during exercise. The chapter starts with physiological description of lactate metabolism. The model and parameter values are discussed. Simulation results are then presented and discussed.

5.1. Lactate metabolism

Lactate is produced when pyruvate acquires two hydrogen ions. In normal aerobic metabolism, pyruvate is broken down into carbon dioxide and water but an amount of pyruvate is always converted to lactate in an equilibrium mechanism by which the ratio of lactate to pyruvate concentration is maintained constant. Lactate production is increased during exercise following the increase of pyruvate production and a quantity of both species flow into the blood stream which increases their concentration in blood (Wasserman et al., 1985). When anaerobic metabolism takes place, a large amount of pyruvate converts into lactate so that lactate concentration becomes higher, resulting in a change that takes the system away from the equilibrium condition. It has been observed that the ratio of pyruvate to lactate concentration is generally constant during rest and moderate exercise, and it drops during conditions with anaerobic metabolism (Rausch et al., 1991; Bertram et al., 1967).

Anaerobic metabolism produces ATP, which can be used to help deal with the load under exercise conditions. Increased anaerobic metabolism, which is indicated by lactate production, helps to reduce the amount of energy required from aerobic metabolism which means, in turn, a reduction of the oxygen requirement. The amount of oxygen conserved by lactate production may be estimated by multiplying the increase of lactate concentration in blood by the litres of body water, and the amount of oxygen which is conserved by the acceptance of 2 hydrogen ions by the pyruvate molecule (11.2 ml O₂/mEq lactate) (Wasserman et al., 1967). This may be expressed quantitatively through the equation:

$$\text{ml O}_2/\text{min} = \Delta \text{ lactate/litre per min} \times \text{body water volume} \times 11.2$$

As the site where lactate is produced, exercising muscle has a higher lactate concentration level ([La]) than blood. At the same time, blood [La] is likely to be higher than the lactate concentration of non exercising muscle and other tissues. However, exact measurement of tissue lactate concentration is not easy because it needs a biopsy which is a highly invasive procedure. Moreover, muscle has two groups of fibres with fast-twitch fibres tending to produce lactate and slow twitch fibres tending to consume lactate and a

biopsy may result in a sample containing both groups so that determination of muscle [La] may not be simple.

Lactate concentration in arterial blood changes very little at moderate exercise although pyruvate production and muscle metabolism, in general, change significantly. This is because lactate production and consumption increase in a similar way at the same time. During heavy exercise, lactate production exceeds lactate consumption so that arterial [La] increases to a level several times higher than the resting value (see Figure 5.1) (Wasserman et al., 1967).

Figure has been removed
due to Copyright restrictions.

Figure 5.1. Lactate concentration in the artery during a step increase in work rate for moderate, heavy and very heavy exercise (Wasserman et al., 1967). Solid lines on each graph are average values.

The effect of exercise on lactate utilization has been observed by several investigators. Hubbard (1973) suggested that the same concentration of lactate injected into the body will be utilized more quickly when the subject is performing exercise than when the subject is at rest. Lactate uptake from blood into splanchnic tissues has been reported to rise progressively during exercise and this is associated with a rise in arterial lactate concentration (Ahlborg and Felig, 1982). Indeed, both the lactic acid production and utilization levels are higher in exercise than at rest even during moderate exercise. However, in moderate exercise there is no net increase in the difference of lactate production and utilization so that lactate concentration will generally be equal to or slightly higher than the resting value without sustained accumulation (Cabrera et al. 1999).

An experiment with radioactive lactate injection suggested that blood radioactivity decreases in a manner described by single exponential or double exponential curves (Hubbard, 1973). For the two-exponential model, the rapid exponential component has been interpreted as the result of at least two processes: distribution of the injected material throughout the lactate space and the lactate utilization. On the other hand, the slow exponential component is believed to be the result of lactate utilization alone. It was

suggested therefore that the model of lactate utilization can be represented by a single exponential.

The rise of lactate production during early exercise or during exercise of short duration may be regarded as an impulsive stimulus to the system of lactate metabolism and from this the system response may be predicted readily. Some experiments using such a stimulus have been conducted e.g. by Hubbard (1973) and Kowalchuk et al. (1988) and others. Hubbard suggests that the rise of arterial [La] during moderate exercise reaches a peak value in about 5 minutes. By means of an experiment involving 30s maximal exercise Kowalchuk et al. have obtained results that are apparently in line with Hubbard's suggestion that the peak time of the impulse response occurs in the period 3 – 6 minutes after exercise onset (see Table 5.6). On the other hand, Freund and Zouloumian (1981) observed that the arterial [La] peak value occurs in the range 5 – 10 minutes after exercise onset with higher exercise levels tending to show later peak attainment than the responses for lower exercise levels.

Freund and Gendry (1978) were in no doubt that the kinetics of arterial [La] after short strenuous exercise fits accurately with a description involving two exponentials. Further investigations have supported their original finding (Freund and Zouloumian, 1981; Zouloumian and Freund, 1981). Table 5.6 which is an excerpt from more recent work by Kowalchuk et al. (1988) suggests similar kinetics of arterial [La].

Table 5.6. Lactate concentration (mEq/l) after 30s maximal exercise and during recovery.

Data taken from (Kowalchuk et al., 1988)

	Rest	Minutes post exercise								
		0	0.5	1	1.5	2.5	3.5	5.5	7.5	9.5
Muscle La	6	-	47	-	-	-	30	-	-	26
Arterial La	1.2	6.3	9.6	12.2	13.5	13.9	13.8	13.8	12.3	12.3

When the exercise level is extremely high, the human body will finally reach exhaustion or a fatigue level at which it can no more withstand the work. The level of exhaustion may vary among subjects but the attainment can always be indicated by the high concentration of blood lactate produced in muscle. However, lactate concentration is not the limiting factor that contributes to exhaustion; rather it is the high concentration of muscle hydrogen ion (or proton) that affects and may paralyze metabolism (Robergs et al., 2004). The release of lactate from muscle to the blood within the mechanism of lactate-proton co-transport helps reduce proton concentration in muscle so lactate release prolongs the ability to sustain exercise.

5.2. Model of Lactate Metabolism

The model structure of lactate metabolism can be extracted from the respiratory model and is shown in Figure 5.2. The muscle block represents the exercising muscle and is both a lactate producer and consumer. The other tissues compartment consists of non-exercising muscle, the liver and other body parts and is a lactate consumer. Lactate production and consumption are influenced by exercise so these blocks of the model have exercise work rate (WR) as their input. The block labelled D is the circulatory delay which represents the time for the blood to move from the tissues to the heart or the lung. In the mixed venous compartment the blood from tissue compartments is mixed so the concentration of lactate here will lie between the values for the muscle and other tissues compartment. It should be noted that heart can be a lactate consumer (Gutierrez et al., 2005; Cabrera et al., 1998) but its role may be included basically in the other tissues compartment and the heart & lung block has been included in the model structure simply to indicate the circulatory function.

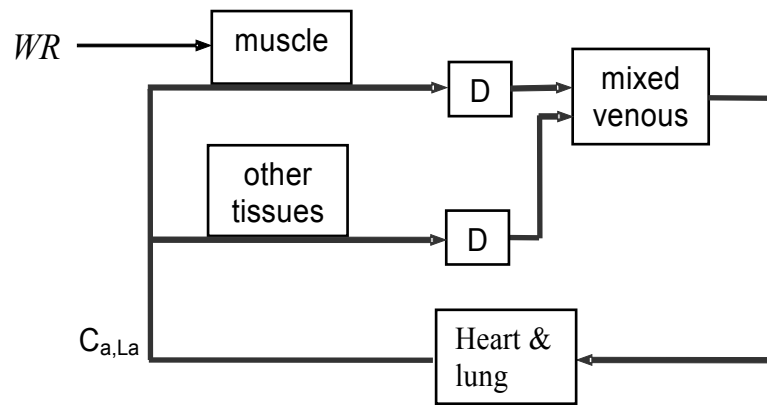


Figure 5.2. Structure of the model for lactate metabolism; the muscle block represents the exercising muscle; the other tissues block consists of non-exercising muscle, the liver and other body parts; block labelled D is circulatory delay; WR is work rate; $C_{a,La}$ is arterial [La].

The other tissues compartment is assumed to be a producer and consumer of lactate. The mass balance equation for lactate metabolism in the other tissue compartment is modelled using the following first order linear equation:

$$V_o \frac{dC_{o,La}}{dt} = P_{o,La} - U_{o,La} + \dot{Q}'_o (C_{a,La} - \sigma_{La} \cdot C_{o,La}) \quad (5.1)$$

where V_o is the effective volume of lactate contained in other tissues, $C_{o,La}$ and $C_{a,La}$ are lactate concentrations in other tissues and artery respectively, $U_{o,La}$ is the lactate utilization factor and \dot{Q}'_o is the other tissues blood flow. The quantity σ_{La} is the blood tissue partition coefficient for lactate. This partition coefficient represents how much lactate can be transported between the blood capillary and the relevant compartment and, in this case, is

equal to $C_{v_o,La}/C_{o,La}$ where $C_{v_o,La}$ is the venous concentration in the other tissues. Lactate production in the muscle tissue block is constant, which represents a steady state condition unaffected by exercise. Lactate utilization is proportional to lactate concentration which is consistent with the idea that the kinetics of lactate utilization is described by a single exponential.

The mass balance equation for lactate metabolism in the muscle compartment follows the equation:

$$V_m \frac{dC_{m,La}}{dt} = P_{m,La} - U_{m,La} + \dot{Q}'_m (C_{a,La} - \sigma_{La} \cdot C_{m,La}) \quad (5.2)$$

where V_m is the effective volume of the muscle compartment, $C_{m,La}$ and $C_{a,La}$ are lactate concentrations in the muscle compartment and in the blood artery respectively, $P_{m,La}$ and $U_{m,La}$ are the production and utilization of lactate in the muscle compartment respectively and \dot{Q}'_m is muscle blood flow.

Equations (5.1) and (5.2) above are derived based upon the mass balance principle (see Appendix D), where the change of mass of a species is equal to the production and utilization of the species within a compartment and the movement of the species into and out of the compartment. Lactate transport into and out of the body tissues depends on a mechanism called proton-lactate co-transport and is represented as the third term in the equations. This modelling procedure is essentially similar to Fick's principle.

5.3. Parameter values

In equations (5.1) and (5.2), the volume of the muscle compartment is estimated using the information that total volume of muscle is 29.14 litres, volume of other tissue is 9.6 litres and blood volume is 5 litres (Saunders et al., 1980), where the total muscle volume is made up of exercising and non-exercising muscle. To estimate the effective volume of the exercising muscle which is required in equation (5.2), information in Table 5.7 is used.

Table 5.7. Muscle volume in kg of several body organs (Kida et al., 2006)

Average muscle volume (kg)	
Whole body	21.8 ± 2.8
Superior limb	1.3 ± 0.2
Inferior limb	4.9 ± 0.6
Thigh	3.0 ± 0.5
Crus	2.0 ± 0.3

Table 5.7 is extracted from Kida et al. (2006). Hence the total muscle volume is 29.14 litres or 21.8 kg and the exercising muscle volume (i.e. thigh) is 3 kg which implies that the thigh volume is $3/21.8 * 29.14$ or approximately 4 litres.

The total body tissue volume, not including blood, is $29.14 + 9.6 = 38.74$ litres which means that the volume of other tissues, including non exercising muscle, is $38.74 - 4 = 34.74$ litres.

Another parameter estimation process, which leads to a different result, is based on the observation that muscle density is a little less than 1.112 g/cm^3 (Ward and Lieber, 2005). Combining this information with the observation of Kida et al. (2006) suggests that a 3 kg thigh weight would represent a volume of $3 \text{ kg} / 1.112 \text{ g/cm}^3 \approx 2.70 \text{ l}$. Hence the exercising muscle volume would be 2.7 l and other tissues volume would be 26.7 l. Other estimation suggests that contracting muscle is 9 kg (Coyle et al., 1988), which leads to muscle volume = 7.5 l.

The partition coefficient for lactate is $\sigma_{\text{La}} = 0.55$, which is a value obtained from tests on muscle (Cabrera et al., 1998). According to the definition of partition coefficient, the venous [La] would always be lower than the tissue [La] and this is true for a lactate producer such as exercising muscle. For a lactate consumer, the reverse may be assumed to be true. Note that in the case of the lung, the alveolar O_2 concentration is generally assumed to be equal to the arterial concentration so would be parameterized with partition coefficient, $\sigma_{\text{O}_2} = 1$.

Many investigators have measured that the arterial lactate concentration at rest is 1 – 2 mEq/l (Wasserman, 1994; Kowalchuk et al., 1988). Some others suggest an approximate value in the range of 0.6 – 1.1 mEq/l (van Hall et al., 2003; Jorfeldt et al., 1978). During moderate exercise, the arterial [La] increases slightly or does not increase at all. At the steady state of heavy exercise, the arterial [La] can yield a value beyond 9 mEq/l. In the model, the value of arterial lactate concentration for unloaded exercise conditions is put at 1.2 mEq/l.

Lactate production and utilization rates are not known and have never been measured in vivo in human (Cabrera et al., 1999). However some researchers suggest that, both at rest and during exercise, lactate is removed from the blood and metabolized and that during exercise this metabolism is much more rapid (Hubbard, 1973). Even though lactate metabolism is more rapid during exercise, the concentration of lactate in blood tends to increase which indicates that its production is more rapid.

Jorfeldt et al. (1978) state that lactate release to blood is proportional to muscle lactate concentration up to 4-5 mmol/min and for levels above this concentration value the relationship levels off. Van Hall et al. (2003) agree with Jorfeldt et al. but they imply that lactate release may increase to a level higher than 10 mmol/min and, if calculated against muscle mass, the critical level is approximately 3-4 mmol/min/kg. In addition van Hall et al.

suggest that lactate uptake from blood has a strong correlation with lactate delivery (i.e. arterial lactate concentration x blood flow to the corresponding tissue).

Using the available information, the lactate production in the muscle compartment of the model is set to increase with work rate. The lactate utilization in the muscle compartment is also set to increase with the work rate and with the muscle lactate concentration while the lactate utilization in the compartment representing the other tissues increases with the lactate concentration in that compartment. Equation (5.3) describes these relationships in quantitative terms, where $k_1 - k_5$ are constants.

$$P_{m,La} = k_1 \times WR + k_2$$

$$U_{m,La} = k_3 \times WR + k_4 \times C_{m,La} \quad (5.3)$$

$$U_{o,La} = k_5 \times C_{o,La}$$

5.4. Simulation Results

Figures 5.3 – 5.7 depict the results of investigations carried out using the simulation model for lactate metabolism. For conditions of unloaded exercise, the arterial lactate concentration reaches a steady-state at 1.24 mEq/l and at the same time the concentration in muscle and the muscle vein are 2.35 mEq/l and 1.29 mEq/l respectively (Figure 5.3). Compared to the experimental data presented in Table 5.6, the simulation result gives a good value for blood lactate concentration but it displays a significant discrepancy for muscle lactate concentration. Another contrast result for muscle lactate concentration is presented by Cabrera et al. (1999) who suggest a value of 1.6 mEq/l. Therefore, it has been decided that the current lactate model is limited to obtain correct values of blood lactate concentration ignoring the values for muscle and other tissues compartments.

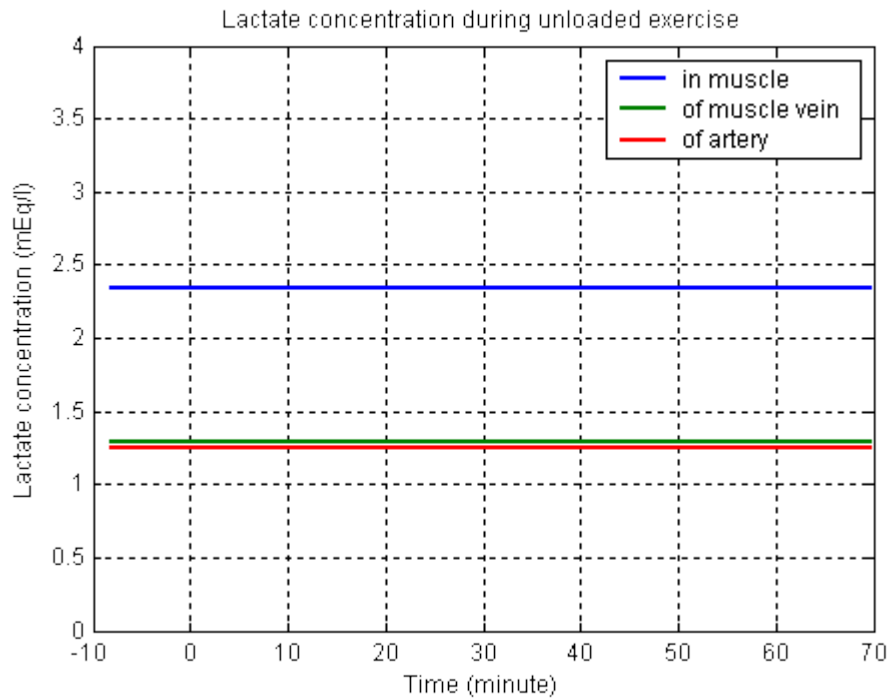


Figure 5.3. Lactate concentration in blood and muscle compartment during unloaded exercise.

Figure 5.4 shows the simulation result for moderate exercise at 100W. The lactate concentration in all the compartments increases slightly. For example, the arterial [La] reaches a steady state value of 1.39 mEq/l and the muscle [La] increases to 2.65 mEq/l.

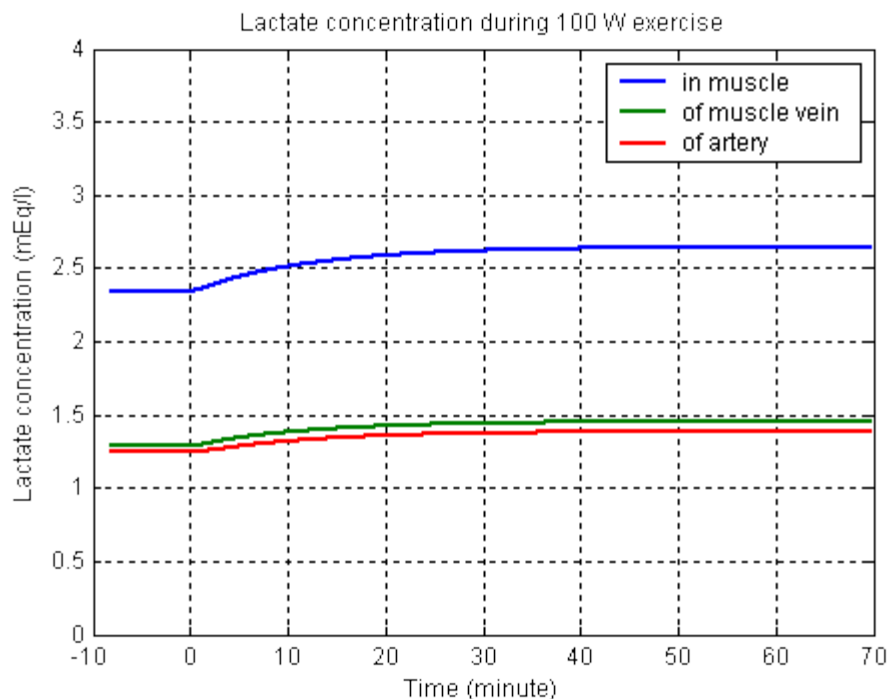


Figure 5.4. Lactate concentration in blood and muscle compartment during 100 W exercise starting at time = 0 min on the base line of unloaded exercise.

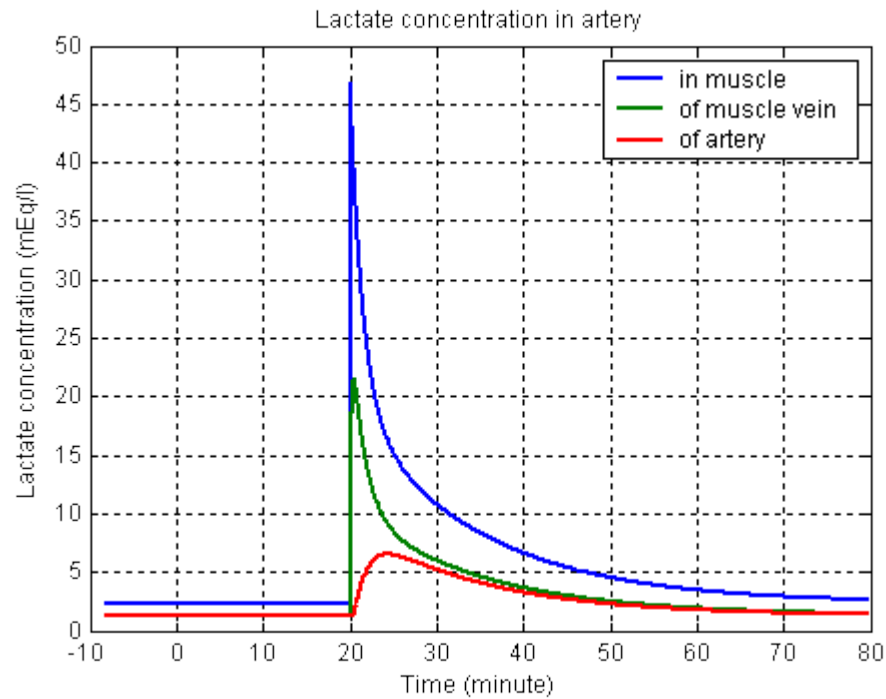


Figure 5.5. Lactate concentration in blood and muscle compartment during unloaded exercise. At time = 20 min, muscle lactate concentration is suddenly increased to 47 mEq/l.

Figure 5.5 shows the simulation result if muscle lactate concentration is immediately increased to 47 mEq/l from the baseline of unloaded exercise. Muscle conditions of this kind have been observed in an experiment by Kowalchuk et al. (1988) when 9 subjects underwent maximal exercise for 30 seconds. The muscle [La] drops quickly for the first 5 minutes, decreases more slowly for the next 20 minutes and then declines slowly. On the other hand, the arterial lactate keeps increasing for the first 5 minutes, peaking at 5.3 mEq/l above the base-line level. In an enlarged view, as depicted in Figure 5.6, it is clear that the decline of arterial [La] follows a pattern that is similar to the decline of muscle [La].

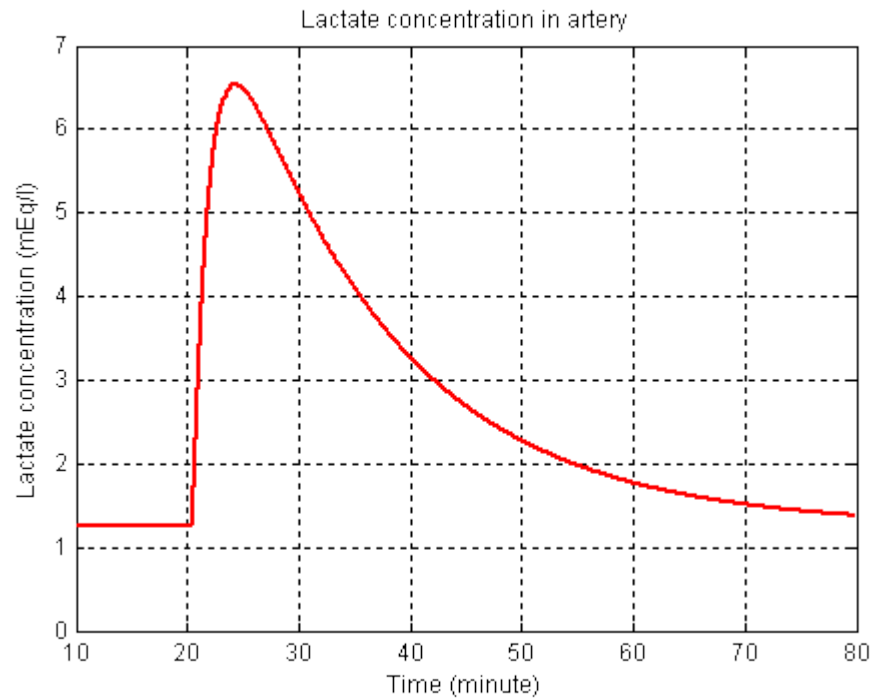


Figure 5.6. Arterial [La] after a sudden increase of muscle [La] at the 20th minute on the base-line of unloaded exercise.

Figure 5.7 shows the simulation result if muscle lactate concentration is increased to 47 mEq/l at 20th minute from the base line of moderate exercise. Compared to the result in Figure 5.5, it may be seen in this case that the muscle [La] drops more quickly during the first few minutes of the response but after the 50th minute the results do not show significant differences. In the first 5 minutes, the arterial [La] increases more slowly reaching a peak at 3.8 mEq/l above the base-line level.

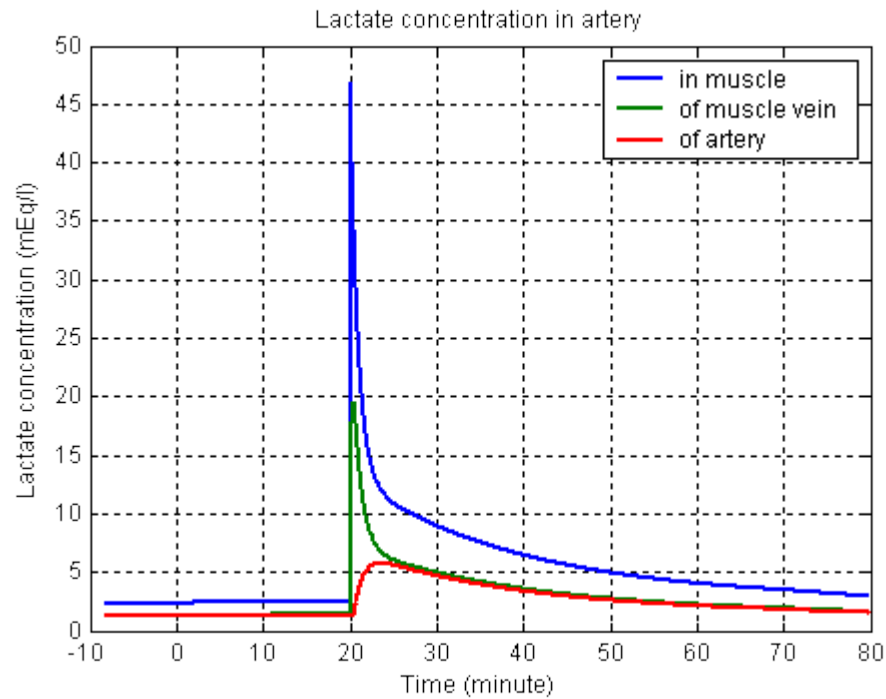


Figure 5.7. Lactate concentration in blood and muscle compartment during 100 W exercise. At time = 20 mins, muscle lactate is suddenly increased to 47 mEq/l to imitate 30s maximal exercise.

5.5. Discussion

Modelling lactate metabolism is an important part in modelling the respiratory control system during exercise, both for the moderate and higher intensity domains. In the moderate intensity domain, the inclusion of lactate metabolism enhances the accuracy of the model if the transient condition at the onset of exercise is of importance. For the higher intensity domain, the model of lactate metabolism is required to calculate acidosis. This enables the estimation of blood bicarbonate deformed in buffering and the prediction of hyperventilation which, in turn, increases the carbon dioxide output at the mouth.

The performance of the current model of lactate metabolism is constrained so the objective of the modelling has been limited to the estimation of the level of acidosis and the kinetics of lactate in the blood artery during exercise and not to calculate other lactate variables involved, such as the lactate concentration in muscle, the lactate release or uptake during exercise, etc. Hence the discussion will focus on how to produce an appropriate form of response in terms of the arterial lactate concentration. Note that the mixed-venous $[La]$ is assumed to be equal to the arterial $[La]$.

The concentration of arterial lactate is approximately 1-2 mEq/l at rest and may increase very slightly at moderate work rates (Wasserman et al., 1967). With the parameter values applied in the model, the simulation results for the steady state condition in Figure 5.3 – 5.4 agree with this statement.

The simulation results shown in Figures 5.5 – 5.7 suggests that the attainment of the peak value of arterial $[La]$ agrees with experiments such as those of Kowalchuk et al.

(1988) and Hubbard (1973) which show that the arterial lactate increase peaks about 3 – 6 minutes after the onset of exercise. Results from experiments by Wasserman et al. (1967), as shown in Figure 5.1, give slightly different figures, suggesting that the arterial [La] peaks about 5 – 10 minutes after the onset of moderate and heavy exercise.

Among the investigations that have been carried out so far, it is probable that the one by Freund and Zouloumian (1981) is the most accurate in that data were taken every 10 or 30 seconds. With such precision, their data are very useful in describing more accurately the kinetics of blood lactate concentrations within the investigated conditions. Figure 5.8 shows one of their experimental results in terms of the lactate concentration in the brachial artery before, during and after a short maximal exercise. The figure shows that after exercise ceases the arterial [La] still increases by 5.27 mEq/l before starting to decline. After approximately 60 minutes, the lactate level has declined to a level close to the base-line value. Comparing this experimental result with the simulation result in Figure 5.6, it is observable that the results show several agreements. In the simulation, where the muscle [La] is increased to a value achievable during maximal exercise, the arterial [La] continues to increase by 5.34 mEq/l after the exercise ceases. By 60 minutes, the arterial [La] has declined to a level close to base line value. Both results also show the same pattern of lactate kinetics in which the arterial [La] decreases exponentially.

Figure has been removed
due to Copyright restrictions.

Figure 5.8. Arterial [La] after 3 minutes maximal exercise. At the end of exercise arterial [La] has reached a level of 5.29 mEq/l; the arterial [La] peaks at 10.56 mEq/l (Freund and Zouloumian, 1981).

Assuming that a short period of maximal exercise can be regarded as an impulsive stimulus of lactate metabolism, the kinetics of arterial [La] closely resemble the response of a second order linear systems. Indeed, Freund and co-workers have described the arterial [La] kinetics as involving a double exponential. They fit the response into a model of a two tank system in which one tank represents “muscle space” and the other tank represents “other space” which includes blood and other tissues.

As depicted in Figure 5.2, changes in arterial [La] depends on the changes of lactate production and utilization in muscle and the other tissue compartment. Assuming that the heart and lung do not significantly produce or consume lactate, there are two possible conditions that generate the kinetics of arterial [La]. Firstly, the kinetics may originate from a combination of tissue compartments and the blood which is similar to the two-tank model proposed by Freund and co workers. The muscle compartment is regarded as the first tank and the blood is regarded as the second tank. The other tissue compartment may only be regarded as the outflow of the second tank. The implementation of this approach using the structure shown in Figure 5.2 necessitates the assumption that blood cells have a significant role in lactate storage. Indeed, the blood volume (i.e. 5 litres) is large enough compared to the thigh muscle volume (2.7 litres) and blood cells comprise approximately 45% of the total volume which means the volume of blood cells that may be involved in lactate metabolism is about 2.25 litres. The heart and lung might be included in the second tank because they are also lactate producers and consumers considering that these two organs work more heavily during exercise, (see e.g. Gutierrez et al. 2005).

Secondly, the kinetics of arterial [La] may originate from muscle and other tissues compartments where mixed-venous blood has a passive role to blend the venous blood from the two compartments. In this approach, the two exponential kinetics of arterial [La] must have come from the muscle itself where other tissues compartment in lactate storage and as lactate producer and consumer.

To establish which of these approaches is more likely to be correct, an experiment needs to be devised to acquire data at the femoral vein and artery that is detailed enough to enable an accurate description of the lactate kinetics at that point compared to the kinetics at the artery. At the moment, the rough data available leads to contradictory inferences. Hermansen and Vaage (1977) for instance suggest that there can be discrepancy between [La] in the artery and in the femoral vein during exercise but experimental results by Bonen et al. (1998) are not consistent with this. More detailed data like those acquired by Freund and co-workers will allow more reliable comparisons between the femoral venous [La] and the arterial [La] and will hopefully contain phase difference which may not be observable using sparse data. Significant differences in terms of the peak time (i.e. phase difference) and the peak value would support the first approach while insignificant differences would give more credibility to the second approach.

The model does not, at present, incorporate any limitation to the lactate release from the muscle compartment. This is inconsistent with the suggestion by Jorfeldt et al. (1978) that the lactate release levels off at 4-5 mmol/min. However, their suggestion is apparently in contradiction with other investigators. For example, a simulation test using

model parameter values to give maximal lactate release at 5 mEq/min gives much slower and lower response in terms of arterial [La] which peaks at 3 mEq/l about 18 minutes after the onset of exercise, which is inconsistent with many of the experimental results quoted in previous paragraphs. Moreover, the model with maximal lactate release results in a linear shape of arterial [La] which does not agree with experimental results by Freund and co-workers. In addition, an experiment has presented values of lactate release up to 20 mmol/min (Wasserman et al., 1997). It appears that Jorfeldt's calculation of lactate release involving multiplication of the femoral arterial and venous difference (v-a diff) of lactate concentration and the leg blood flow may not have achieved a good result because lactate transport is relatively slow compared to the blood flow. This means that the lactate v-a diff value will always be close to zero. As such, the calculation will generate a large relative error. Such a calculation may allow prediction of qualitative trends of lactate metabolism but may not give a sound quantitative result.

5.6. Summary

Blood lactate concentration is a marker of metabolic acidosis occurred during exercise. The model of lactate metabolism is able to reproduce a double exponential response for blood lactate concentration and this is in agreement with experimental evidence found in literatures. However, the value for muscle compartment is still unrealistic.

Chapter 6

Model of Respiratory System for Conditions above the Lactate Threshold

This chapter describes the development of the general model that applies for exercise conditions above the lactate threshold. It provides description of several parameters and variables that show significant changes during exercise above the lactate threshold, i.e. the muscle energetics, oxygen consumption, cardiac output, CO₂ production, acidosis, fibre recruitment, and hyperventilation. Simulation results are then presented and discussed.

6.1. Model structure

The structure of the model for conditions above the lactate threshold does not differ from model structure for moderate exercise condition depicted in Figure 4.1 which is described in Section 4.1. However, the profile of the respiratory system has marked differences when exercise work rate exceeds the lactate threshold.

Above the lactate threshold muscles extract less oxygen than that is required so that some amount of ATP has to be regenerated anaerobically producing lactate. Muscle oxygen consumption is higher than predicted by the profile below lactate threshold, which is related to the policy of muscle fibre recruitment. Cardiac output starts to level off when it approaches maximal value. CO₂ production gets additional components from hyperventilation and buffering mechanism, which serves to reduce metabolic acidosis.

6.2. Energetics of the muscle

During exercise, muscles have to overcome the effects of external loads by contracting their fibres. For that purpose, muscle gets energy from the breakdown of ATP (adenosine tri-phosphate) which is available in its cells. Another energy reservoir, Phosphocreatine (PCr), is also available in the muscle cells, at a level two or three times higher than the concentration of ATP. The PCr energy supply can be used to resynthesize ATP so that in overall, the muscle PCr and ATP can provide maximal muscle power for a period of 10 to 20 seconds (Grassi, 2003; Teschl, 1998).

Aerobic metabolism does not wait for the ATP and PCr to be fully depleted before it starts to resynthesize both species. Investigation using ¹H Magnetic Resonance Spectroscopy suggests that myoglobin is deoxygenized within a 20 s time frame after the onset of exercise (Richardson et al., 1995). Furthermore, not long after exercise onset, muscle starts to absorb oxygen to support oxidative phosphorylation to provide phosphate for the resynthesis of ATP in muscle cell mitochondria. There are different views about the initial response of muscle oxygen consumption. Some suggest that there is a slight delay (of the order of 2s) before muscle oxygen uptake (Q'O₂) starts to increase and at 25s it reaches half of its peak value (Bangsbo et al., 2000). Others suggest that on average there is a slight initial increase of Q'O₂ within 10-15 s before it shows a more significant rise with an exponential fundamental component (Grassi et al., 1996). Individual data sets

either show a slight delay or a slight increase of $\dot{V}O_2$ as depicted in Figure 6.1. The dominant exponential increase of the response has also been suggested by many other investigators, e.g. (Mahler, 1985).

Figure has been removed
due to Copyright restrictions.

Figure 6.1. Two samples of individual data taken during cycle ergometer exercise at a level 50W less than the ventilatory threshold; ● muscle O_2 consumption, ○ alveolar O_2 uptake (Grassi et al., 1996).

The available energy stored in the muscle in the form of ATP and PCr together with the energy provided by aerobic metabolism is not always sufficient to balance the work load. A situation of this kind can occur, for example, at supra maximal work load, i.e. the work load which needs more oxygen than the maximum amount of O_2 that body can uptake and transport to muscle. In addition, at the start of exercise at a level below the maximal exercise level, when energy requirement suddenly increases, the level of oxygen concentration in muscle is not sufficient to be used in burning metabolic fuel to form ATP.

When aerobic metabolism does not meet the requirements for more ATP, anaerobic metabolism takes place. As described in Section 2.2, during aerobic metabolism each glycogen molecule can be oxidized to produce 36 ATP molecules. This process involves the breakdown of each glycogen molecule to 2 pyruvate molecules which produces 2 ATP and then the oxidation of each pyruvate molecule to produce 17 ATP molecules together with CO_2 and water. Pyruvate oxidation takes time because it involves many chemical reactions, (known as the Krebs cycle), including the transport of pyruvate from cytosol to mitochondria. When the ATP requirement is larger than can be

supplied in oxidative phosphorylation, additional ATP is obtained from glycogen breakdown to pyruvate. Most of these pyruvate molecules will react with protons from ATP breakdown and convert to lactate.

It is important to note that the conversion from pyruvate to lactate is a reversible reaction so both species are present in equilibrium. During exercise, the increase in the breakdown of glucose means an increase in pyruvate concentration and at the same time an increase in lactate concentration. It is therefore a common situation that blood lactate concentration increases during steady state exercise, even in the moderate exercise domain.

The ATP usage is similar to the process of discharging and recharging a capacitor in an electronic system. ATP releases its high energy phosphate (P~):



which is used by the contracting myofibril. ATP is then re-synthesized from ADP and phosphate (see Section 2.2). The process of ATP usage and resynthesis (also called ATP recycle or ATP turn over) is complex and the overall kinetics is assumed to be of first order for exercise in moderate intensity domain. During heavy exercise, the kinetics of ATP turn-over rate has been observed to have a slow component increase that is similar to the slow component increase of O₂ uptake (Whipp et al., 2002).

In our model, the increase of muscle ATP requirements (ΔR_{ATP}) is assumed to be dependent on work rate having two components, each of which is represented as a linear differential equation:

$$\begin{aligned} \tau_f \frac{d(\Delta R_{\text{ATP}})_f}{dt} + (\Delta R_{\text{ATP}})_f &= G_f \cdot \text{WR} \\ \tau_s \frac{d(\Delta R_{\text{ATP}})_s}{dt} + (\Delta R_{\text{ATP}})_s &= G_s \cdot \text{WR} \cdot \mu \\ \Delta R_{\text{ATP}} &= (\Delta R_{\text{ATP}})_f + (\Delta R_{\text{ATP}})_s \end{aligned} \quad (6.1)$$

where WR is the work rate in watt, G and τ are the gain and time constant (s) respectively, and subscripts f and s represent variables for fundamental and slow component respectively. The constant μ is defined as:

$$\mu = 0 \text{ for } \text{WR} \leq \text{LT}$$

$$\mu = 1 \text{ for } \text{WR} > \text{LT}$$

where LT is the lactate threshold. Equation (6.1) can be expressed as:

$$\Delta R_{\text{ATP}}(t) = \text{WR}(t) \cdot \{G_f(1 - e^{-t/\tau_f}) + G_s(1 - e^{-t/\tau_s}) \cdot \mu\} \quad (6.2)$$

If compared to the equivalent increase of muscle oxygen extraction ($\Delta Q'O_2$), ΔR_{ATP} is slightly higher during the steady state of moderate exercise thereby resulting in

anaerobic metabolism to meet the ATP requirement, i.e. G_f of equation (6.1) is slightly bigger than G_f of equation (6.3). In higher exercise domain, both R_{ATP} and $Q'O_2$ has a slow component increase but the increase of R_{ATP} is larger than the equivalent increase of $Q'O_2$ (G_s of eq. (6.1) > G_s of eq. (6.3)). The kinetics of R_{ATP} is faster than the kinetics of $Q'O_2$ resulting in early anaerobiosis, i.e. τ_f and τ_s of eq. (6.1) < τ_f and τ_s of eq. (6.3). The difference in kinetics between R_{ATP} and $Q'O_2$ is evident from experimental findings, e.g. (Rossiter et al., 2002) but the difference in slow component increase is a logical assumption.

6.3. Oxygen consumption and maximum oxygen consumption

At the onset of exercise in humans, oxygen uptake ($V'O_2$) responds quite rapidly with a fundamental component showing first-order kinetics for all work rates below the lactate threshold (LT). However, beyond the lactate threshold an additional component of $V'O_2$ starts to appear and develops slowly, superimposing on the fundamental component (Barstow and Mole, 1991; Whipp and Wasserman, 1972). Therefore, the steady state value of $V'O_2$ for high intensity exercise work rates lies above the point predicted by calculating the relationship between $V'O_2$ and work rate at levels below the lactate threshold.

The magnitude of the additional component can be 1 l O_2 /min or even more (Poole et al., 1994). For moderate exercise conditions, the increase of $V'O_2$ relative to the increase of work rate is approximately 10 ml/min/watt but for higher exercise conditions the relative increase can be as high as 13 ml/min/watt.

The underlying process that causes the slow component to emerge is still not fully understood but it has been argued that more than 80% of the additional $V'O_2$ arises inside the exercising muscle. Some ideas proposed include metabolic stimulation by species such as lactate, H^+ or K^+ , recruitment of a progressively increasing proportion of lower-efficiency fast-twitch fibres, the rising muscle temperature, and reduced efficiency of ATP synthesis or work ability due to the accumulation of metabolites (Krustrup et al., 2004a; Poole et al., 1991).

The emergence of the slow component is always followed by an increase in blood lactate concentration and a higher exercise work rate leads to an increased magnitude of the slow component and thus to higher levels of blood lactate concentration. Although there is a correlation between the additional increase of oxygen uptake during high intensity exercise and lactate concentration, it is in doubt whether or not this is a cause and effect relationship. Experiments with dog gastrocnemius muscle, which is the largest of the calf muscles, shows that an increase of lactate concentration by infusion does not increase the oxygen uptake which means that lactate does not intrinsically stimulate the slow component of $V'O_2$ (Poole et al., 1994). Another study has also confirmed that

manipulation of lactate concentration has no significant effect on the $\dot{V}O_2$ slow component during recovery (Roth et al., 1988).

A contrasting result, however, was obtained in a previous investigation where sodium lactate was injected into a dog vein at rest. After the injection, there was no change in the pulmonary CO_2 production but the O_2 consumption was increased. Following the lactate metabolism, which reduced lactate concentration, O_2 consumption was found to decrease (Bertram et al., 1967).

The dynamics of oxygen consumption is affected not only by the level of work rate but also by the location of the work rate in the exercise domain. In an experiment on subjects with different the lactate thresholds, it has been shown that the rise time of oxygen consumption for the fitter subject with a higher the lactate threshold is shorter than the rise time for a less fit subject even though both are exercising at the same work rate (Whipp, 1987).

When the human body is forced to work with higher and higher power levels, for example in an incremental exercise test, it will take more and more oxygen until it reaches a certain critical level called the maximum oxygen uptake ($\dot{V}O_{2max}$). This is the level where the human body can provide maximal aerobic energy. It is important to note that the human body is capable of performing muscular work at a higher power level than the maximal aerobic energy supply at the maximum oxygen uptake (Rowell, 1993). It has been found that, with proper training, the maximum oxygen uptake can be upgraded (Osteras et al., 2005; Butler and Turner, 1988).

In essence there are three major factors determining the maximal oxygen uptake: 1.) the cardiac output; 2.) the oxygen carrying capacity of the blood; and 3.) the amount of exercising skeletal muscle and the ability of muscle to utilize the supplied oxygen. Hence $\dot{V}O_{2max}$ is partially limited by the ability of the cardio respiratory system to deliver oxygen to the exercising muscles. According to Basset and Howley (2000), the evidence for this limitation arises from from three factors: 1.) when oxygen delivery is altered (e.g. by blood doping or hypoxia), $\dot{V}O_{2max}$ changes accordingly; 2.) the increase in $\dot{V}O_{2max}$ with training results primarily from an increase in the maximal cardiac output (not an increase in the arteriovenous O_2 difference); and 3.) when a small muscle mass is overperfused during exercise, it has an extremely high capacity for consuming oxygen. Thus, they conclude that O_2 delivery, not skeletal muscle O_2 extraction, should be viewed as the primary limiting factor for $\dot{V}O_{2max}$ in exercising humans.

However, some other investigators have argued that it is the muscle's capability to extract oxygen that limits oxygen supply to the muscle for aerobic metabolism because oxygen delivery to the muscle is essentially high even during intense exercise (Bangsbo et al., 2000). Oxygen delivery is higher than the amount required for muscle work yet the muscle does not absorb it. A possible explanation to this extraction limitation is that

oxygen may not be able to diffuse completely from the blood capillary into muscle cells when the O_2 pressure difference is not high enough and this allows only a portion of the oxygen to be released from the blood haemoglobin.

The increase of muscle oxygen extraction ($\Delta Q'O_2$) has been modelled using two differential equations, one for the fundamental component and the other for the slow component:

$$\begin{aligned}\tau_f \frac{d(\Delta \dot{Q}O_2)_f}{dt} + (\Delta \dot{Q}O_2)_f &= G_f \cdot WR \\ \tau_s \frac{d(\Delta \dot{Q}O_2)_s}{dt} + (\Delta \dot{Q}O_2)_s &= G_s \cdot WR \cdot \mu \\ \Delta \dot{Q}O_2 &= (\Delta \dot{Q}O_2)_f + (\Delta \dot{Q}O_2)_s\end{aligned}\tag{6.3}$$

where WR is the work rate in watt, G and τ are the gain and time constant (s) of the $Q'O_2$ components respectively, and subscripts f and s represent variables for fundamental and slow component respectively. The constant μ is defined as:

$$\mu = 0 \text{ for } WR(t) \leq LT$$

$$\mu = 1 \text{ for } WR(t) > LT$$

where LT is the lactate threshold. Equation (6.3) can be expressed as follows:

$$\Delta \dot{Q}O_2(t) = WR(t) \cdot \{G_1(1 - e^{-t/\tau_1}) + G_2(1 - e^{-t/\tau_2}) \cdot \mu\}\tag{6.4}$$

The actual value of $Q'O_2$ is obtained by adding eq. (6.4) with the base line value $Q'O_2(0) = 300$ ml/min. The increase of $Q'O_2$ is subject to limitation so that the muscle venous O_2 content does not drop below zero (or below a certain level which effectively limits muscle O_2 extraction).

Similar to the situation with the model for moderate exercise, oxygen extraction below the LT is set at 10 ml/min/watt and the kinetics involves a time constant of 32 s. Oxygen extraction above the LT is much higher but the kinetic behaviour is much slower. The slow component of oxygen uptake is assumed to originate solely from the exercising muscle and is linked to the recruitment of type II fibres (see Section 6.7). Type II fibre recruitment is immediate when the work rate passes the lactate threshold, which is set at 100 W. Based on these assumptions, muscle O_2 extraction ($Q'O_2$) for 200 W exercise would have the form shown in Figure 6.2. This assumption in one and another way does not accurately match what is expected from experiment. As suggested in Section 2.6 (see Figure 2.5), oxygen uptake for exercise work rate above LT has a slow component increase that arises “later” than the onset of exercise.

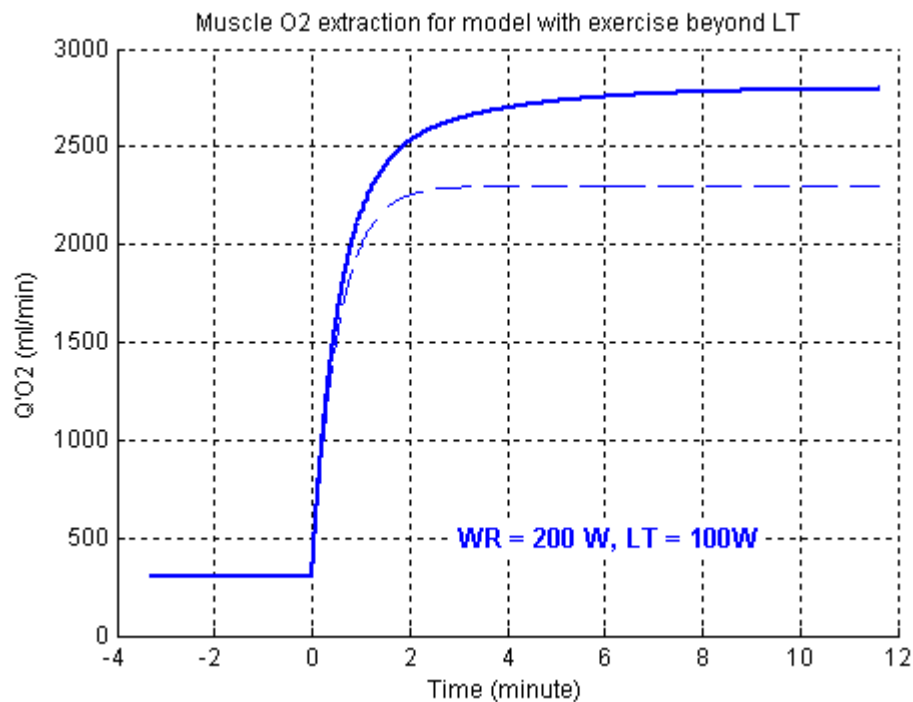


Figure 6.2. Model response of muscle O₂ extraction (Q'O₂) for exercise at 200 watt where LT is assumed to be 100 watt; the dashed curve represents the Q'O₂ prediction based on kinetics below LT.

6.4. Cardiac output at high intensity exercise

During moderate intensity exercise, blood flow adjusts to a steady value that is appropriate for the metabolic demand. The increase is linearly related to the increase of work rate and has a close relationship with the increase of oxygen uptake. For steady state conditions involving moderate exercise the cardiac output is sufficient to supply oxygen to the exercising muscle so that the muscle has the ability to sustain the work for a long period. Not long after exercise ceases, the cardiac output recovers to the pre-exercise baseline level which indicates that there is only a short period needed to pay the oxygen debt that occurs at the onset of exercise (Van Beekvelt et al., 2001). The off transient response of oxygen uptake has been observed to be symmetrical with the on transient response (Ozyener et al., 2001) which supports the suggestion that the oxygen supply during the steady state of moderate exercise is at a sufficient level and the off transient oxygen uptake is necessary solely to repay the oxygen debt.

For conditions of high intensity exercise, however, the off transient response for cardiac output is different from the on transient response and during the off-transient the blood flow remains high for several minutes after the exercise ceases (Van Beekvelt et al., 2001). These investigators have interpreted this as a way of prolonging the oxygen supply for recovery to compensate for a high debt not only at the onset of exercise but also during the period when the muscle is performing the exercise. One of the reasons for the insufficiency of oxygen supply to the exercising muscle is that the blood flow level is not high enough to support the requirements of the muscle.

As pointed out in Section 5.4, the cardiovascular system does not supply a sufficient amount of oxygen to muscle in order to withstand intense muscular work. There is a limit of blood flow that the heart can pump and this limit is called maximum cardiac output.

Hence for heavy exercise, cardiac output may increase proportionally with the work rate until it approaches its maximum level at which point it starts to level off. Rowell (1993) seems to suggest that the proportionality of cardiac output and oxygen uptake is applicable for moderate exercise and extends to the higher intensity domain until the maximal level is approached. Since oxygen uptake has a slow component, cardiac output may also have the same feature because a constant work rate of exercise above the lactate threshold has a constant steady-state arteriovenous O_2 difference so that the slow component of O_2 uptake should be accompanied by a similar slow component of cardiac output (Richard et al., 2004).

The maximal cardiac output varies among subjects just like $V'O_{2max}$. Both are somehow related to the lactate threshold (LT) but no strict quantitative relationship has been defined although some investigators such as Grassi et al. (1999) and Katz and Sahlin (1988) suggest that LT occurs when the exercise load is about 50-70 % of the work rate at $V'O_{2max}$.

Similar to the condition below LT, the increase of cardiac output ($\Delta Q'$) during exercise above LT is modelled as:

$$\begin{aligned}\tau_c \frac{d(\Delta \dot{Q})_i}{dt} + (\Delta \dot{Q})_i &= 0.05 \cdot k \cdot WR \\ \tau_f \frac{d(\Delta \dot{Q})_f}{dt} + (\Delta \dot{Q})_f &= 0.05 \cdot (1 - k) \cdot WR \cdot e^{TD_f} \\ \Delta \dot{Q} &= (\Delta \dot{Q})_i + (\Delta \dot{Q})_f\end{aligned}\tag{6.5}$$

where WR is work rate in watt, TD and τ are time delay (s) and time constant (s) of the Q' components, and subscripts c and f indicate that the variables are for cardiodynamic (phase 1) and fundamental (phase 2) component respectively. The constant k represent the relative magnitude of phase 1 component compared to the magnitude of the fundamental component. Equation (6.5) can be expressed as follows:

$$\Delta \dot{Q}(t) = 0.05 \cdot WR \cdot \{k \cdot (1 - e^{-t/\tau_c}) + (1 - k) \cdot (1 - e^{-(t-TD_f)/\tau_f})\}\tag{6.6}$$

Note that $\Delta Q'$ is limited so that Q' is always below Q'_{max} .

We wish to assess whether cardiac output has a slow component increase. For this purpose, $\Delta Q'$ will be expressed as:

$$\Delta \dot{Q}(t) = 0.05 \cdot WR \cdot \{k \cdot (1 - e^{-t/\tau_c}) + (1 - k) \cdot (1 - e^{-(t - TD_f)/\tau_f})\} + \mu \cdot (1 - e^{-(t - TD_s)/\tau_s}) \quad (6.7)$$

where TD_s and τ_s are time delay and time constant of the slow component increase respectively, and μ is defined as

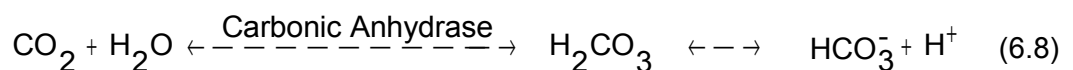
$$\mu = 0 \text{ for } WR \leq LT$$

$$\mu = \text{constant for } WR > LT$$

6.5. Carbon dioxide production

By keeping the assumption that all extracted oxygen in the muscle is immediately converted to carbon dioxide, muscle CO_2 production from aerobic metabolism would show an additional slow component in its response. The kinetics of the CO_2 slow component may be slower than that of oxygen because of muscle CO_2 storage effects. Carbon dioxide production in muscle is the main source of CO_2 output at the mouth and there are two other contributors that increase CO_2 output during heavy exercise, i.e. bicarbonate buffering and hyperventilation.

During heavy exercise muscle CO_2 production gets an extra component from buffering of hydrogen ions produced in hydrolysis of ATP during glycolysis (Wasserman et al., 2005; Peronnet and Aguilaniu, 2005). The existence of carbonic anhydrase means that bicarbonate is present in the muscle and bicarbonate reaction with hydrogen ions produces carbon dioxide. As described in Section 2.4, carbon dioxide is stored and transported partially in the form of bicarbonate and dissolved CO_2 and bicarbonate has an equilibrium reaction described by the following equation:



where carbonic anhydrase is the enzyme that accelerates the hydration of CO_2 and dehydration of carbonic acid (H_2CO_3). In acidosis, some amount of proton will react with bicarbonate to form carbonic acid which will then dissociate into CO_2 and water.

It has been shown that the concentration of muscle bicarbonate can decrease from approximately 10 mEq/l at rest down to about 3 mEq/l after exhaustive exercise (Sahlin et al., 1978). If the volume of exercising muscle is 2.7 litres, CO_2 production from buffering hydrogen ions can amount to approximately 18.9 mmol or 420 ml. However, bicarbonate buffering in muscle does not produce carbon dioxide per se. There is no way of CO_2 to escape from muscle in the form of gas. Rather, muscle bicarbonate diffuses out and supports blood buffering (Peronnet and Aguilaniu, 2005).

Bicarbonate buffering is also present in the blood. Blood has an approximate volume of 5 litres and the bicarbonate concentration may drop by 14 mEq/litres during

intense exercise, Therefore, blood buffering can result in an additional CO₂ output ($V'\text{CO}_2$) of as much as 70 mmol or, in terms of litres, 1500 ml.

Another source of CO₂ output is hyperventilation. As described in Section 4.3.1 and further discussed in Section 4.9.2, ventilation and CO₂ output are closely related. When the ventilation increases above its “normal” control level, additional CO₂ will leave the system via the mouth. This additional volume of CO₂ comes from storage of CO₂ in the blood and the lung. More information about hyperventilation is presented in Section 6.8.

6.6. Metabolic acidosis

Every time ATP is broken down to ADP and free phosphate, one hydrogen ion or proton is released. A proton is consumed when mitochondria perform complete aerobic metabolism known as oxidative phosphorylation. Aerobic metabolism produces more ATP from the same amount of fuel (glycogen or triglyceride) and is a preferred mechanism to supply ATP. When the ATP demand of muscle contraction is met by aerobic metabolism, the same amount of proton is released and used so that there is no proton accumulation in the cell (Robergs et al., 2004).

Oxidative phosphorylation involves many reaction cycles so it is relatively slow. When the exercise intensity increases and ATP demand cannot be met by aerobic metabolism, ATP can be regenerated immediately through anaerobic metabolism also known as glycolytic phosphorylation which is much faster. Glycolytic phosphorylation takes place outside mitochondria and does not consume proton. Therefore high intensity exercise has a consequence that proton accumulates in muscle cell.

On the other hand, lactate is always present and has an equilibrium reaction with pyruvate which is indicated by the constant proportion of lactate-pyruvate concentration (Sahlin et al., 1987). Catabolism starts with glycolysis, i.e. breakdown of fuel such as glucose or glycogen into pyruvate which generates anaerobic ATP. In oxidative phosphorylation, pyruvate is oxidized which produces carbon dioxide and water. An increase in exercise intensity elevates the breakdown of fuel and it consequently increases the pyruvate concentration but if ATP demand is still met by oxidative phosphorylation, the lactate to pyruvate ratio will still be constant.

However, when the exercise is intense, the large amount of ATP is obtained more and more from glycolytic phosphorylation and in this situation proton accumulates and pyruvate concentration raises. Under this condition, lactate production increases to prevent pyruvate accumulation and at the same time to reduce proton accumulation and support further glycolysis. The overall result is that lactate and pyruvate leaves the equilibrium state and the ratio of lactate to pyruvate is much higher than at rest or at moderate exercise. In the steady-state, the amount of lactate production is equal to the

amount of proton released in ATP breakdown which used to be interpreted erroneously as lactic acid production (Robergs et al., 2004).

While protons may diffuse out of muscle, lactate removal needs a special mechanism called lactate-proton co-transport which transfers both lactate and proton in one go and is quite slow (e.g. (Juel, 1997)). When a high concentration of lactate is present in muscle, it can take 3-5 minutes before the lactate concentration in blood increases to a peak level (Kowalchuk et al., 1988; Hubbard, 1973). Although proton may drain out of the muscle without the accompanying transport of lactate, it happens mainly outside steady state condition and therefore the lactate release remains a good marker of proton release (Robergs et al., 2004).

A high concentration of proton is not desirable because it affects metabolism, contributes to fatigue. High concentration of H^+ influences energy production and muscle contraction and at a very low pH of 6.4, glycolysis can cease completely (Myers and Ashley, 1997). It is important to note that lactate ion is not a major contributor to fatigue and degeneration of metabolism but rather the hydrogen ion (or the acidity) that matters more (Robergs et al., 2004).

The proton and lactate generated in the muscle cells can either be buffered and removed within the cells or released to the interstitial space. The cellular mechanisms of proton buffering and lactate clearance represent the first line of defence against acidosis and lactate accumulation. Muscle buffering and lactate clearance mechanisms enable the muscle to produce more lactate and protons before reaching lactate accumulation and pH limits. The release of lactate and H^+ ions to the outside of the muscle cell represents the major protective mechanism against intracellular pH decrease and lactate accumulation.

In our model, proton release from muscle is assumed to be equal to the lactate release. This would lead to acidosis that is lower than it should be, especially in transient conditions. With this assumption, the increase of blood [La] simultaneously decreases the buffer base and base excess which simplifies the pH calculation since it eliminates the need to acquire the change in proton concentration. Note that in pH calculation (see Section 4.6.2 for details of calculation of pH), the increase of acidity reduces the buffer base and base excess.

6.7. Muscle fibre type recruitment

It has been mentioned in Section 2.2 that muscle has two types of fibres: Type I and Type II and the latter may be further divided to two different groups called Type IIa and Type IIx. Every type of muscle fibre has properties that may be different from the other types.

It is suggested that to perform work, muscle recruits specific muscle fibres which are suitable for the kind of the work involved. For intense work of short duration, muscle

tends to recruit Type IIx fibres which are fast and large (and hence strong). On the other hand for moderate work over longer periods of time, muscle Type I fibres are preferred because this type of fibre is oxidative so that it produces more ATP from the same amount of fuel.

The recruitment policy is reflected in the kinetics and amount of oxygen required for performing the exercise. Pringle et al. (2003) reported that muscle with a high percentage of Type I fibres had a faster kinetics of oxygen uptake and had a lower amplitude of VO_2 slow component. Several observations indicate that the emergence of a VO_2 slow component has a link with the recruitment of Type II fibres (Carter et al., 2006; Krusturup et al., 2004a; Krusturup et al., 2004b). On the other hand, Altenburg et al. (2007) suggest that the policy of fibre type recruitment seems unchanged as long as the work rate is constant. In an investigation for subjects performing 75% maximal exercise, they found that the same proportion of muscle fibres was recruited during the 45 min of exercise.

An important property of muscle fibre relates to lactate metabolism. Slow twitch fibres are rich in mitochondria and myoglobin so they can produce ATP using a complete cycle of oxidation (oxidative phosphorylation). On the other hand, fast twitch fibres have a small amount of mitochondria so fuel does not usually fully oxidize and the need for ATP is fulfilled with a glycolytic reaction which produces lactate. Interestingly, slow twitch fibres consume lactate, by which lactate reverts to pyruvate and pyruvate is put in the oxidation cycle in mitochondria (van Hall et al., 2003).

Our model incorporates a simple policy for recruitment of different types of fibre. Below the lactate threshold (LT), only Type I fibre is recruited. Above LT, all Type I fibres are recruited and additional work rate above the LT involves Type II fibres. Recruitment policy does not change as long as the exercise work rate does not change. When Type II fibres are recruited, it is assumed that a portion of the ATP requirement is met anaerobically so that lactate is also produced even in the steady state condition. Among the consequences of this policy is the fact that $\dot{Q}\text{O}_2$ will immediately show a slow component at the onset of a step increase of exercise above the LT, as depicted in Figure 6.2.

6.8. Hyperventilation

In Chapter 2 it was pointed out that the exact mechanisms involved in the control of ventilation are not clear. At a condition of rest, changes in arterial PO_2 , PCO_2 and pH stimulate changes in ventilation such that these humoral variables shift back to their "normal" levels. These variables have been long regarded as the regulatory variables in the ventilatory feedback control system.

In moderate exercise conditions, it appears that the arterial PO_2 is not regulated as strictly as PCO_2 and pH. Whipp (1990) suggests that during moderate exercise ventilation is controlled in such a way as to maintain arterial PCO_2 and pH relatively constant. In this condition, however, there is a large increase in ventilation but no significant change in arterial PCO_2 or pH. Consequently, it is hard to envision ventilation being controlled by sustained “errors” in arterial PCO_2 and pH and its control should involve other factors for example the neural drives from the working muscle and higher brain centres. It is now generally accepted that the control of \dot{V}_E in exercise is multifactorial and based on a high degree of redundancy so that no single factor is responsible (Paterson, 1992; Cunningham, 1987).

Regardless of what causes ventilation, a good and solid equation has been established that relates ventilation, arterial PCO_2 and CO_2 output for an ideal lung (see Section 4.3). The equation, which is rewritten below as equation (6.9) for convenience, enables the model to estimate ventilation in order to maintain $PaCO_2$ for any value of $\dot{V}'CO_2$, or calculate $PaCO_2$ if ventilation and $\dot{V}'CO_2$ are known.

$$\dot{V}_E = \frac{863 \cdot \dot{V}'CO_2}{PaCO_2(1 - VD/VT)} \quad (6.9)$$

Hyperventilation is a state where the lung breaths more deeply and frequently than is normally needed, and so $PaCO_2$ falls. When the exercise work rate is higher than a certain level in the high intensity domain, the lung ventilates more than is predicted by equation (6.9), i.e. the lung hyperventilates. It is not known exactly how hyperventilation is stimulated during high-intensity exercise but the consequence is obvious. Hyperventilation increases the CO_2 output, which according to equation (6.8) would decrease proton concentration. Apparently, hyperventilation is stimulated to compensate metabolic acidosis which becomes more severe in the high intensity domain (Rausch et al., 1991).

With the limited information available, it is not possible to decide how hyperventilation can be introduced into our model. Many researchers have observed that blood potassium concentration ($[K^+]$) has a good correlation with ventilation and they suggest that $[K^+]$ may be the controlling factor for ventilation (Paterson, 1992; McCoy and Hargreaves, 1992; Paterson et al., 1989). However, potassium is not included in our model so it cannot be used to build an expression for ventilation. Instead, we will try express hyperventilation using changes in proton concentration or work rate..

6.9. Simulation Results

6.9.1. Simulation with incremental exercise

The purpose of this simulation is to assess whether the model behaves satisfactorily. It is important therefore to compare the simulation with experimental results

and ideally with experimental results that have not been applied in establishing the structure and parameter values used in developing the model itself. The experimental evidence provided by Sun et al. (2001) has been taken as the target for tuning the model for several reasons. They provide descriptions of kinetics of several important variables: blood O₂ and CO₂ content, PCO₂ and. The information is for incremental exercise so it applies for work rates below and beyond LT and the interval between measurements (the measurement precision) is 1 minute which may be considered fairly good. They also provide numerical values of several other variables for conditions of unloaded and maximal exercise (Table 6.8). Note that the original table does not provide value for unloaded exercise so we have made estimation for it based on the percentage of oxygen uptake that they provide on their paper.

Table 6.8. Mean values of variables as presented in Sun et al. (2001); *) our estimation

Variables	Value at rest	Estimated value at unloaded exercise *)	Value at maximal exercise	Increase
V'O ₂ (l/min)	0.37	0.72	3.91	3.19
V'CO ₂ (l/min)	0.29	0.45	4.84	4.39
Q' (l/min)	7.06	12.06	25.38	13.32

Sun et al. (2001) conducted their observations on five men using exercise testing involving incremental work rate from the base line of unloaded exercise up to maximal exercise within 10 minutes. The mean value of LT is 126 watt and the work rate which achieves V'O_{2,max} is 302 watt. The gain factor in terms of mean value of oxygen uptake to work rate is $\Delta V'O_2/\Delta WR = 10.3$ ml/min/watt. Haemoglobin concentration changes with work rate (or with time) from 15.8 at unloaded exercise to 16.9 at maximal exercise.

For the purpose of this simulation, several parameters have been adjusted to mimic the condition similar to the experiment conducted by Sun et al. (2001). The lactate threshold is set at 125 watt. Steady state increase of ventilation is modelled as an exponentially increasing function of work rate, thus hyperventilation is implicitly contained. The decision to model ventilation in that way is based on information in a report that ventilation and arterial [La] are strongly correlated (McCoy and Hargreaves, 1992). Thus,

$$\Delta \dot{V}E_{ss} = k_1 \cdot e^{k_2 \cdot WR} \quad (6.10)$$

where $\Delta \dot{V}E_{ss}$ is steady state increase of ventilation, and k_1 and k_2 are constants.

The total magnitude of cardiac output is limited to $Q'_{max} = 22$ l/min. All of the increase of cardiac output is assumed to flow to the exercising muscle. With this limitation, the muscle O₂ extraction ($Q'MO_2$) may become larger than the quantity that the blood can deliver and that could make the muscle venous O₂ concentration ($CvMO_2$) drop below

zero, which cannot be allowed. To avoid this, $Q'MO_2$ is limited such that $CvMO_2 \geq 0.02$ l/l.

Figures 6.3 – 6.6 depict the responses of the model during incremental exercise from unloaded to maximal exercise (300 W) for PCO_2 , blood O_2 and CO_2 content and pH. The responses have been drawn on top of the experimental results from Sun et al. (2001) for convenient comparison. Several other variables such as $V'CO_2$ and $V'O_2$ are presented in Table 6.9.

Table 6.9. Base line value of O_2 uptake, CO_2 output and cardiac output

Variables	Base line value (unloaded exercise)	Value at maximal exercise	Increase
$V'O_2$ (l/min)	0.72	4	3.28
$V'CO_2$ (l/min)	0.45	3.87	3.545
Q' (l/min)	10	24.6	14.6

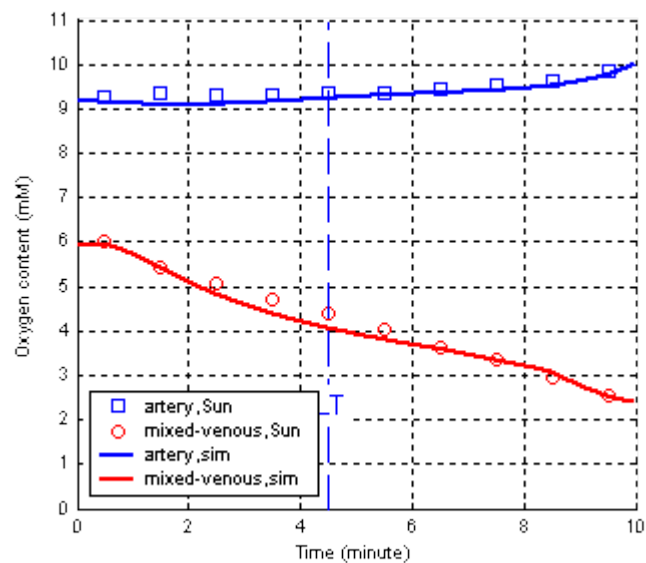


Figure 6.3. Model response for arterial and mixed venous O_2 content during incremental exercise from unloaded condition to 300 W in 10 minutes; Square and circled points indicate experimental results conducted by Sun et al. (2001); The blue vertical dashed line indicates the lactate threshold (LT).

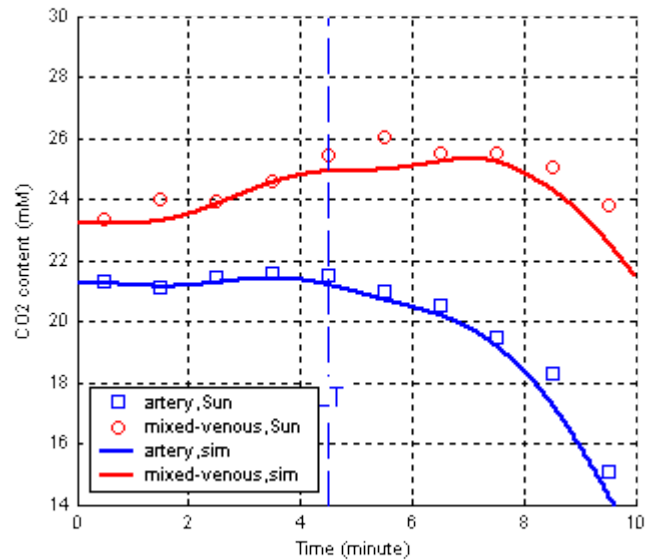


Figure 6.4. Model response for arterial and mixed venous CO₂ content during incremental exercise from unloaded condition to 300 W in 10 minutes. Square and circled points indicate experimental results conducted by Sun et al. (2001). The blue vertical dashed line indicates the lactate threshold (LT).

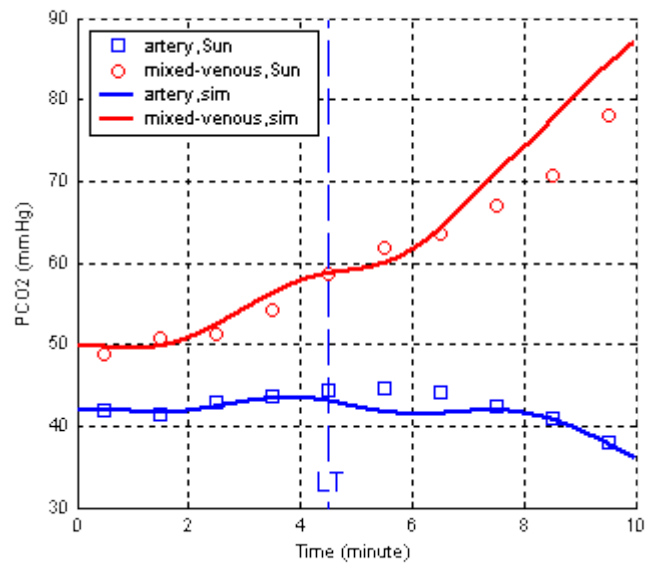


Figure 6.5. Model response for arterial and mixed venous CO₂ partial pressure during incremental exercise from unloaded condition to 300 W in 10 minutes. Square and circled points indicate experimental results conducted by Sun et al. (2001). The blue vertical dash line represents the assigned LT.

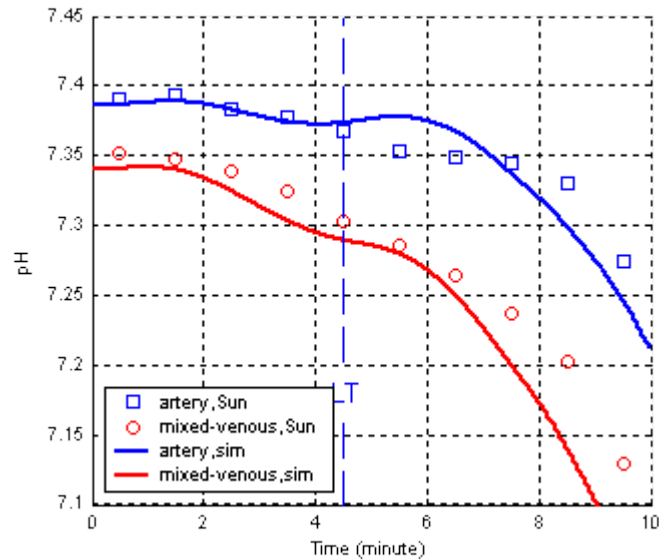


Figure 6.6. Model response for arterial and mixed venous pH during incremental exercise from unloaded condition to 300 W in 10 minutes. Square and circled points indicate experimental results conducted by Sun et al. (2001).

By comparing the response of experimental results and the respective simulation result as shown in Figures 6.3 – 6.6, it may be inferred that the model behaviour is rather satisfactory in terms of patterns of the response. The kinetics of O_2 and CO_2 content shows similar patterns between simulation and experimental results. Other variables such as arterial pH and PCO_2 show noticeable deviations and mixed venous pH and PCO_2 show significant discrepancies.

With the selected parameter values, we obtain the kinetics of $V'E$, $V'O_2$ and $V'CO_2$ as depicted in Figure 6.7. All the variables increase more or less linearly below the lactate threshold. Above LT, $V'E$ and $V'CO_2$ increase further which make the curves appear to be upward at about the LT point. This additional increase of $V'E$ is the hyperventilation component. On the other hand, $V'O_2$ appears to be linearly increased until the end of the exercise test. Model response for oxygen ventilatory equivalent ($V'E/V'O_2$) and ventilatory efficiency ($V'E/V'CO_2$) are depicted in Figure 6.8. Comparing these simulation results with experiments, e.g. Wasserman, et al. (1973) and Whipp (1994a), we may say that there is a fair agreement in terms of the $V'O_2$, $V'CO_2$ and $V'E$ kinetics (see e.g. Figure 6.9) although $V'E/V'O_2$ is expected to level off below the lactate threshold (Whipp, 1994a).

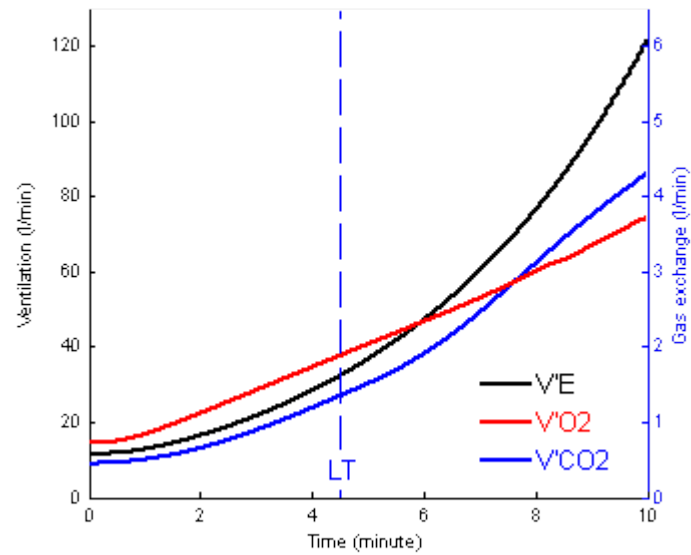


Figure 6.7. Model response for kinetics of pulmonary gas exchange during incremental exercise. The blue vertical dash line represents the assigned LT.

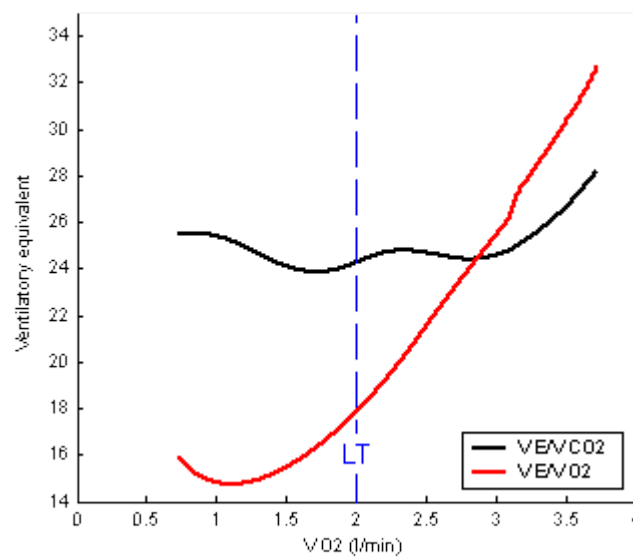


Figure 6.8. Model response for kinetics of ventilatory equivalent during incremental exercise. The blue vertical dash line represents the assigned LT.

Figure has been removed
due to Copyright restrictions.

Figure 6.9. Breath by breath measurement of pulmonary gas exchange of a relatively fit subject during incremental exercise. Diagram taken from fig. 8 of the work by Wasserman et al. (1973).

6.9.2. Simulation with constant work rates

Figures 6.15 – 6.17 depict the kinetics of $\dot{V}O_2$, $\dot{V}CO_2$ and $\dot{V}E$ for several constant work rates within the moderate (30, 60 and 90 W) and higher intensity domains (120W, 150W and 180W). In the model, the lactate threshold is set at 100 W and haemoglobin concentration is set at 15 g/dl. Hyperventilation takes place once the work rate passes the lactate threshold. Equation (6.10) which is used for hyperventilation during incremental exercise does not work here. Instead, we have used this equation:

$$\tau \frac{d\Delta \dot{V}E_H}{dt} + \Delta \dot{V}E_H = k \cdot WR \quad (6.11)$$

where $\Delta \dot{V}E_H$ is hyperventilation, ΔWR_H is the work rate difference from the lactate threshold, τ is time constant and k is a proportionality constant.

For our model, work rates of 120W, 150W and 180W belong to the heavy exercise domain (see Section 2.6). Comparisons of the model response with an experimental result of Casaburi et al. (1989) (see Figure 6.13) suggest that the model response for $\dot{V}O_2$ (Figure 6.10) is fairly adequate in terms of the fact that the steady state is more delayed for work rates above the lactate threshold. The model response shows that an additional slow component is present during exercise above the LT but it does not show a **late**

increase of the slow component and this is due to inherent model limitations (see Section 6.3).

The model response for $\dot{V}E$ (Figure 6.11) appears acceptable. The steady state magnitude for the response above LT shows an additional component, i.e. the hyperventilation. However, when compared with an experimental result by Casaburi et al. (1989), the kinetics of the model looks too fast and the magnitude of the response seems too small.

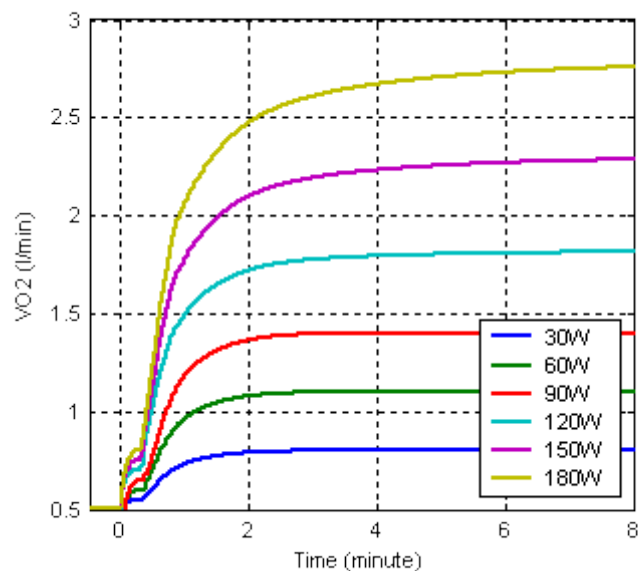


Figure 6.10. Model response for pulmonary oxygen uptake ($\dot{V}O_2$) at different work rates; Below LT, $\dot{V}O_2$ increase exponentially reaches a steady state in 3 minutes; Above LT, the attainment of steady state is delayed.

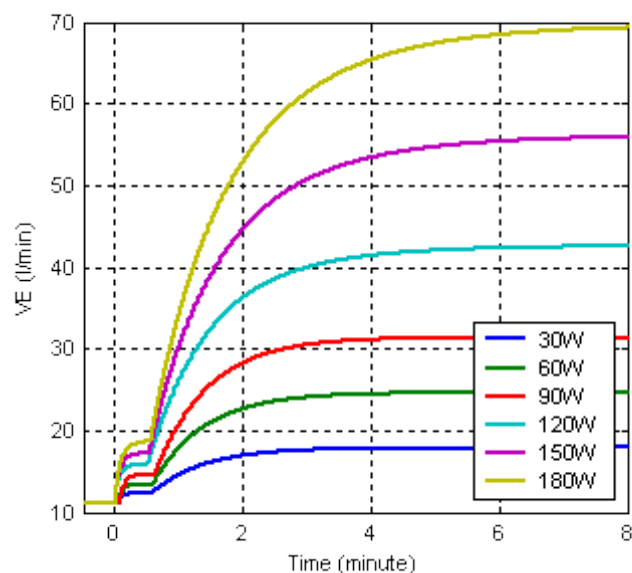


Figure 6.11. Model response for ventilation at different work rates; Below LT, $\dot{V}E$ attains a steady state in approx. 4 min; Above LT, $\dot{V}E$ is hyperventilation is superimposed.

The model response for $\dot{V}CO_2$ does not show significantly different time constants at different exercise level (Figure 6.12), which is what Casaburi et al. (1989) have

suggested in their work. In the case of the steady state magnitude, it is clear that during heavy exercise $\dot{V}'\text{CO}_2$ has additional components which are not visible for work rates below LT. It is worth considering why, despite the slower kinetics of $\dot{V}'\text{O}_2$ and $\dot{V}'\text{E}$, the kinetics of $\dot{V}'\text{CO}_2$ do not change much. The answer lies in the fact that there are several sources of CO_2 production or release. The increase of muscle O_2 extraction leads to the increase in muscle CO_2 production but with the ability of muscle to store CO_2 , muscle CO_2 production shows slower kinetics than muscle O_2 extraction. Blood buffering during metabolic acidosis releases CO_2 and the kinetics of the CO_2 released is similar to the kinetics of lactate concentration (Figure 6.15). Lastly, hyperventilation increases the CO_2 release from blood stores (and also from the lung dead space).

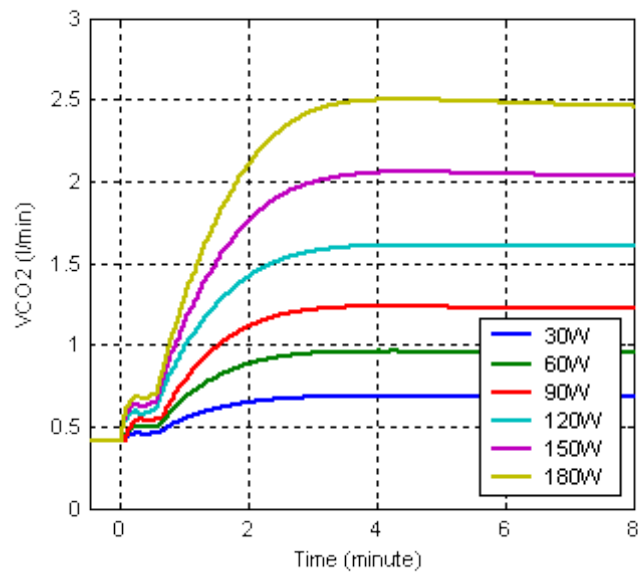


Figure 6.12. Model response for CO_2 output at different work rates. Below LT, the kinetics of $\dot{V}'\text{CO}_2$ is slower than the kinetics of $\dot{V}'\text{O}_2$; Above LT, $\dot{V}'\text{CO}_2$ appears to have a slight overshoot; Time constant is similar for different work rates below and above LT.

Figure has been removed
due to Copyright restrictions.

Figure 6.13. Second by second response of a subject conducting exercise at several constant work rates from the base line of unloaded exercise. The work rates are evenly spaced below 205W. Diagram is taken from Casaburi et al. (1989).

6.9.3. Lactate kinetics at different work rates

Figures 6.17 – 6.18 show model responses for arterial lactate concentration during moderate, heavy and very heavy exercise. At all levels of exercise, arterial [La] increases temporarily at the onset of exercise and peaks at approximately 6 – 10 minutes. During moderate exercise, arterial [La] slowly decreases to a level slightly above the base line. In heavy exercise, the arterial [La] decreases to a level much higher than the base line and in very heavy exercise (in this case 220W), the arterial [La] keeps increasing until a point in time when the simulation halts, apparently because acidosis has become too high. The kinetics of the model response is in good agreement with experimental result, for example the study by Wasserman et al. (1967) (see Figure 5.1). Their experimental data apparently have numerous variations in terms of the pattern, peak time and magnitude of arterial [La] but the simulation result appears to exhibit only one peak time for moderate and heavy exercise.

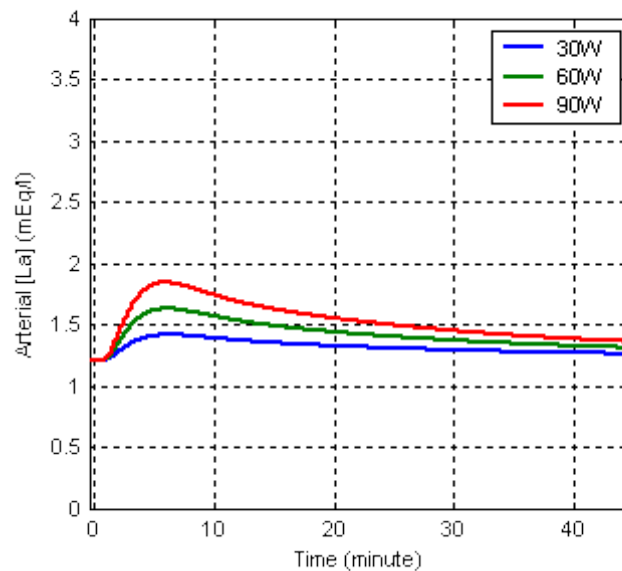


Figure 6.14. Model response for arterial [La] at work rates below LT; Arterial [La] suggests early acidosis, peaking at approx. 5 minutes after exercise onset and dropping back to the level at base line or slightly higher.

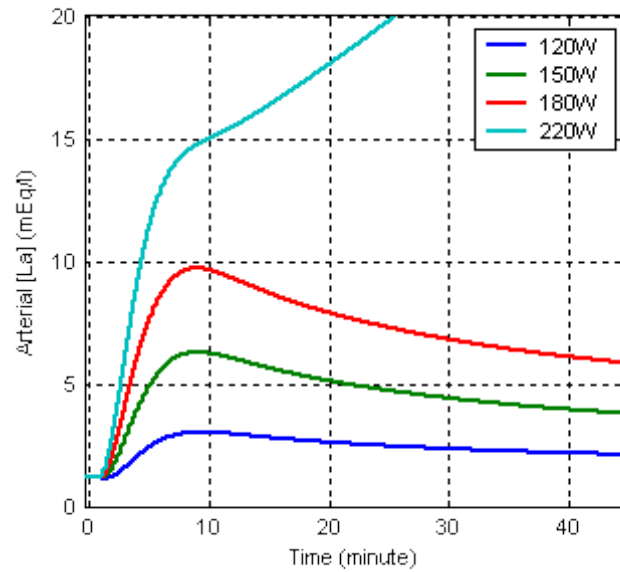


Figure 6.15. Model response for arterial [La] at work rates above LT; Arterial [La] suggests a much higher early acidosis, then it may decrease to a steady state level or keep increasing until simulation halts.

6.9.4. Sensitivity to changes of [Hb]

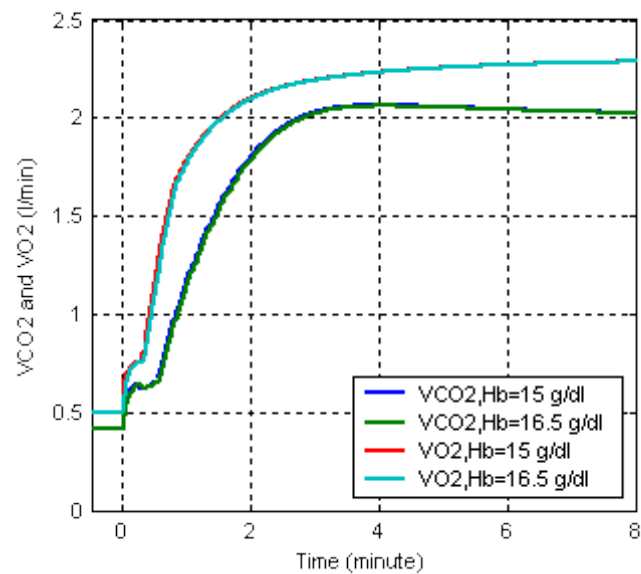


Figure 6.16. Pulmonary gas exchange during 150W exercise for different [Hb]; $V'CO_2$ (lower curves) and $V'O_2$ (upper curves) do not visibly change when blood Hb concentration is higher.

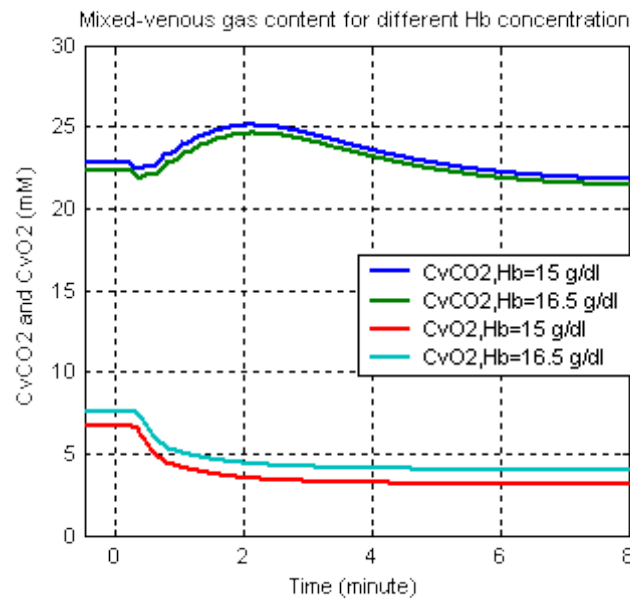


Figure 6.17. Mixed-venous gas content during 150 W exercise for different [Hb]; Mixed-venous O₂ content (lower curves) is higher when [Hb] is higher; Mixed-venous CO₂ content (upper curves) is lower for higher [Hb].

When the haemoglobin concentration increases, e.g. by 10%, the profile of pulmonary gas exchange hardly changes (Figure 6.16) which shows that the cost of the work does not change. However, the blood gas content is clearly altered (Figure 6.17), the CO₂ content decreases and the O₂ content is raised, which can effectively raise the maximum amount of oxygen that can be extracted by muscle. This suggests that a subject with higher blood [Hb] is more likely to achieve a high work level. Indeed, Haemoglobin concentration is among the markers of subject fitness, where a subject with higher [Hb] is considered fitter.

6.9.5. Effect of changes in cardiac output

Cardiac output (\dot{Q}) is related to oxygen uptake ($\dot{V}O_2$) following Fick's principle:

$$\dot{V}O_2 = \dot{Q} \cdot C(a-v)O_2 \quad (6.12)$$

where $C(a-v)O_2$ is the arterial mixed-venous oxygen content difference. Equation (6.12) has been used to estimate cardiac output by measuring the oxygen uptake considering the linear relationship between $C(a-v)O_2$ and the percentage of maximal $\dot{V}O_2$ (Stringer et al., 1997). A similar equation is used to estimate the amount of oxygen extracted by muscle after adjusting the variables to involve the quantities that are of relevance for muscle.

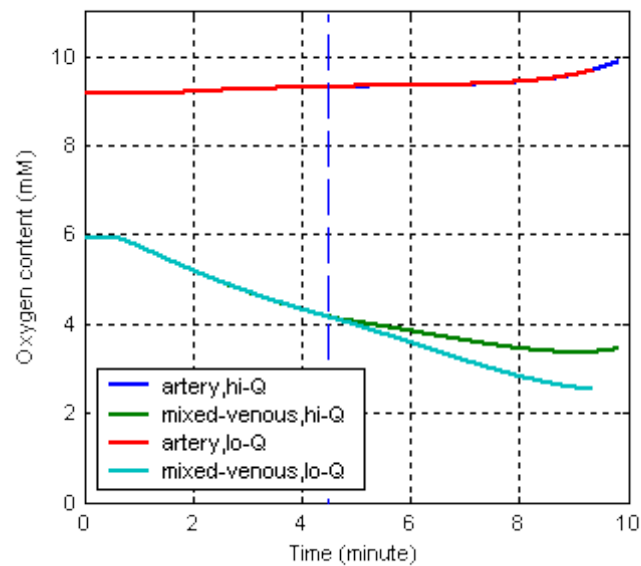


Figure 6.18. Arterial and mixed venous O_2 content in simulation for different cardiac output levels; In the legend, hi-Q means the variables when cardiac output is higher, and lo-Q when lower; Arterial O_2 content does not differ and mixed-venous O_2 content is higher when Q' is higher, resulting in a smaller O_2 content difference for higher Q' .

Figures 6.21 – 6.22 depict the model response for O_2 content and O_2 content difference during incremental exercise with two different cardiac output levels above LT. Below LT, the cardiac output increases with the work rate and is proportional to the $\dot{V}O_2$ increase. Above LT, the cardiac output increases in two different ways in these simulation studies. In one case the increase is proportional to the work rate, following the pattern that applies below the lactate threshold (denoted by Lo-Q in the figures). In the other case the increase is proportional to $\dot{V}O_2$, having a slow component increase (denoted by Hi-Q).

The arterial and mixed-venous oxygen difference is smaller when the cardiac output is higher (Figure 6.18), as would be expected following the Fick's principle (Equation 6.12). Figure 6.19 shows the arterial mixed-venous O_2 content difference ($C(a-v)O_2$) plotted against $\dot{V}O_2/\dot{V}O_{2,max}$. $C(a-v)O_2$ looks more linear for conditions involving low cardiac output (Lo-Q) than for high cardiac output (Hi-Q) conditions suggesting that if $C(a-v)O_2$ is linearly related to the percentage of maximal $\dot{V}O_2$ then the cardiac output is more likely to increase with work rate and may not have slow component increase above LT.

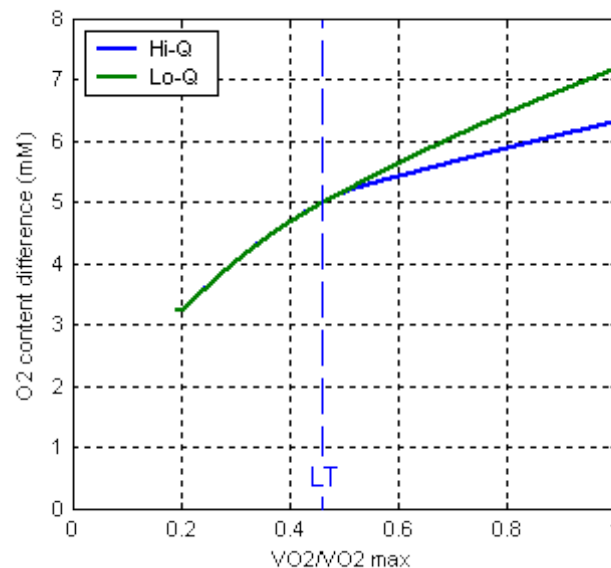


Figure 6.19. Arterial mixed venous O₂ content difference against the ratio of $\dot{V}'O_2$ to $\dot{V}'O_2$ max as determined from simulation studies with different cardiac output values.

6.9.6. Changes in CO₂ Stores During Exercise

The carbon dioxide that flows out of the mouth comes from two sources. One source is the aerobic CO₂ production in the muscle and other body tissues and the other is the release of CO₂ from the blood and tissue stores. The kinetics of total body CO₂ stores can be quantified by calculating the difference between the pulmonary CO₂ output and the CO₂ produced by the tissues. Figure 6.20 depicts the model response for the kinetics of the increase and the accumulation of CO₂ stores during a constant work rate at 60 W, which resembles the kinetics for exercise in the moderate intensity domain. The total CO₂ accumulated is a little more than 0.3 litres with the peak increase being 0.3 l/min at 0.6 minutes after the onset of exercise. This simulation result shows more rapid kinetics than the experimental result presented by Chuang et al. (1999) (see Figure 6.21), which shows a peak increase of approximately 250 ml/min occurring one minute after the onset of exercise, but the total accumulated CO₂ is similar. This discrepancy in CO₂ store kinetics might well be due to the difference in the kinetics of ventilation used in the model, as compared with the ventilation kinetics of the subject observed in the experiment.

During exercise above LT (Figure 6.22), the stored CO₂ increases during the first 2 minutes of exercise, associated to the increased production of CO₂. However, the storage is later reduced slowly and when it attains a steady state the accumulated CO₂ has decreased by more than 20%. This reduction of CO₂ storage can be attributed to the acidosis that occurs during heavy exercise.

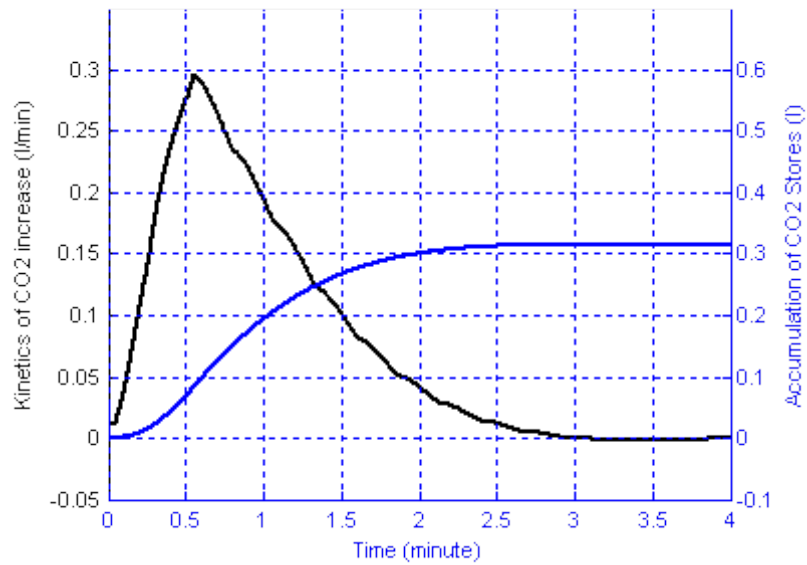


Figure 6.20. Kinetics of the total body CO₂ stores during 60 W exercise; the black curve shows the increase and blue curve is the accumulation of CO₂ stores.

Figure has been removed
due to Copyright restrictions.

Figure 6.21. Kinetics of body CO₂ stores calculated from experimental data. Diagram taken from (Chuang et al., 1999).

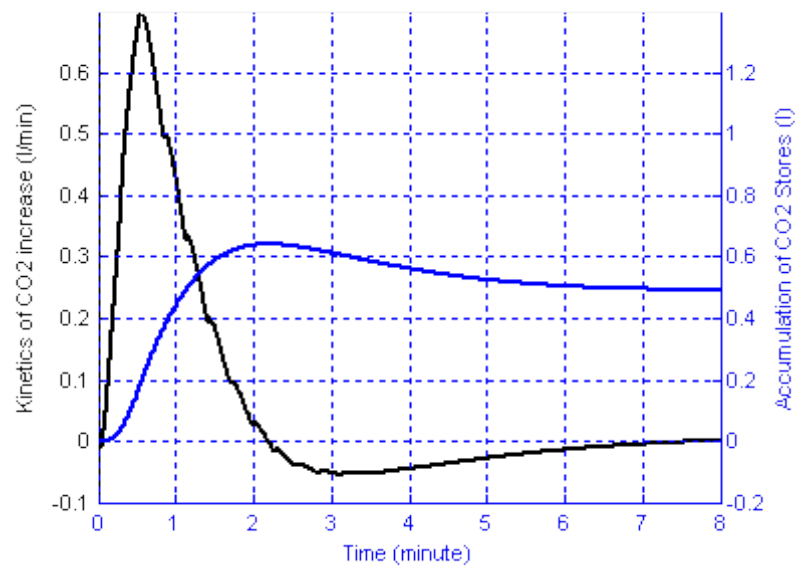


Figure 6.22. Kinetics of CO₂ stores during exercise above LT (150W); CO₂ is added into the stores during the first minutes but is later reduced due to acidosis.

6.10. Discussion

6.10.1. General Impressions

The overall results of the simulation investigations for conditions above the lactate threshold and their comparison with experimental results suggest that the model is broadly satisfactory. In incremental simulation, several variables, such as O₂ and CO₂ content, behave in the expected manner but several other variables show noticeable deviations from what is observed in experiments. Such differences may be present because of a number of reasons. For example, the developed model is based upon assumptions which may not be completely true for the condition of the subjects who participated in the experiments, For example, one or two parameters have been assigned as constants while in reality they are known to vary with work rate. Physiological parameters also have a large variability among subjects so that a set of parameters that is appropriate for one group of subjects may not be adequate for another group. In other words, a model that is tuned using data from one group may not fit well into data from another group. In addition, the experimental results of Sun et al. (2001) were obtained by averaging data over 30-second intervals and the data are presented at intervals of one minute which may smear detailed variations that occur over shorter intervals of time.

Significant discrepancies between simulation and experimental results have been observed for mixed-venous pH and PCO₂. These discrepancies apparently arise not only because of model limitation but also because of the calculation method. In our model, mixed-venous pH and PCO₂ are not involved in the main simulation and have been calculated from the simulation result for mixed-venous CO₂ content. The calculation is problematic. Using the algorithm from Douglas et al. (1988) to calculate PCO₂ requires

that the values of CO₂ content and pH to be known. On the other hand, using the Siggaard-Andersen nomogram to calculate pH (Andersen and Engel, 1960) requires one to know the values of CO₂ content and PCO₂. Thus, the fairly good simulation result for mixed-venous CO₂ content (Figure 6.4) has not led to similar quality for the mixed-venous pH and PCO₂ (Figures 6.5 and 6.6). Therefore, it is sensible with the present model to discard the results for mixed-venous pH and PCO₂ and not to use them in analysis.

The result of simulation with constant work rates is also broadly satisfactory. Responses of arterial lactate concentration show changes of the expected kind for changes of exercise intensity. Changes in the responses in terms of O₂ uptake and CO₂ output are also adequate but responses in terms of ventilation show some deviation from what is expected.

To our knowledge, this work is one of the first attempts to model the respiratory system for levels of exercise that include conditions above the lactate threshold. Most models created so far have limited their applicability to work rates below the lactate threshold. The reason for this restricted range in previous models is that at lower levels of exercise many variables change proportionally to changes in work rate or with percentage of O₂ uptake. Beyond the lactate threshold, complexity arises and some variables lose their proportionality or involve additional components which are not present during exercise below LT.

6.10.2.Potential Application

The model may be used to get insight into the behaviour of various variables in the respiratory control system for all domains of exercise. Several variables have been shown to behave fairly well so that further study may be conducted based on these particular variables. Three studies have been attempted so far and the results are shown in sections 6.9.4 – 6.9.6. However, it is accepted that this represents only a start in modelling the system at and above LT and a more thorough study is needed to achieve useful objectives.

In Section 6.9.4, it is shown that different values of Hb concentration result in different levels of mixed-venous CO₂ and O₂ content but the difference barely affects pulmonary gas exchange. This simulation may show the effect of different levels of [Hb] in terms of the ability to perform exercise and may describe the effect of [Hb] increase during incremental exercise.

In Section 6.9.5, it is shown that cardiac output increases in a more or less linear fashion with work rate. As a consequence, the correlation between cardiac output and oxygen uptake diminishes when exercise goes into the heavy exercise domain. The simulation therefore suggests that cardiac output might be better estimated using the work rate to calculate the increase in addition to the base line value at unloaded exercise.

Section 6.9.6 shows how the CO₂ stores may change during exercise with constant work rate below and above the lactate threshold. The simulation shows that below LT, a quantity of produced CO₂ does not leave human body and is stored somewhere. When the work rate increases, the amount of stored CO₂ is also increased. However, when the work rate is in the higher exercise domain, metabolic acidosis increases which reduces bicarbonate concentration to buffer the increased hydrogen ion level so that the stored CO₂ is later reduced.

Studies of the stored CO₂ may be conducted using the model for incremental exercise conditions. From simulation investigations of this kind, it is possible to see how bicarbonate concentration and blood CO₂ content change during exercise. However, with the present model, observation of CO₂ stores within compartments is not possible because the model does not calculate the CO₂ content of each compartment.

6.10.3. Limitation and Improvement

Despite some positive results and possible application, the model can (and needs to) be improved to perform better, especially at work rates within the heavy exercise domain. Such improvement would require reformulation of the kinetics for several variables and adjustment of some parameter values which include ventilation and hyperventilation, acidosis and muscle fibre recruitment.

Hyperventilation for incremental exercise has been formulated differently from the modelling for constant work rates, one being dependent on arterial [La] and the other being dependent on work rate. Although dependency on arterial [La] is justifiable to some extent in terms that there is a report suggesting the close correlation between ventilation and arterial [La] (Hardarson et al., 1998; McCoy and Hargreaves, 1992), those investigators, among many others (e.g. Paterson et al. (1989)), also suggest that potassium has an important role in the control of ventilation. In our model, using arterial [La] to estimate the increase of ventilation during incremental exercise may be considered acceptable. However, the same estimate does not work when applied to simulation with constant work rates because lactate increase during early exercise would make the estimate become too large (although it can be used to estimate the increase for steady state conditions).

Apparently, the control of ventilation during exercise may be separated into two conditions. In the aerobic condition, the increase of ventilation relates to the increase of body metabolism of respiratory gases. In the anaerobic condition, the increase of ventilation relates to the offset of the total ATP required from the amount of ATP that is aerobically regenerated. During moderate exercise, ATP requirements are fulfilled aerobically so ventilation can be observed to increase linearly with pulmonary gas exchange. During heavy exercise, when anaerobic ATP regeneration increases,

ventilation increases likewise. During very heavy exercise, when anaerobic ATP regeneration soars, ventilation increases greatly. One important feature of the control of ventilation that has not been fully implemented so far in our model is that it has to be applicable for all types of exercise stimuli (e.g. step, incremental, or sinusoidal patterns).

It might not be very good to assume that acidosis is equal to the lactate increase particularly when dealing with simulation for transient conditions. Lactate and proton are produced through different mechanisms in exercise metabolism (Robergs et al., 2004). Proton originates from ATP hydrolysis. Hence once ATP is utilized, proton is released. On the other hand, lactate is produced when pyruvate reacts with proton, where both pyruvate and proton are the product of glycolysis (i.e. breakdown of glucose/glycogen). The delayed start of muscle oxygen extraction might suggest that glycolysis starts later than ATP hydrolysis and consequently proton production may occur earlier than lactate production.

In incremental exercise, when the system can be considered to be in a transient condition all the time, the level of muscle O_2 extraction always lags the level of ATP hydrolysis. In such a condition, proton release may become higher than the lactate release resulting in acidosis that is higher than predicted by the increase of lactate concentration. Furthermore, lactate release is quite slow so that the amount of proton released at any time may exceed the lactate release. The discrepancy can be more significant when the muscle energy demand is larger than that can be provided by aerobic metabolism, e.g. when work rate increases beyond the rate equivalent to maximal $V'O_2$.

The current model assumes a simple policy in terms of the recruitment of muscle fibres of different types. This assumption has led to relatively simple kinetics of muscle O_2 extraction and it may have simplified the profile of lactate uptake and release for the muscle compartment. On the other hand, it has been observed that O_2 uptake can have a delayed slow component increase during heavy exercise (Whipp et al., 1982) which implies that some fibres can be recruited after the onset of exercise. Indeed, Carter et al. (2006) pointed out that muscle fibre recruitment can be altered and that this influences the VO_2 slow component. Incorporation of the Henneman Principle of fibre recruitment (Henneman et al., 1965) might improve the model characteristics as this would introduce a delayed VO_2 slow component which would affect the CO_2 kinetics. Delayed additional muscle fibre recruitment would be expected to affect the kinetics of lactate concentration and pH. The attainment of the peak value of arterial [La] would consequently be delayed but this is just what has been observed experimentally by Freund and Zouloumian (1981).

6.11. Summary

The model gives various quality of response when compared to various sources of published literature. Simulation result for pulmonary gas exchange, arterial gas content

and lactate concentration is good. However, the result for arterial partial pressure and pH shows noticeable deviations. Nevertheless, the model has several potential applications, for example to show the effect of Hb concentration and to describe the changes in CO₂ stores during exercise. Improvement is still needed especially in the formulation of ventilation.

Chapter 7

Overall Discussion, Conclusions and Future Work

7.1. Summary, Model Assumptions and Limitations

The human respiratory control system is highly complex and a model is therefore a very helpful tool in describing, interpreting and explaining the system. Many models of this system have been developed in the past with different purposes and with various levels of success. However, there has been little previous work aimed at the development of a general model that describes the behaviour of respiratory control system for exercise conditions below and above the lactate threshold. Therefore the research work undertaken in the project and presented in this thesis has had, as its objective, the development of a general model that can be applied to exercise conditions in all domains.

7.1.1. Reconstruction of Saunders, Bali and Carson model

A general review of models developed in the past was conducted at an early stage in the work and specific model, i.e. the model developed by Saunders, Bali and Carson (1980), was selected to further assess the possibility of modifying and improving an existing description of the system so that it could become applicable for conditions of exercise. The inclusion of a muscle compartment in that model and the initial work by Saunders and his colleagues to simulate exercise conditions was the main reason why this particular model was selected. The inclusion of cyclic respiration was a further positive aspect of the model that contributed to its selection in the initial stages of the study.

Reconstruction of the Saunders, Bali and Carson model has been conducted using modern simulation software (Simulink), as presented in Chapter 3. The reconstructed model gives similar simulation results to that obtained in the original model suggesting a fairly successful replication. However, the Saunders, Bali and Carson model was found to be unable to accurately describe the results of exercise tests because several assumptions within the model are not physiologically appropriate. Both cardiac output and the gain of the ventilatory controller have been assumed, in that model, to increase abruptly at the onset of exercise. The resulting ventilation increases too rapidly and shows an overshoot at the onset of exercise which is not found in experimental test results.

Modifications of the Saunders, Bali and Carson model have been tried to make the model applicable for conditions of exercise. The modelling of cardiac output has been modified so that this quantity increases exponentially following the kinetics of a first-order system. Moreover, a ventilatory control component has been introduced which will cause the ventilation to have kinetics of a first-order exponential system in addition to the control component that depends on PaCO_2 and PaO_2 . The results obtained from the modified simulation model are more realistic in that they correspond more closely to experimental

findings. In the modified model ventilation does not show an overshoot at the onset of exercise and PaCO_2 does not show an undershoot, just as is usually observed in real experiments.

However, further modification of the Saunders, Bali and Carson model is constrained because several assumptions within that model are physiologically inappropriate for exercise conditions. Adjustment of the ventilatory controller gain is not sufficient to explain what happens in exercise because it is assumed in the structure of the model that ventilation is fully dependent on PaCO_2 and PaO_2 , which contradicts the idea, which is well-supported by experimental evidence, that there should be at least one other factor that contributes to ventilation during exercise. The method of calculation of the tidal volume which is an essential element of the cyclic description of ventilation may not apply for high values of ventilation, which is common in heavy exercise conditions. Also the calculation of gas partial pressures in the tissue compartment is hard to verify and is dependent on the assumption that the tissue compartment has a constant volume which may not be the case for muscle under exercise conditions.

7.1.2. Model for exercise conditions below the lactate threshold

A new model has therefore been developed in which an attempt has been made to omit the features of the Saunders, Bali and Carson model that may be inadequate in attempting to describe the respiratory system for exercise conditions and to add features that make the model applicable for such conditions. Chapter 4 describes the development of the new model along with the corresponding simulation results. The new model is not necessarily more complex in all respects than the Saunders, Bali and Carson description. In fact, some of the compartmental representations that provide the sub-models in the new simulation model are actually simpler in form than the corresponding sub-models in the earlier description.

The lung compartment has been heavily simplified and it does not feature cyclic respiration in the new description. The alveolar O_2 and CO_2 ventilation is assumed equal to the lung ventilation and is calculated based on Fick's principle. The arterial partial pressure of oxygen and carbon dioxide are calculated based on ideal lung conditions, in which it is assumed that there is no right-to-left blood shunt and no diffusion limitation, and that there is perfect matching of ventilation to perfusion.

In the tissue compartment, the O_2 and CO_2 partial pressures are not calculated and therefore there is no need to make an assumption about the constancy of tissue volume. The tissue O_2 consumption and CO_2 production directly modify the tissue venous partial pressure and the calculation is based on Fick's principle. This leads to a simpler formulation, yet the parameter values may be experimentally estimated. For example, muscle O_2 consumption may be estimated experimentally by measuring the O_2 content in

the muscle artery and muscle vein and measuring the blood flow into the muscle. This approach is positive in that it cuts out the need to use the pressure-content relationship of O_2 or CO_2 inside the tissue compartment because that relationship has not been convincingly validated.

The time course of muscle O_2 consumption has been approximated by a first-order exponential function with a magnitude which is proportional to the increase of exercise work rate. The muscle CO_2 production is calculated based on the O_2 consumed, the fuel utilized in the metabolism (i.e. the RQ factor) and the muscle CO_2 storage capacity. The O_2 consumption and the CO_2 production of other tissues are assumed constant.

Blood that transports oxygen and carbon dioxide shows a two-phase increase in flow. The first phase (phase 1) is short and rapid and the second phase (phase 2) is first-order exponential. The increase of cardiac output during exercise is assumed to go to muscle, so blood flow to other tissues is assumed constant.

Blood storage of O_2 and CO_2 depends on the partial pressure of the respective gas considering the Haldane and Bohr Effect. Kelman's equation is used to relate the oxygen partial pressure and content in blood. Douglas's approach is used to calculate CO_2 content and partial pressure relationship which is applicable in exercise conditions. Other factors such as acidity (blood pH) and haemoglobin concentration is also taken into account but temperature is assumed constant at 37°C.

Blood acidity is calculated using the Siggaard-Andersen nomogram which takes into account the variation of buffer base, base excess and CO_2 partial pressure. The calculation will achieve greater accuracy if major ions that change during exercise are involved. However, in this model only lactate is included. Because lactate transport out of the muscle is always accompanied by hydrogen ions (protons) in a lactate-proton co-transport mechanism, addition of lactate into the blood stream is equivalent to addition of strong acid, which means a reduction in base excess. Calculation of normal buffer base depends on the value of blood haemoglobin content, which increases during exercise.

Modelling ventilation during exercise proved the most difficult aspect of model development because the exact mechanism that rules the control of ventilation has not yet been revealed from experimental studies. Therefore, for moderate exercise, ventilation has been approximated using an empirical relationship which states that ventilation increases linearly with CO_2 output up to the ventilatory compensation point.

Simulation results for moderate exercise conditions using the new model show generally good agreement with experimental findings for the following observed quantities: ventilation, O_2 uptake, CO_2 output, gas partial pressure in artery and mixed-venous, lactate concentration in the early period of exercise (which resembles early acidosis), and mixed-venous and arterial pH. The model response during phase 1 supports the notion that pulmonary O_2 uptake has a correlation with cardiac output and CO_2 output has a

correlation with ventilation (at least during phase 1). A model test has been carried to check whether or not muscle has the capacity to store CO₂. Simulation supports the suggestion that muscle is capable of storing CO₂ which slows down the kinetics of muscle CO₂ production compared to the kinetics of O₂ consumption. However, the slowing of muscle CO₂ production does not necessarily imply that the kinetics of pulmonary CO₂ output is slower than O₂ uptake because the effects of acidosis may change the kinetics of V'CO₂ for higher exercise work rates.

7.1.3. Lactate metabolism

Lactate metabolism is discussed in Chapter 5. Lactate concentration in muscle changes in two different ways. In normal conditions, lactate and pyruvate are in an equilibrium state where concentration changes of one species will lead to proportional changes of the other species. This equilibrium state materializes in the form of a constant lactate to pyruvate ratio and is attained in steady-state conditions. During steady state conditions of exercise, lactate concentration tends to be higher than at rest due to the higher pyruvate concentration. In the condition of acidosis, hydrogen ion and pyruvate tend to react to form lactate so that lactate concentration increases resulting in a higher value of the lactate to pyruvate ratio. Acidosis occurs at the onset of exercise, which is called early acidosis, and during heavy exercise.

A portion of muscle lactate is transported into the blood stream by a slow mechanism called lactate proton co-transport. In a 30 second maximal exercise test that results in a peak muscle lactate concentration at the end of the exercise, it can take 3 – 10 minutes before the arterial lactate concentration attains its peak value. Longer still is the recovery, which can take 60 minutes before arterial lactate gets close to the rest value.

The kinetics of arterial lactate concentration has been observed to be similar to a model of two first order systems (see Figures 6 and 8 of Chapter 5). Freund and co-workers (Freund and Zouloumian, 1981; Freund and Gendry, 1978) have used a two-tank system to describe this characteristic where one tank represents muscle and the other tank represents blood and other tissues. Although the output of this model fits the experimental result well, their model cannot be combined conveniently with our model of the respiratory control system. Instead, we suggest that the two first-order system characteristic is an inherent response of the muscle itself and the blood cannot be represented as the other tank in the two-tank system. An experiment needs to be devised to establish which of these two hypotheses is more likely to be correct.

7.1.4. Model for exercise above the lactate threshold

During heavy exercise, at least two quantities show non linearity: muscle O₂ consumption and ventilation. This is described in Chapter 6. Muscle O₂ consumption has

an additional slow component increase, which has been suggested to relate to the recruitment of new muscle fibres in the course of exerting the work. The present model, however, incorporates a simple policy of fibre recruitment so the slow component increase is not visible during exercise tests with constant work rates.

Ventilation also gets an additional component. During heavy exercise, ventilation is higher than required to maintain PaCO_2 at or near resting level. That is why the lung is called upon to hyperventilate, which is apparently needed to reduce acidosis. The occurrence of hyperventilation complicates the modelling of ventilation. In the incremental exercise test, an additional component of ventilation during heavy exercise has been approximated using a linear function of lactate concentration, which has been observed to correlate well with ventilation. However, this is inapplicable for exercise with constant work rates, so for that specific situation ventilation is estimated using the work rate increase above the lactate threshold.

With these approximations and estimates incorporated in the model, simulation results show that ventilation increases too quickly in the early period of exercise. This is most apparent during incremental exercise where the kinetics of ventilation is too fast compared to the kinetics of O_2 uptake before the lactate threshold and is slightly faster than the kinetics of CO_2 output in the period around the lactate threshold (see Figures 6.7 and 6.8).

7.1.5. Limitation and potential application

This modelling process has not taken into account the condition of recovery (the off-transient at the end of the exercise period). During moderate exercise, the off-transient kinetics of O_2 uptake is in shape symmetrical to the on-transient kinetics of the fundamental component, but the cardiac output response does not show this symmetry (Yoshida and Whipp, 1994) which means that the formulation for the recovery transition has to be different from the formulation for on-transient condition. During heavy exercise such symmetry does not exist completely (Rossiter et al., 2002). Therefore, the model does not apply for the recovery condition or for an exercise stimulus that contains a diminishing value of work rate (e.g. repeated bouts or a sinusoidal pattern of exercise level).

Nevertheless, the developed model has the potential to be used to study the effect or contribution of certain variables to the response of the respiratory control system. As described in Chapter 6, the model may be used to describe the contribution of haemoglobin in exercise performance. The model may also be used to investigate how cardiac output changes during heavy exercise. Furthermore, the model may be used to describe body CO_2 store changes during heavy exercise. Other studies are possible and should be well conducted to achieve useful objectives.

Development of the model involves collection and use of relationships and parameter values from many published sources. This process is inevitable because of the complexity of the respiratory system. Moreover, the number of quantities that may be acquired from one single experiment is small compared to the overall number of variables involved in the model. Therefore, the parameters and relationships that are used in the model and the data for tuning and validation of the model have all come from different experiments with different methods, subjects and conditions. In this situation, external validation may not allow quantitative or statistical point by point comparison between model response and experimental data. Therefore, validation of our model has been conducted by comparing the qualitative features between the simulation and experimental results, such as the trends, patterns and steady state levels.

It is reasonable to expect a better model in terms of better characteristics and response when the modelling process involves experimental data obtained in an experiment that acquires as many quantities as possible. Although, the process may not directly produce a “good model”, it gives a better chance to reveal some aspects that may have not been accounted for so that suggestions can be raised whether to restructure or refine the model or to devise an experiment. Measurement precision (or the interval of data measurement) also contributes to model quality because a finer precision would certainly allow better tuning and validation and may reveal particular detail that is not visible in a gross data. Therefore it is desirable to obtain a large data set with good precision from within a single experiment.

7.2. Conclusions

1. Reconstruction of the Saunders, Bali and Carson (SBC) model has been conducted. The reconstructed model shows characteristics that are close to the SBC model and to experimental results in most cases. The SBC model is proved to perform well when tested with disturbances in rest condition. However, the application of the SBC model for conditions of exercise is constrained for the following reasons. The model controller equation is dependent solely on gas arterial partial pressure which is not the case for exercise conditions. Gas partial pressures inside tissues are hard to measure thus the variable value in the model is hard to verify
2. Therefore, a model of the human respiratory control system for exercise conditions has been established. The simulation results of the model during moderate exercise condition are in good agreement with experimental findings. The model is able to reproduce the system responses for pulmonary gas exchange, gas partial pressure and

- content in arterial and mixed-venous blood, lactate concentration during early acidosis, pH and bicarbonate content.
3. Inclusion of lactate metabolism in the model is useful to describe acidosis which occurs in the early period of exercise and during work rates above the lactate threshold. The model of lactate metabolism shows a good profile of blood lactate concentration but still has unrealistic value for muscle compartment.
 4. Model responses for exercise conditions above the lactate threshold are broadly satisfactory in terms that many of the model responses have similar trends with experimental findings obtained from published sources. The responses in terms of pulmonary gas exchange and arterial gas content are close to those obtained in experiments but several other variables show deviations from experimental results. The kinetics for ventilation is too rapid suggesting that the control of ventilation in the model needs further improvement and reformulation.

7.3. Suggestions for Further Work

Various results have been obtained from the simulation of the developed model and some areas for possible improvements have already been hinted at. Further research on this model could well be beneficial in terms of improving the structure and parameter values of the current model and thus maximising its potential as a tool to assist in experimental physiological research.

The most important improvements relate to defining a better ventilation controller equation. Two approaches can be taken. Firstly, without having to change the structure of the model and include modelling of other chemical substances, an empirical controller description could be formulated using experimental data that relate ventilation and work rate. A proposal of this kind has already been made by Fujihara (1973a). Secondly, the model structure could be changed to include changes in potassium concentration because this substance has been widely suggested as providing a stimulus for ventilation during exercise conditions. The work by Ursino and Magosso (2004), Rowlands (2005) and McLoughlin (1994) could be taken as a starting point in such a study.

The muscle compartment could be restructured to contain a number of smaller compartments. Each of the small compartments may represent muscle fibre of different types with its own O_2 consumption, blood flow, and recruitment time. The advantage of this kind of modelling is the ability to reproduce O_2 kinetics that shows a delayed slow component increase.

The present model is not applicable to the recovery condition. The off-transient kinetics of cardiac output and pulmonary gas exchange are not symmetrical with the on-

transient kinetics. Therefore, the model has to differentiate between these transients and incorporate an appropriate formulation accordingly. The work by Yoshida and Whipp (1994) and Rossiter et al. (2002) provides a useful starting point to define the formulation. Inclusion of the recovery condition into the model has an advantage that the model would be applicable to simulate exercise with repeated bouts, exercise with prior intense exercise and exercise involving a sinusoidal pattern.

Bibliography

1. Ahlborg G, Felig P (1982) Lactate and glucose exchange across the forearm, legs, and splanchnic bed during and after prolonged leg exercise. *J Clin Invest* 69: 45-54
2. Altenburg TM, Degens H, van Mechelen W, Sargeant AJ, de Haan A (2007) Recruitment of single muscle fibers during submaximal cycling exercise. *J Appl Physiol* 103: 1752-1756
3. Andersen OS, Engel K (1960) A new acid-base nomogram an improved method for the calculation of the relevant blood acid-base data. *Scandinavian Journal of Clinical and Laboratory Investigation* 12: 177-186
4. Andersen OS, Engel K, rgensen K, Astrup P (1960) A micro method for determination of pH, carbon dioxide tension, base excess and standard bicarbonate in capillary blood. *Scandinavian Journal of Clinical and Laboratory Investigation* 12: 172-176
5. Andersen OS (1962) The pH-log pCO₂ acid-base nomogram revised. *Scandinavian Journal of Clinical and Laboratory Investigation* 14: 598-604
6. Bache, Richard A. Time-Domain System Identification Applied to Non-Invasive Determination of Cardio-Pulmonary Quantities. 1-370. 1981. University of Glasgow.
7. Bangsbo J, Krstrup P, Gonzalez-Alonso J, Boushel R, Saltin B (2000) Muscle oxygen kinetics at onset of intense dynamic exercise in humans. *Am J Physiol Regul Integr Comp Physiol* 279: R899-R906
8. Barstow TJ, Mole PA (1991) Linear and nonlinear characteristics of oxygen uptake kinetics during heavy exercise. *J Appl Physiol* 71: 2099-2106
9. Barstow TJ, Mole PA (1987) Simulation of pulmonary O₂ uptake during exercise transients in humans. *J Appl Physiol* 63: 2253-2261
10. Bassett DRJ, Howley ET (2000) Limiting factors for maximum oxygen uptake and determinants of endurance performance. *Medicine & Science in Sports & Exercise* 32: 70-84
11. Batzel JJ, Tran HT (2000a) Stability of the human respiratory control system 1. *Journal of Mathematical Biology* 41: 45-79
12. Batzel JJ, Tran HT (2000b) Stability of the human respiratory control system 2. *Journal of Mathematical Biology* 41: 80-102
13. Beaver WL, Wasserman K, Whipp BJ (1986) Bicarbonate buffering of lactic acid generated during exercise. *J Appl Physiol* 60: 472-478
14. Bertram FW, Wasserman K, Van Kessel AL (1967) Gas exchange following lactate and pyruvate injections. *J Appl Physiol* 23: 190-194
15. Bonen A, McCullagh KJ, Putman CT, Hultman E, Jones NL, Heigenhauser GJ (1998) Short-term training increases human muscle MCT1 and femoral venous lactate in relation to muscle lactate. *Am J Physiol Endocrinol Metab* 274: E102-E107
16. Brice AG, Forster HV, Pan LG, Funahashi A, Lowry TF, Murphy CL, Hoffman MD (1988) Ventilatory and PaCO₂ responses to voluntary and electrically induced leg exercise. *J Appl Physiol* 64: 218-225
17. Butler PJ, Turner DL (1988) Effect of training on maximal oxygen uptake and aerobic capacity of locomotory muscles in tufted ducks, *Aythya fuligula*. *J Physiol (Lond)* 401: 347-359
18. Cabrera M, Saidel G, Kalhan S (1998) Role of O₂ in Regulation of Lactate Dynamics during Hypoxia: Mathematical Model and Analysis. *Annals of Biomedical Engineering* 26: 1-27
19. Cabrera ME, Saidel GM, Kalhan SC (1999) Lactate metabolism during exercise: analysis by an integrative systems model. *Am J Physiol Regul Integr Comp Physiol* 277: R1522-R1536

20. Capek JM, Roy RJ (1988) Noninvasive measurement of cardiac output using partial CO₂ rebreathing. *Bio Eng , IEEE Trans* 35: 653-661
21. Carter H, Pringle JSM, Boobis L, Jones AM, Doust JH (2006) Muscle glycogen depletion alters oxygen uptake kinetics during heavy exercise. *Medicine & Science in Sports & Exercise* 36: 965-972
22. Casaburi R, Barstow TJ, Robinson T, Wasserman K (1989a) Influence of work rate on ventilatory and gas exchange kinetics. *J Appl Physiol* 67: 547-555
23. Casaburi R, Daly J, Hansen JE, Effros RM (1989b) Abrupt changes in mixed venous blood gas composition after the onset of exercise. *J Appl Physiol* 67: 1106-1112
24. Cerretelli P, Shindell D, Pendergast DP, Prampero PED, Rennie DW (1977) Oxygen uptake transients at the onset and offset of arm and leg work. *Respiration Physiology* 30: 81-97
25. Cheriack NS, Longobardo GS (1970) Oxygen and carbon dioxide gas stores of the body. *Physiol Rev* 50: 196-243
26. Chuang ML, Ting H, Otsuka T, Sun XG, Chiu FYL, Beaver WL, Hansen JE, Lewis DA, Wasserman K (1999) Aerobically generated CO₂ stored during early exercise. *J Appl Physiol* 87: 1048-1058
27. Cobelli C, Carson E (2001) An Introduction to Modelling Methodology. In *Modeling Methodology for Physiology and Medicine*, Carson, E., Cobelli, C. (eds) pp 1-13. Academic Press: San Diego
28. Cohen R, Overfield EM, Kylstra JA (1971) Diffusion component of alveolar-arterial oxygen pressure difference in man. *J Appl Physiol* 31: 223-226
29. Coyle EF, Coggan AR, Hopper MK, Walters TJ (1988) Determinants of endurance in well-trained cyclists. *J Appl Physiol* 64: 2622-2630
30. Cruz JC, Rahn H, Farhi LE (1969) Mixed venous PO₂, PCO₂, pH, and cardiac output during exercise in trained subjects. *J Appl Physiol* 27: 431-434
31. Cunningham DJ (1987) Studies on arterial chemoreceptors in man. *J Physiol (Lond)* 384: 1-26
32. Davis JA, Vodak P, Wilmore JH, Vodak J, Kurtz P (1976) Anaerobic threshold and maximal aerobic power for three modes of exercise. *J Appl Physiol* 41: 544-550
33. Davis JA, Whipp BJ, Wasserman K (1980) The relation of ventilation to metabolic rate during moderate exercise in man. *Eur J App Physiol* 97-108
34. De Cort SC, Innes JA, Barstow TJ, Guz A (1991) Cardiac output, oxygen consumption and arteriovenous oxygen difference following a sudden rise in exercise level in humans. *J Physiol (Lond)* 441: 501-512
35. Defares JG (1964) Principles of feedback control and their application to the respiratory control system. In *Handbook of Physiology - Respiration I*, pp 649-680.
36. Dolensek, Janez, Podnar, Tomaz, Runovc, Franc, and Kordas, Marjan. Analog simulation of cardiovascular physiology: exercise in man. 2[1]. 2007. Slovenia, Eurosim/Slosim. *Proc. EUROSIM 2007*. Zupancic, Borut, Karba, Rihard, and Blazic, Saso.
37. Douglas AR, Jones NL, Reed JW (1988) Calculation of whole blood CO₂ content. *J Appl Physiol* 65: 473-477
38. Douglas CG, Haldane JS (1909) The regulation of normal breathing. *J Physiol (Lond)* 38: 420-440
39. Farhi LE, Rahn H (1960) Dynamics of changes in carbon dioxide stores. *Anesthesiology* 21 : 604-614
40. Fenn WO, Craig AB, Jr. (1963) Effect of CO₂ on respiration using a new method of administering CO₂. *J Appl Physiol* 18: 1023-1024
41. Forster HV, Pan LG, Funahashi A (1986) Temporal pattern of arterial CO₂ partial pressure during exercise in humans. *J Appl Physiol* 60: 653-660
42. Fowle ASE, Matthews CME, Campbell EJM (1964) The rapid distribution of h₂O and co₂ in the body in relation to the immediate carbon dioxide capacity. *Clinical Science* 27: 51-65
43. Freund H, Gendry P (1978) Lactate kinetics after short strenuous exercise in man. *Eur J App Physiol* 39: 123-135

44. Freund H, Zouloumian P (1981) Lactate after exercise in man: I. Evolution kinetics in arterial blood. *Eur J App Physiol* 46: 121-133
45. Fujihara Y, Hildebrandt J, Hildebrandt JR (1973a) Cardiorespiratory transients in exercising man. II. Linear models. *J Appl Physiol* 35: 68-76
46. Fujihara Y, Hildebrandt JR, Hildebrandt J (1973b) Cardiorespiratory transients in exercising man. I. Tests of superposition. *J Appl Physiol* 35: 58-67
47. Geers C, Gros G (2000) Carbon dioxide transport and carbonic anhydrase in blood and muscle. *Physiol Rev* 80: 681-715
48. Grassi B, Poole DC, Richardson RS, Knight DR, Erickson BK, Wagner PD (1996) Muscle O₂ uptake kinetics in humans: implications for metabolic control. *J Appl Physiol* 80: 988-998
49. Grassi B (2003) Oxygen uptake kinetics: old and recent lessons from experiments on isolated muscle in situ. *Eur J App Physiol* 90: 242-249
50. Grassi B, Quaresima V, Marconi C, Ferrari M, Cerretelli P (1999) Blood lactate accumulation and muscle deoxygenation during incremental exercise. *J Appl Physiol* 87: 348-355
51. Gray JS (1946) The multiple factor theory of the control of respiratory ventilation. *Science* 103: 739-744
52. Grodins FS, Buell J, Bart AJ (1967) Mathematical analysis and digital simulation of the respiratory control system. *J Appl Physiol* 22 : 260-267
53. Grodins FS, Gray JS, Schroeder KR, Norins AL, Jones RW (1954) Respiratory responses to CO₂ inhalation. a theoretical study of a nonlinear biological regulator. *J Appl Physiol* 7: 283-308
54. Gutierrez G, Chawla LS, Seneff MG, Katz NM, Zia H (2005) Lactate concentration gradient from right atrium to pulmonary artery. *Critical Care* 9: R425-R429
55. Habedank D, Reindl I, Vietzke G, Bauer U, Sperfeld A, Glaeser S, Wernecke KD, Kleber FX (1998) Ventilatory efficiency and exercise tolerance in 101 healthy volunteers. *Eur J App Physiol* 421-426
56. Hardarson T, Skarphedinsson JO, Sveinsson T (1998) Importance of the lactate anion in control of breathing. *J Appl Physiol* 84: 411-416
57. Henneman E, Somjen G, Carpenter DO (1965) FUNCTIONAL SIGNIFICANCE OF CELL SIZE IN SPINAL MOTONEURONS. *J Neurophysiol* 28: 560-580
58. Henry RP (1996) Multiple Roles of Carbonic Anhydrase in Cellular Transport and Metabolism. *Annual Review of Physiology* 58: 523-538
59. Hermansen L, Vaage O (1977) Lactate disappearance and glycogen synthesis in human muscle after maximal exercise. *Am J Physiol Gastrointest Liver Physiol* 233: G422-G429
60. Hill DK (1940) The time course of the oxygen consumption of stimulated frog's muscle. *J Physiol (Lond)* 98: 207-227
61. Hubbard JL (1973) The effect of exercise on lactate metabolism. *J Physiol (Lond)* 231: 1-18
62. Hughson RL, Cochrane JE, Butler GC (1993) Faster O₂ uptake kinetics at onset of supine exercise with than without lower body negative pressure. *J Appl Physiol* 75: 1962-1967
63. Hughson RL, Morrissey M (1982) Delayed kinetics of respiratory gas exchange in the transition from prior exercise. *J Appl Physiol* 52: 921-929
64. Hughson RL, Tschakovsky ME (1999) Cardiovascular dynamics at the onset of exercise. *Medicine & Science in Sports & Exercise* 31: 1005-1010
65. Hultman E, Greenhaff PL (1991) Skeletal muscle energy metabolism and fatigue during intense exercise in man. *Science Progress* 361-370
66. Johnson AT (1991) *Biomechanics and Exercise Physiology*. John Wiley & Sons: New York
67. Jorfeldt L, Juhlin-Dannfelt A, Karlsson J (1978) Lactate release in relation to tissue lactate in human skeletal muscle during exercise. *J Appl Physiol* 44: 350-352
68. Juel C (1997) Lactate-proton cotransport in skeletal muscle. *Physiol Rev* 77: 321-358

69. Juel C, Klarskov C, Nielsen JJ, Krstrup P, Mohr M, Bangsbo J (2004) Effect of high-intensity intermittent training on lactate and H⁺ release from human skeletal muscle. *Am J Physiol Endocrinol Metab* 286: E245-E251
70. Katz A, Sahlin K (1988) Regulation of lactic acid production during exercise. *J Appl Physiol* 65: 509-518
71. Kelman GR (1966) Digital computer subroutine for the conversion of oxygen tension into saturation. *J Appl Physiol* 21: 1375-1376
72. Kelman GR (1967) Digital computer procedure for the conversion of PCO₂ into blood CO₂ content. *Respiration Physiology* 3: 111-115
73. Khoo MC, Kronauer RE, Strohl KP, Slutsky AS (1982) Factors inducing periodic breathing in humans: a general model. *J Appl Physiol* 53: 644-659
74. Kida K, Osada N, Akashi YJ, Sekizuka H, Izumo M, Ishibashi Y, Shimozato T, Hayashi A, Yoneyama K, Takahashi E, Suzuki K, Tamura M, Inoue K, Omiya K, Miyake F (2006) Functional capacity, skeletal muscle strength, and skeletal muscle volume in patients with myocardial infarction. *International Heart Journal* 47: 727-738
75. Kofranek, Jiri, Matousek, Stanislav, and Andriik, Michal. Border flux balance approach towards modelling acid-base chemistry and blood gases transport. 11-9-2007. Slovenia, Eurosim/Slosim.
76. Koga S, Poole DC, Shiojiri T, Kondo N, Fukuba Y, Miura A, Barstow TJ (2005) Comparison of oxygen uptake kinetics during knee extension and cycle exercise. *Am J Physiol Regul Integr Comp Physiol* 288: R212-R220
77. Kowalchuk JM, Heigenhauser GJ, Lindinger MI, Sutton JR, Jones NL (1988) Factors influencing hydrogen ion concentration in muscle after intense exercise. *J Appl Physiol* 65: 2080-2089
78. Krogh A, Lindhard J (1913) The regulation of respiration and circulation during the initial stages of muscular work. *J Physiol (Lond)* 47: 112-136
79. Krstrup P, Soderlund K, Mohr M, Bangsbo J (2004a) The slow component of oxygen uptake during intense, sub-maximal exercise in man is associated with additional fibre recruitment. *Pfluegers Archive* 447: 855-866
80. Krstrup P, Soderlund K, Mohr M, Bangsbo J (2004b) Slow-twitch fiber glycogen depletion elevates moderate-exercise fast-twitch fiber activity and O₂ uptake. *Medicine & Science in Sports & Exercise* 36: 973-982
81. Lador F, Azabji Kenfack M, Moia C, Cautero M, Morel DR, Capelli C, Ferretti G (2006) Simultaneous determination of the kinetics of cardiac output, systemic O₂ delivery, and lung O₂ uptake at exercise onset in men. *Am J Physiol Regul Integr Comp Physiol* 290: R1071-R1079
82. Lamarra N, Ward SA, Whipp BJ (1989) Model implications of gas exchange dynamics on blood gases in incremental exercise. *J Appl Physiol* 66: 1539-1546
83. Levitzky MG (2003) *Pulmonary physiology*. McGraw-Hill: New York
84. Lewis SF, Taylor WF, Graham RM, Pettinger WA, Schutte JE, Blomqvist CG (1983) Cardiovascular responses to exercise as functions of absolute and relative work load. *J Appl Physiol* 54: 1314-1323
85. LLoyd BB, Jukes MGM, Cunningham DJC (1958) The relation between alveolar oxygen pressure and the respiratory response to carbon dioxide in man. *Q J Exp Physiol Cogn Med Sci* 43: 214-227
86. MacDonald MJ, Shoemaker JK, Tschakovsky ME, Hughson RL (1998) Alveolar oxygen uptake and femoral artery blood flow dynamics in upright and supine leg exercise in humans. *J Appl Physiol* 85: 1622-1628
87. Mahler M (1985) First-order kinetics of muscle oxygen consumption, and an equivalent proportionality between QO₂ and phosphorylcreatine level. Implications for the control of respiration. *J Gen Physiol* 86: 135-165
88. McCoy M, Hargreaves M (1992) Potassium and ventilation during incremental exercise in trained and untrained men. *J Appl Physiol* 73: 1287-1290
89. McLoughlin P, Popham P, Linton RA, Bruce RC, Band DM (1994) Exercise-induced changes in plasma potassium and the ventilatory threshold in man. *J Physiol (Lond)* 479: 139-147

90. Moeller DPF (1993) State of the art and future aspects of modeling and simulation in physiology and biomedical engineering. In *Biomedical Modelling and Simulation on a PC, A Workbench for Physiology and Biomedical Engineering*, van Brievingh RP, Moeller DPF (eds) pp 1-34. Springer-Verlag: New York
91. Murray-Smith DJ (1995) *Continuous system simulation*. Chapman & Hall: Glasgow
92. Murray-Smith DJ, Carson ER (1988) The Modelling Process in Respiratory Medicine. In *The Respiratory System*, Cramp DG, Carson ER (eds) pp 296-333. CROOM HELM: London & Sydney
93. Myers J, Ashley E (1997) Dangerous curves: a perspective on exercise, lactate and the anaerobic threshold. *Chest* 111 : 787-795
94. Neder JA, Nery LE, Peres CLOV, Whipp BJ (2001) Reference values for dynamic responses to incremental cycle ergometry in males and females aged 20 to 80. *Am J Respir Crit Care Med* 164: 1481-1486
95. Nichols G (1958) Serial changes in tissue carbon dioxide content during acute respiratory acidosis. *J Clin Invest* 37: 1111-1122
96. Olszowka AJ, Shykoff BE, Pendergast DR, Lundgren CEG, Farhi LE (2003) Cardiac output: a view from buffalo. *Eur J App Physiol* 90: 292-304
97. Osteras H, Hoff J, Helgerud J (2005) Effects of High-Intensity Endurance Training on Maximal Oxygen Consumption in Healthy Elderly People. *Journal of Applied Gerontology* 24: 377-387
98. Ozyener F, Rossiter HB, Ward SA, Whipp BJ (2001) Influence of exercise intensity on the on- and off-transient kinetics of pulmonary oxygen uptake in humans. *J Physiol (Lond)* 533: 891-902
99. Paterson DJ (1992) Potassium and ventilation in exercise. *J Appl Physiol* 72: 811-820
100. Paterson DJ, Robbins PA, Conway J (1989) Changes in arterial plasma potassium and ventilation during exercise in man. *Respiration Physiology* 78: 323-330
101. Peronnet F, Aguilaniu B (2005) Lactic acid buffering, nonmetabolic CO₂ and exercise hyperventilation: a critical reappraisal. *Resp Physiol & Neur.* 150: 4 – 18.
102. Poole DC, Gladden LB, Kurdak S, Hogan MC (1994) L-(+)-lactate infusion into working dog gastrocnemius: no evidence lactate per se mediates VO₂ slow component. *J Appl Physiol* 76: 787-792
103. Poole DC, Schaffartzik W, Knight DR, Derion T, Kennedy B, Guy HJ, Prediletto R, Wagner PD (1991) Contribution of excising legs to the slow component of oxygen uptake kinetics in humans. *J Appl Physiol* 71: 1245-1260
104. Powers SK, Beadle RE, Thompson D, Lawler J (1987) Ventilatory and blood gas dynamics at onset and offset of exercise in the pony. *J Appl Physiol* 62: 141-148
105. Radegran G (1997) Ultrasound Doppler estimates of femoral artery blood flow during dynamic knee extensor exercise in humans. *J Appl Physiol* 83: 1383-1388
106. Radegran G, Saltin B (1998) Muscle blood flow at onset of dynamic exercise in humans. *Am J Physiol Heart Circ Physiol* 274: H314-H322
107. Rausch SM, Whipp BJ, Wasserman K, Huszczuk A (1991) Role of the carotid bodies in the respiratory compensation for the metabolic acidosis of exercise in humans. *J Physiol (Lond)* 444: 567-578
108. Raynaud J, Bernal H, Bourdarias JP, David P, Durand J (1973) Oxygen delivery and oxygen return to the lungs at onset of exercise in man. *J Appl Physiol* 35: 259-262
109. Rice AJ, Thornton AT, Gore CJ, Scroop GC, Greville HW, Wagner H, Wagner PD, Hopkins SR (1999) Pulmonary gas exchange during exercise in highly trained cyclists with arterial hypoxemia. *J Appl Physiol* 87: 1802-1812
110. Richard R, Lonsdorfer-Wolf E, Dufour S, phane [2], Doutreleau S, phane [2], Oswald-Mammosser M, Billat V, ronique [3], Lonsdorfer J (2004) Cardiac output and oxygen release during very high-intensity exercise performed until exhaustion. *Eur J App Physiol* 93: 9-18
111. Richardson RS, Noyszewski EA, Kendrick KF, Leigh JS, Wagner PD (1995) Myoglobin O₂ desaturation during exercise. Evidence of limited O₂ transport. *J Clin Invest* 96: 1916-1926

112. Robergs RA, Ghiasvand F, Parker D (2004) Biochemistry of exercise-induced metabolic acidosis. *Am J Physiol Regul Integr Comp Physiol* 287: R502-R516
113. Rossiter HB, Ward SA, Kowalchuk JM, Howe FA, Griffiths JR, Whipp BJ (2002) Dynamic asymmetry of phosphocreatine concentration and O₂ uptake between the on- and off-transients of moderate- and high-intensity exercise in humans. *J Physiol (Lond)* 541: 991-1002
114. Roth DA, Stanley WC, Brooks GA (1988) Induced lactacidemia does not affect postexercise O₂ consumption. *J Appl Physiol* 65: 1045-1049
115. Rowell LB (1993) *Human cardiovascular control*. Oxford University Press: Oxford
116. Rowlands DS (2005) Model for the behaviour of compartmental CO₂ stores during incremental exercise. *Eur J App Physiol* 93: 555-568
117. Sahlin K, Alvestrand A, Brandt R, Hultman E (1978) Intracellular pH and bicarbonate concentration in human muscle during recovery from exercise. *J Appl Physiol* 45: 474-480
118. Sahlin K, Katz A, Henriksson J (1987) Redox state and lactate accumulation in human skeletal muscle during dynamic exercise. *Biochem J* 245: 551-556
119. Saunders KB (1980) Oscillations of arterial CO₂ tension in a respiratory model: some implications for the control of breathing in exercise. *J Appl Physiol* 84: 163-182
120. Saunders KB, Bali HN, Carson ER (1980) A Breathing Model Of The Respiratory System: The Controlled System. *J Theor Biol* 84 : 135-161
121. Saunders NR, Tschakovsky ME (2004) Evidence for a rapid vasodilatory contribution to immediate hyperemia in rest-to-mild and mild-to-moderate forearm exercise transitions in humans. *J Appl Physiol* 97: 1143-1151
122. Siggaard-Andersen O, Fogh-Andersen N (1995) Base excess or buffer base (strong ion difference) as measure of a non-respiratory acid-base disturbance. *Acta Anaesthesiologica Scandinavica - Supplementum* 39: 123-128
123. Singer RB, Hastings AB (1948) An improved clinical method for the estimation of disturbances of the acid-base balance of human blood. *Medicine (Baltimore)* 27: 223-242
124. Stringer W, Casaburi R, Wasserman K (1992) Acid-base regulation during exercise and recovery in humans. *J Appl Physiol* 72: 954-961
125. Stringer WW, Hansen JE, Wasserman K (1997) Cardiac output estimated noninvasively from oxygen uptake during exercise. *J Appl Physiol* 82: 908-912
126. Stuhmiller JH, Stuhmiller LM (2005) A mathematical model of ventilation response to inhaled carbon monoxide. *J Appl Physiol* 98: 2033-2044
127. Sun XG, Hansen JE, Garatachea N, Storer TW, Wasserman K (2002) Ventilatory efficiency during exercise in healthy subjects. *Am J Respir Crit Care Med* 166: 1443-1448
128. Sun XG, Hansen JE, Stringer WW, Ting H, Wasserman K (2001) Carbon dioxide pressure-concentration relationship in arterial and mixed venous blood during exercise. *J Appl Physiol* 90: 1798-1810
129. Sylvester JT, Cymerman A, Gurtner G, Hottenstein O, Cote M, Wolfe D (1981) Components of alveolar-arterial O₂ gradient during rest and exercise at sea level and high altitude. *J Appl Physiol* 50: 1129-1139
130. Teschl, Susanne. A global model for the Cardiovascular and Respiratory System. 1998. Karl-Franzens-Universit of Graz.
131. Ursino M, Magosso E (2004) Interaction among humoral and neurogenic mechanisms in ventilation control during exercise. *Annals of Biomedical Engineering* 32: 1286-1299
132. Van Beekvelt MCP, Shoemaker JK, Tschakovsky ME, Hopman MTE, Hughson RL (2001) Blood flow and muscle oxygen uptake at the onset and end of moderate and heavy dynamic forearm exercise. *Am J Physiol Regul Integr Comp Physiol* 280: R1741-R1747
133. van Hall G, Jensen-Urstad M, Rosdahl H, Holmberg HC, Saltin B, Calbet JAL (2003) Leg and arm lactate and substrate kinetics during exercise. *Am J Physiol Endocrinol Metab* 284: E193-E205

134. Ward SR, Lieber RL (2005) Density and hydration of fresh and fixed human skeletal muscle. *Journal of Biomechanics* 38: 2317-2320
135. Ward SA (2004a) Physiology of Breathing I. *Surgery* 22: i-v
136. Ward SA (2004b) Physiology of Breathing II. *Surgery* 22: 230-234
137. Wasserman K (1994) Coupling of external to cellular respiration during exercise: the wisdom of the body revisited. *Am J Physiol Endocrinol Metab* 266: E519-E539
138. Wasserman K, Beaver WL, Davis JA, Pu JZ, Heber D, Whipp BJ (1985) Lactate, pyruvate, and lactate-to-pyruvate ratio during exercise and recovery. *J Appl Physiol* 59: 935-940
139. Wasserman K, Hansen JE, Sue DY, Whipp BJ, Casaburi R (2005) *Principles of Exercise Testing and Interpretation*. Lippincott Williams & Wilkins: Philadelphia
140. Wasserman K, Van Kessel AL, Burton GG (1967) Interaction of physiological mechanisms during exercise. *J Appl Physiol* 22: 71-85
141. Wasserman K, Whipp BJ, Koyn SN, Beaver WL (1973) Anaerobic threshold and respiratory gas exchange during exercise. *J Appl Physiol* 35: 236-243
142. Wasserman K, Stringer WW, Casaburi R, Zhang YY (1997) Mechanism of the exercise hyperkalemia: an alternate hypothesis. *J Appl Physiol* 83: 631-643
143. Whipp BJ (1990) The control of exercise hyperpnoea. In *The control of breathing in man*, Whipp BJ (ed) pp 87-118. Manchester University Press: Manchester
144. Whipp BJ (1983) Ventilatory control during exercise in humans. *Annual Review of Physiology* 45: 393-413
145. Whipp BJ (1987) Dynamics of pulmonary gas exchange. *Circ* 76 : VI-18
146. Whipp BJ, Ward SA (1980) Ventilatory Control Dynamics during Muscular Exercise in Man. *International Journal of Sports Medicine* 1: 146-159
147. Whipp BJ, Ward SA (1982) Cardiopulmonary coupling during exercise. *J Exp Biol* 100: 175-193
148. Whipp BJ, Wasserman K (1969) Alveolar-arterial gas tension differences during graded exercise. *J Appl Physiol* 27: 361-365
149. Whipp BJ, Wasserman K (1972) Oxygen uptake kinetics for various intensities of constant-load work. *J Appl Physiol* 33: 351-356
150. Whipp BJ (1994a) The bioenergetic and gas exchange basis of exercise testing. *Clinics in Chest Medicine* 15: 173-192
151. Whipp BJ (1994b) The slow component of O₂ uptake kinetics during heavy exercise. *Medicine and Science in Sports and Exercise* 26: 1319-1326
152. Whipp BJ (1998) Breathing during exercise. In *Fishman's Pulmonary Diseases and Disorders*, Fishman AP (ed) pp 229-241. McGraw-Hill: New York
153. Whipp, Brian J., Rossiter, H. B., and Ward, Susan A. (2002) Exertional oxygen uptake kinetics: a stamen of stamina? 30_[4], 237-247. 5-2-2002. England. *Biochemical Society Transactions*. 5-2-2002.
154. Whipp BJ, Ward SA, Lamarra N, Davis JA, Wasserman K (1982) Parameters of ventilatory and gas exchange dynamics during exercise. *J Appl Physiol* 52: 1506-1513
155. Yoshida T, Whipp BJ (1994) Dynamic asymmetries of cardiac output transients in response to muscular exercise in man. *J Physiol (Lond)* 480: 355-359
156. Zouloumian P, Freund H (1981) Lactate after exercise in man: II. Mathematical model. *Eur J App Physiol* 46: 135-147

Appendix

A. Diagram of Saunders, Bali and Carson Model

Simulation parameters:

Solver	ode45 (Dormand-Prince)
Step size	Variable
Max step size	0.1 s
Relative tolerance	0.0001

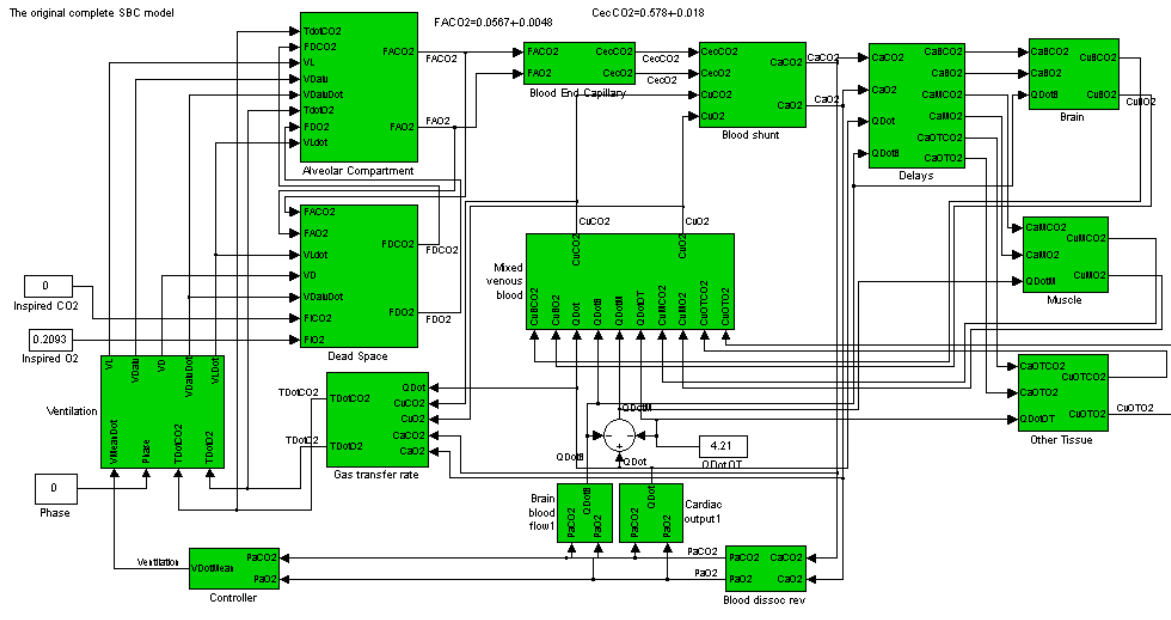


Fig A-1. Main diagram

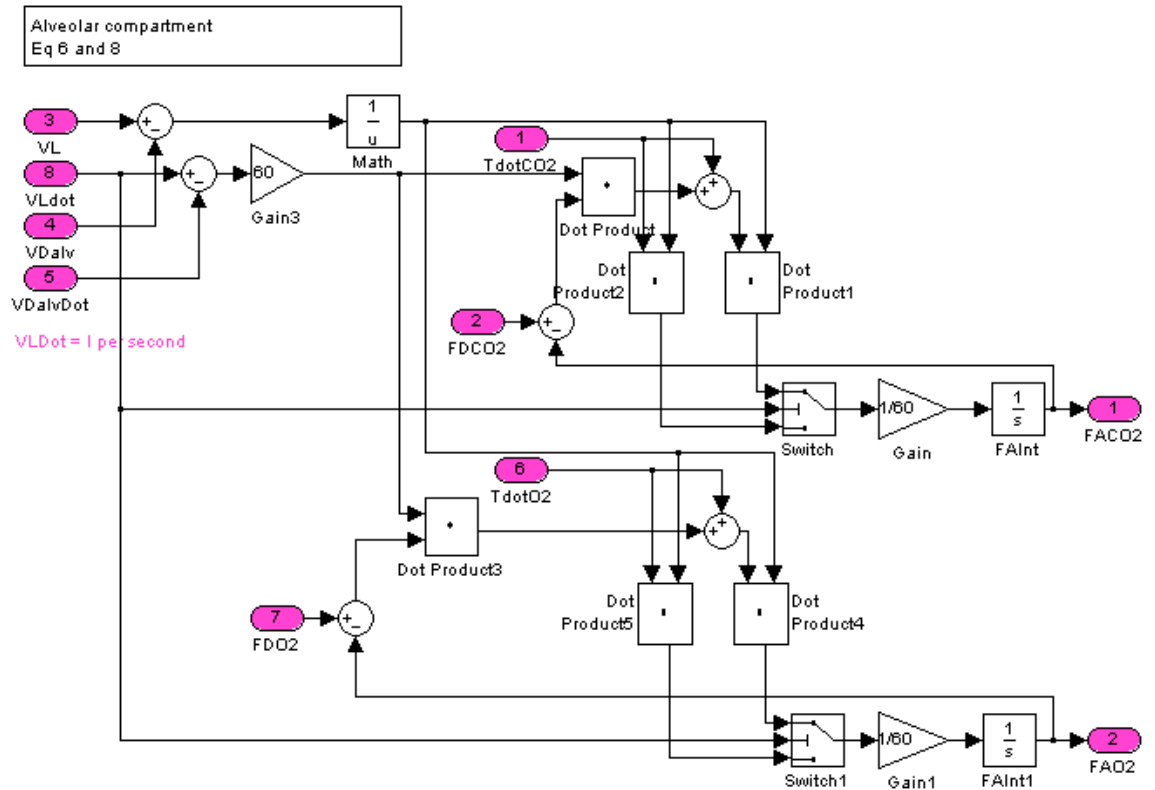


Fig A-2. Alveolar compartment

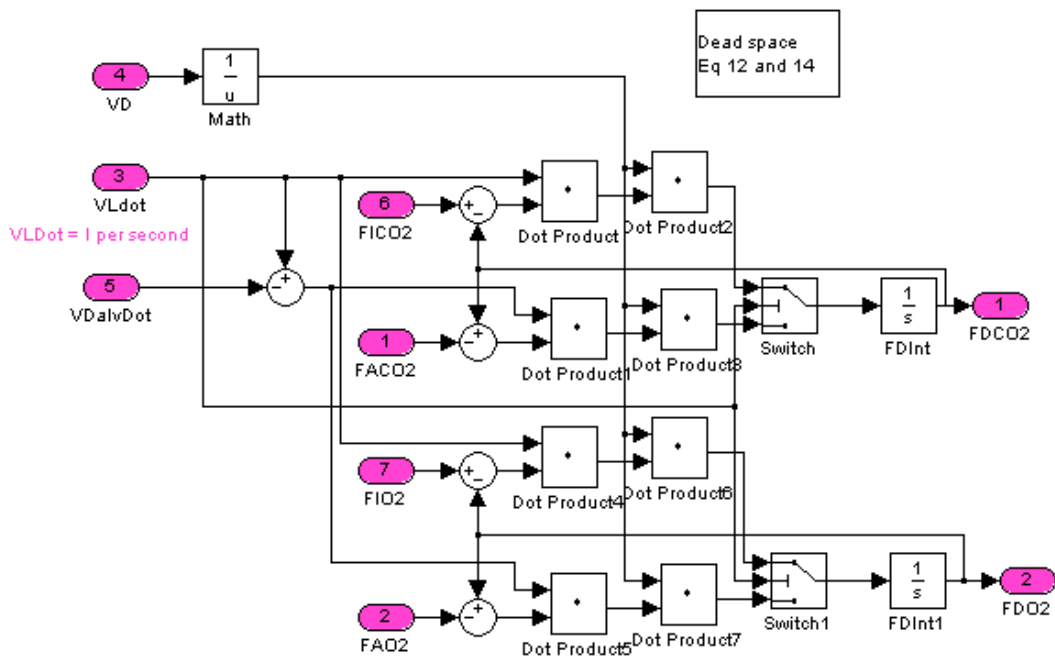


Fig A-3. Dead space

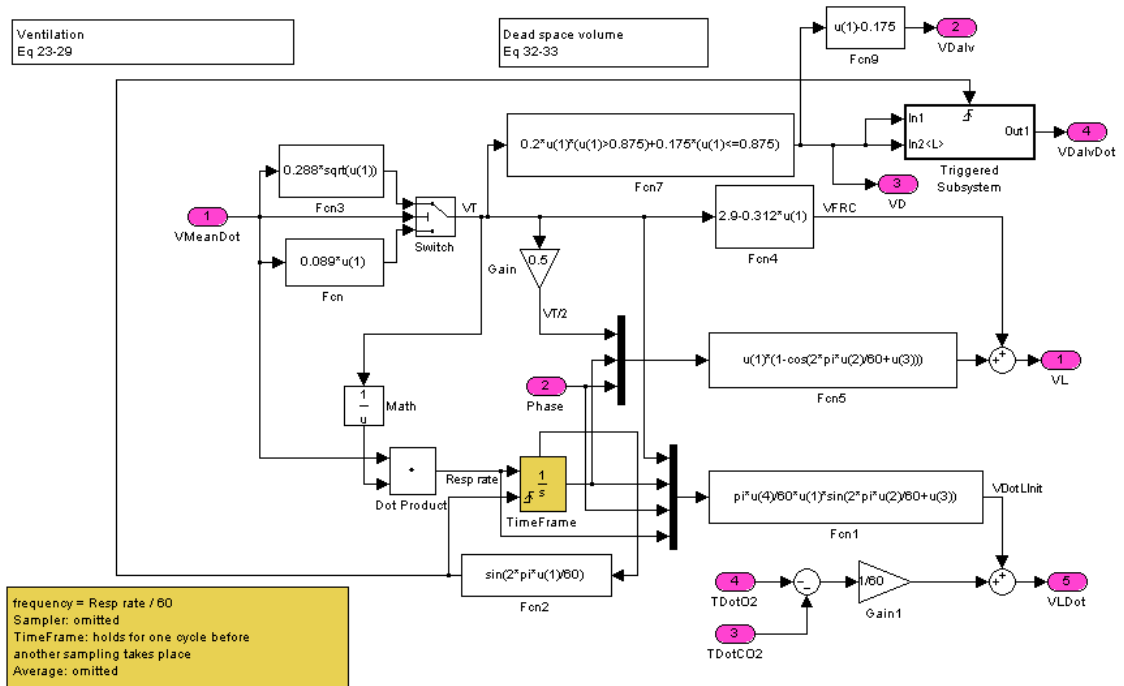


Fig A-4. Ventilation

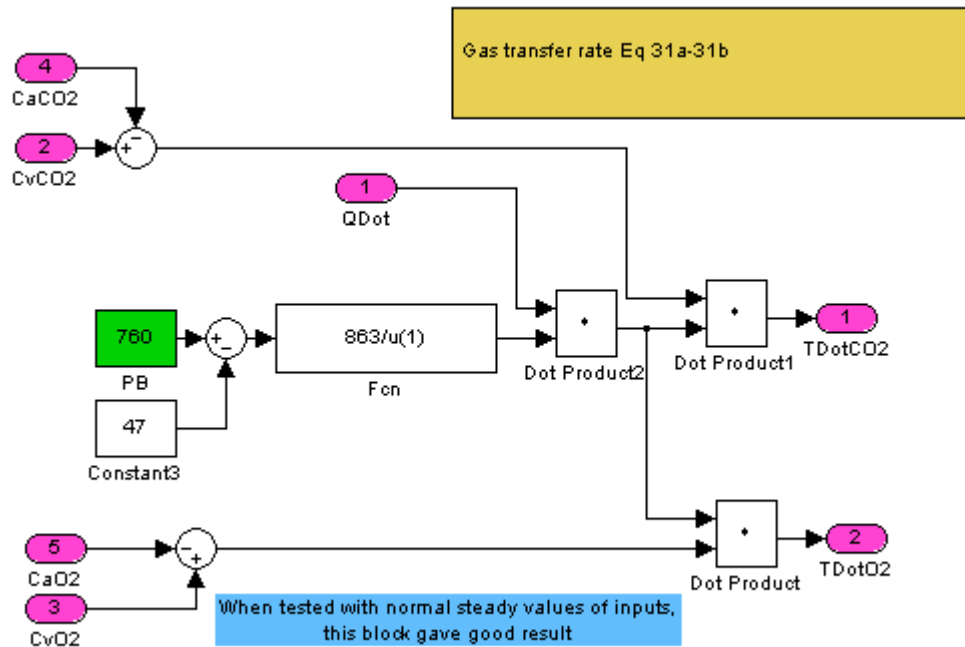


Fig A-5. Gas transfer rate

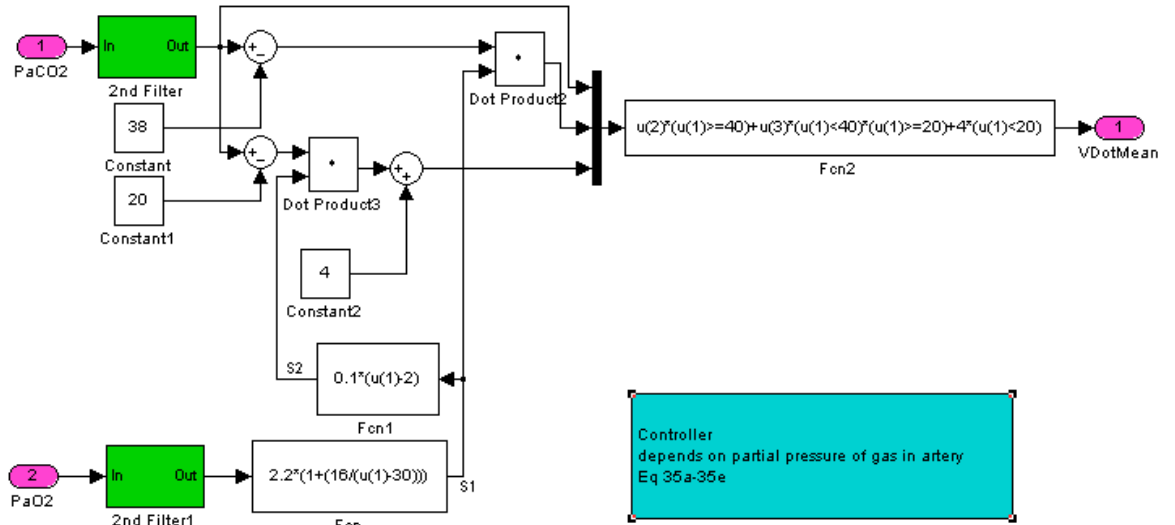


Fig A-6. Controller equation

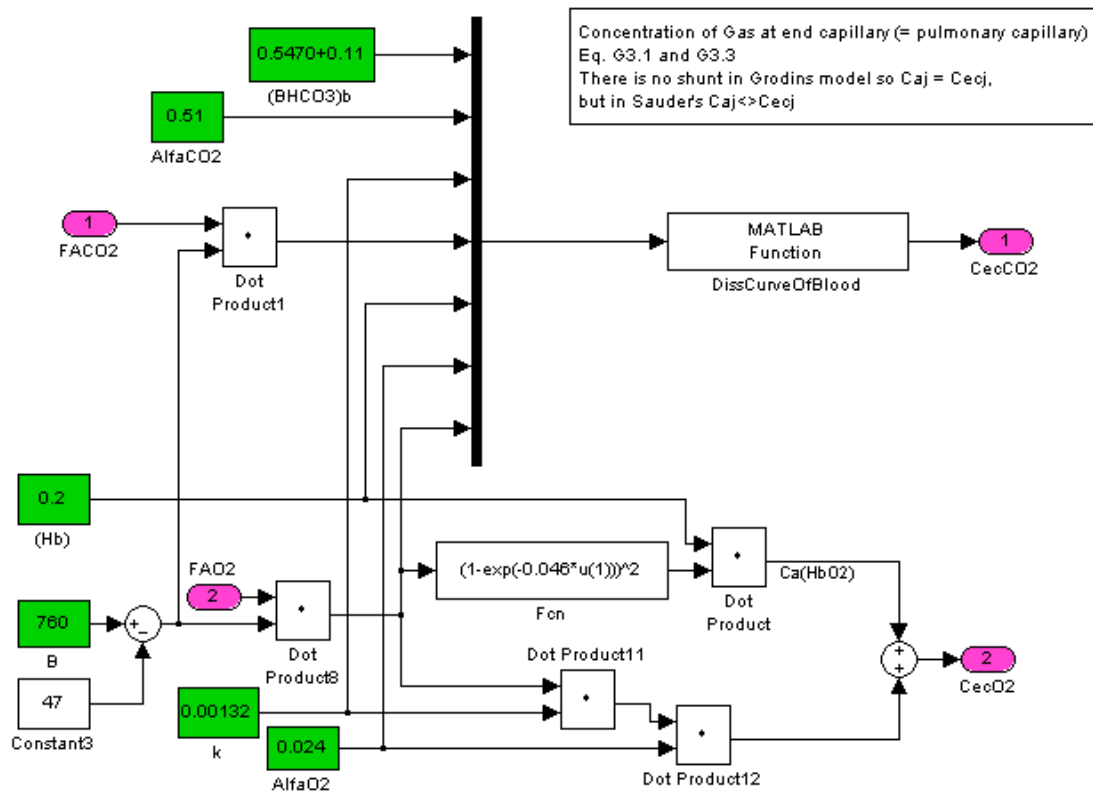


Fig A-7. End capillary

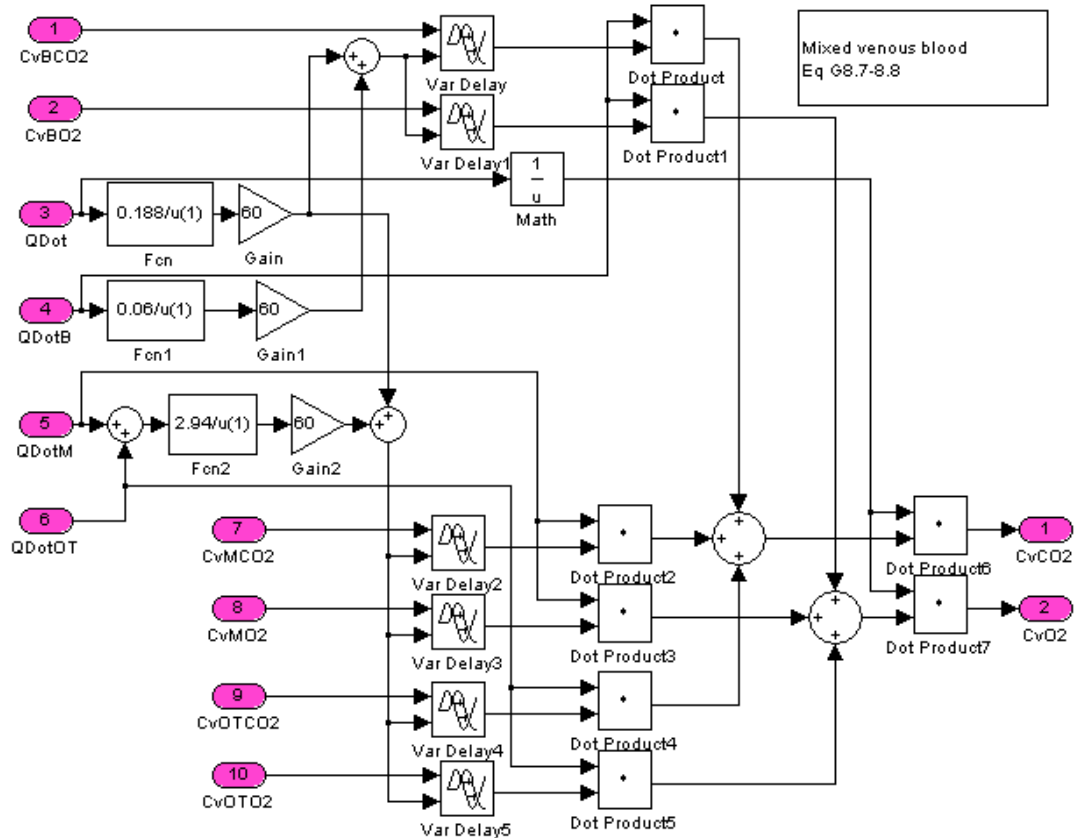


Fig A-8. Mixed venous blood

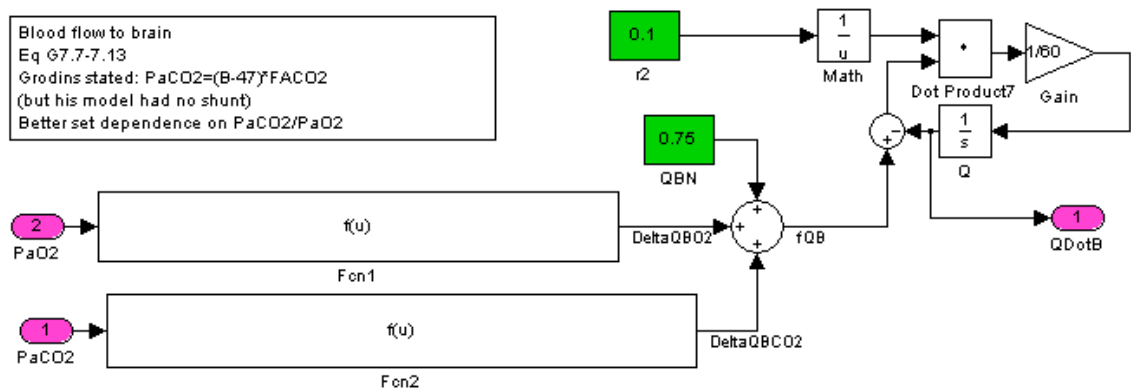


Fig A-9. Brain blood flow

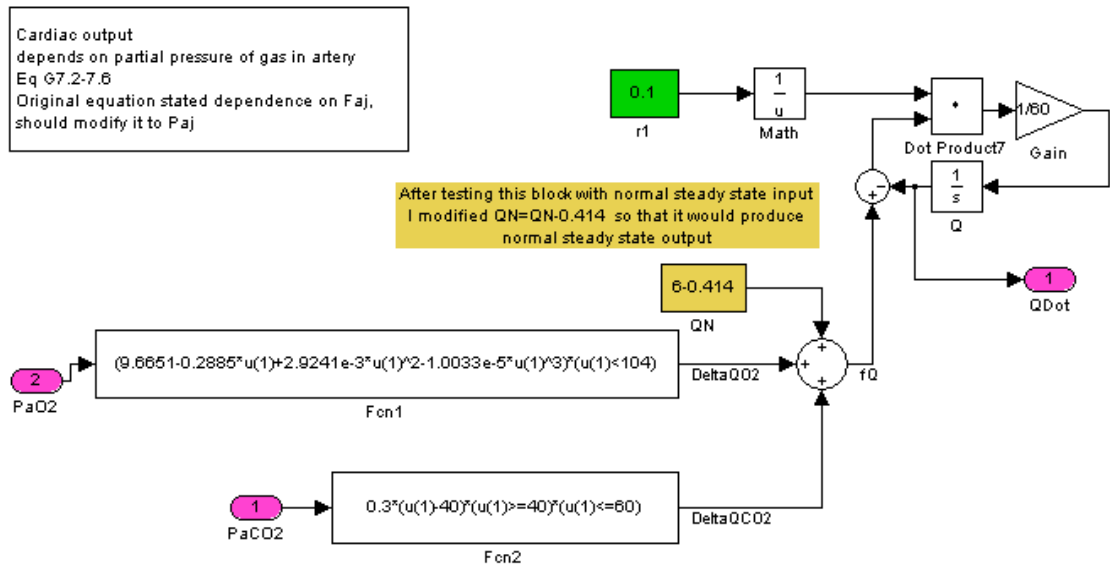


Fig A-10. Cardiac output

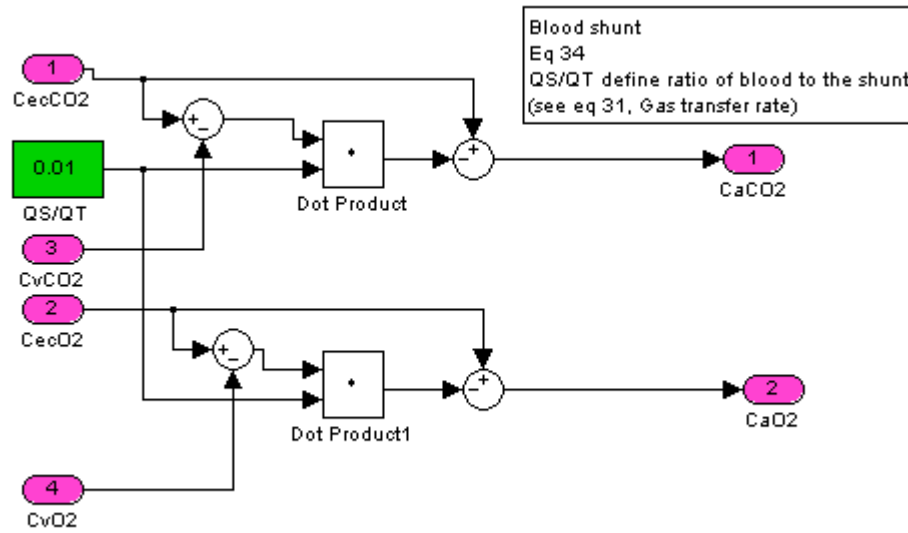


Fig A-11. Blood shunt

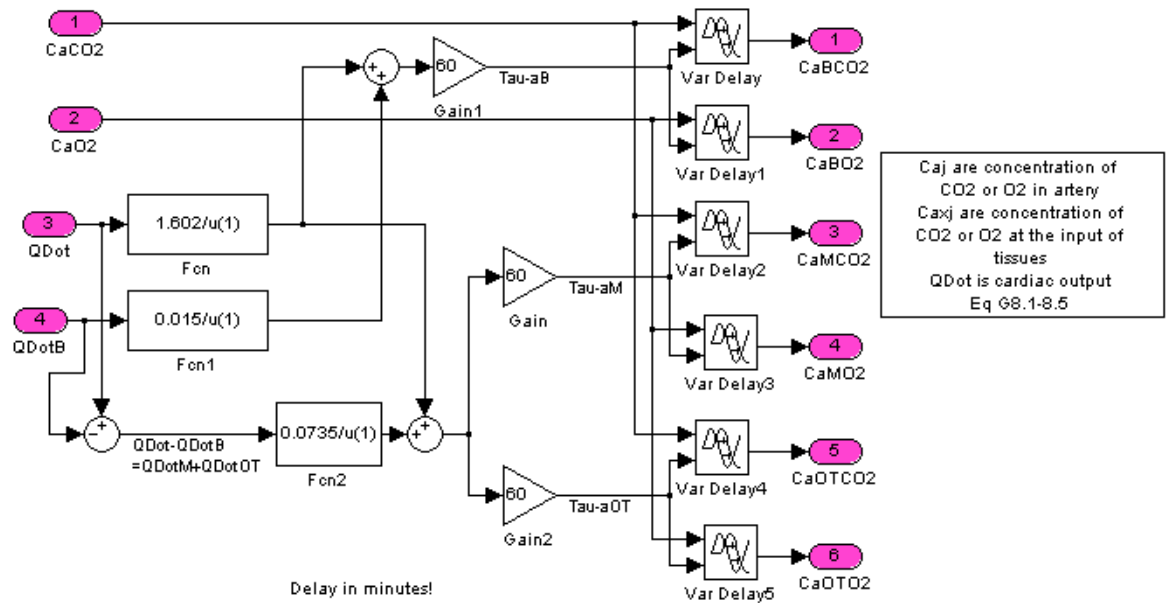


Fig A-12. Delay calculation

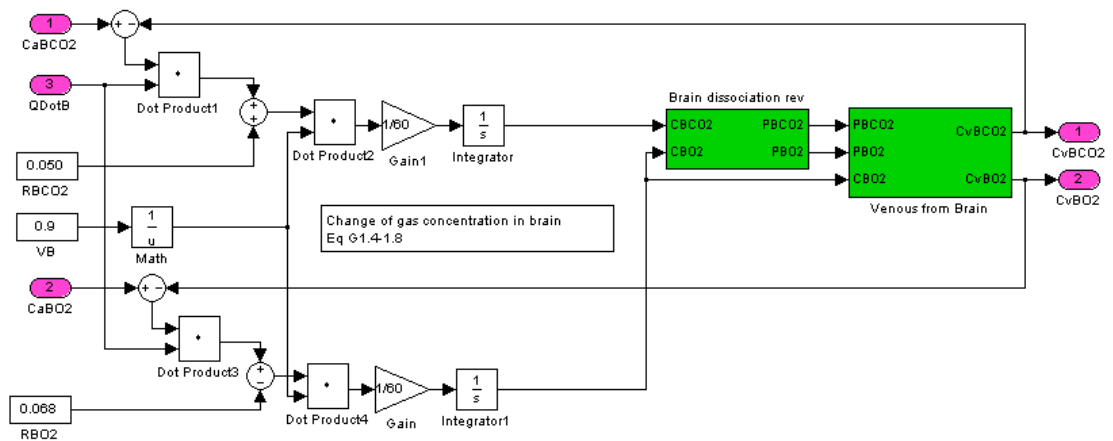


Fig A-13. Brain compartment

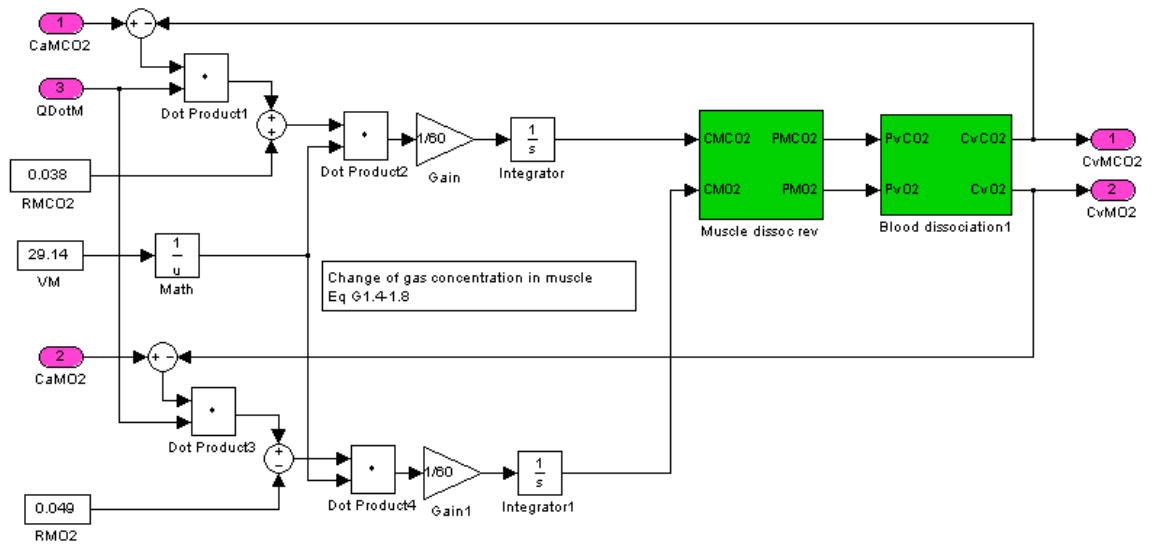


Fig A-14. Muscle compartment

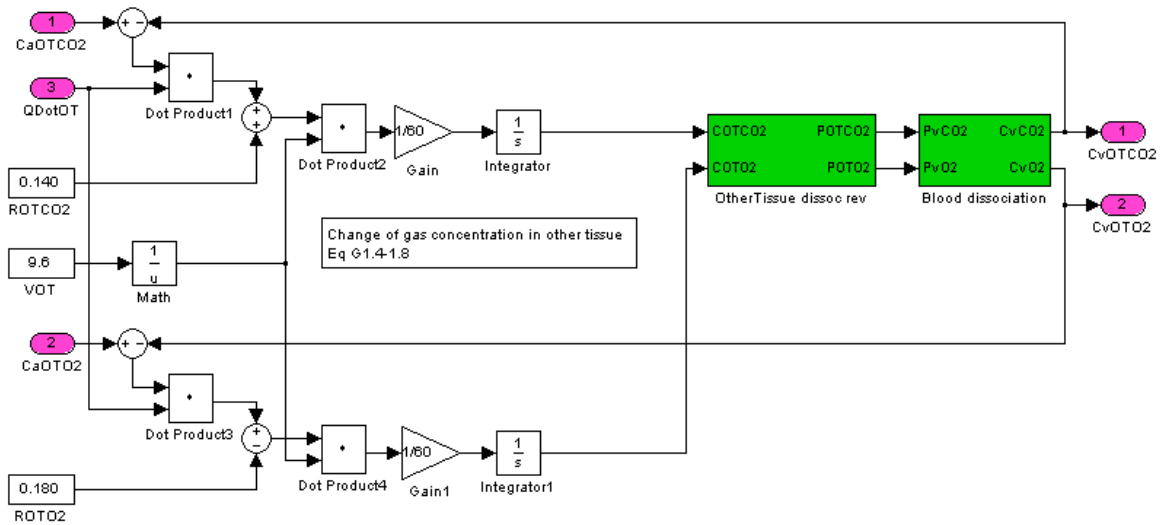


Fig A-15. Other tissue compartment

B. Diagram of the Developed Model

Simulation parameters:

Solver	ode45 (Dormand-Prince)
Step size	Variable
Max step size	0.1 s
Relative tolerance	0.0001

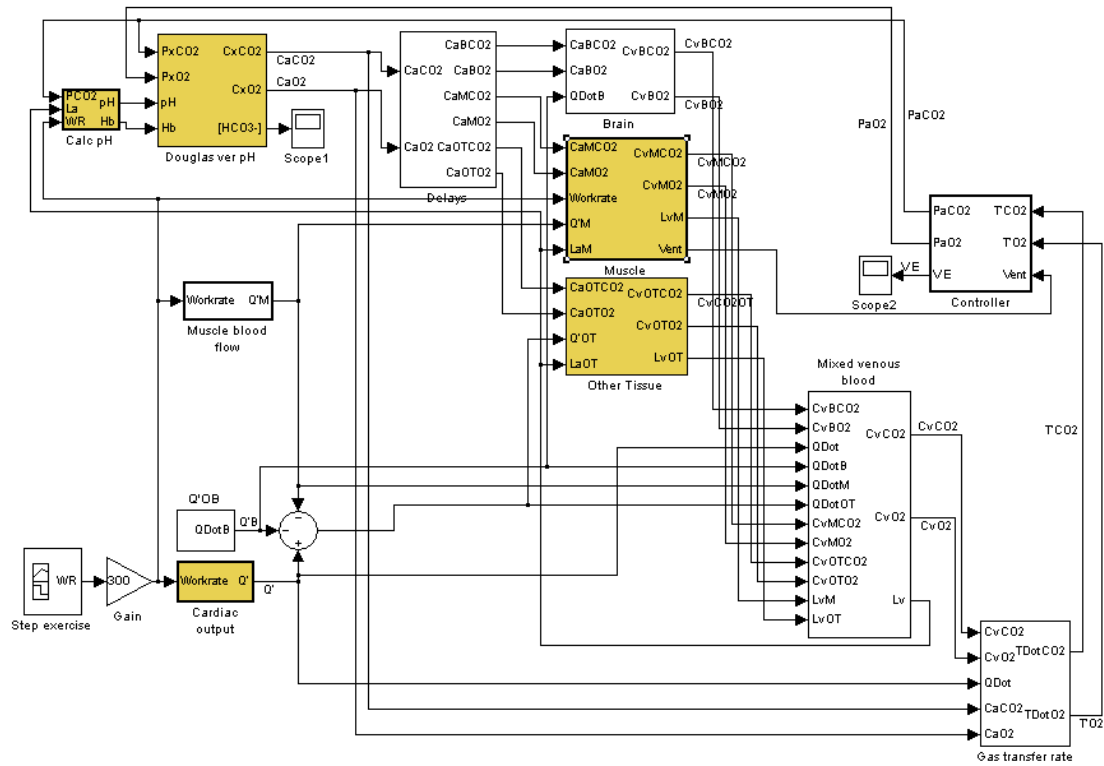


Fig B-1. Main diagram

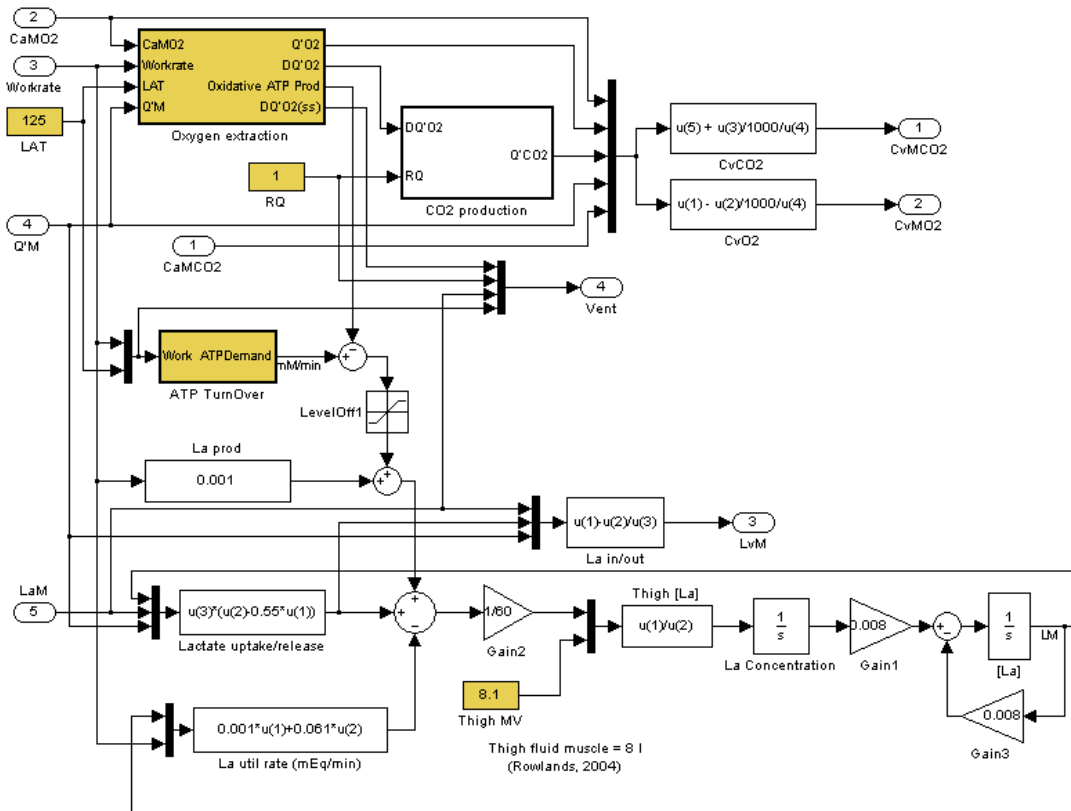


Fig B-2. Muscle compartment

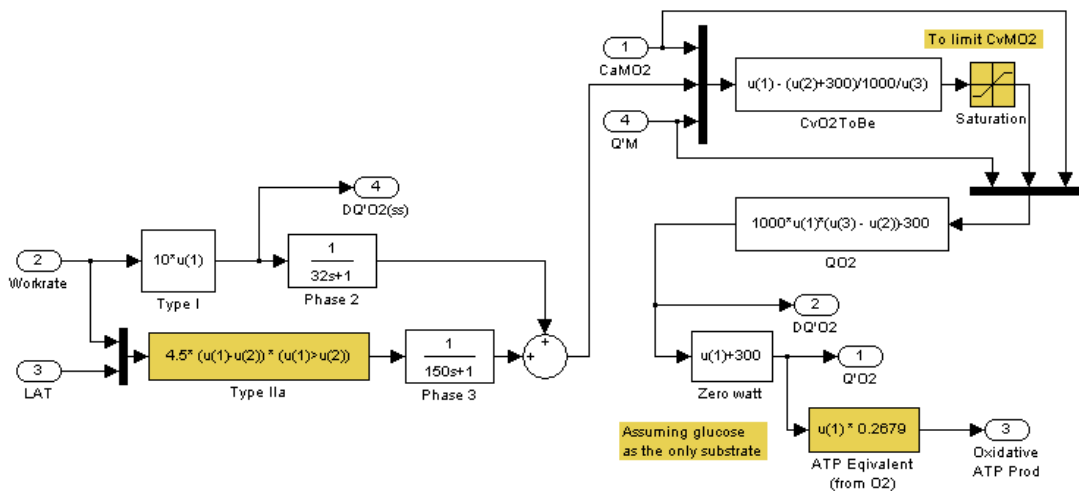


Fig B-3. Muscle oxygen extraction

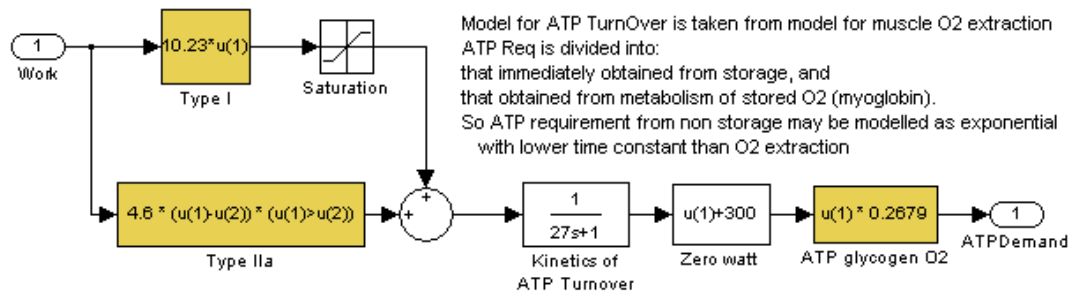


Fig B-4. Muscle ATP Turn-over rate

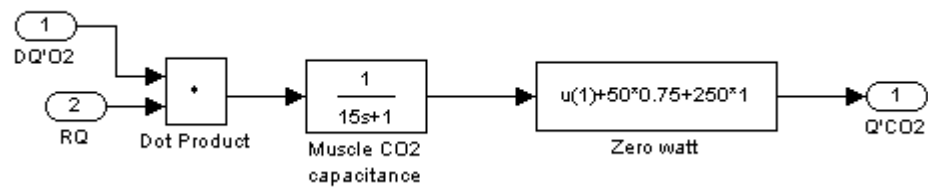


Fig B-5. Muscle CO₂ production

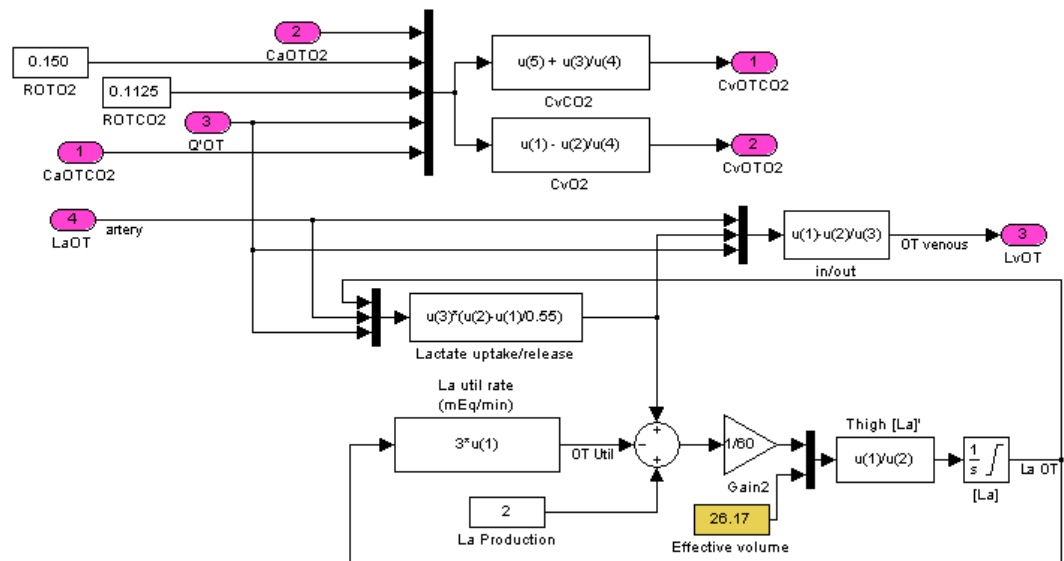


Fig B-6. Other tissue compartment

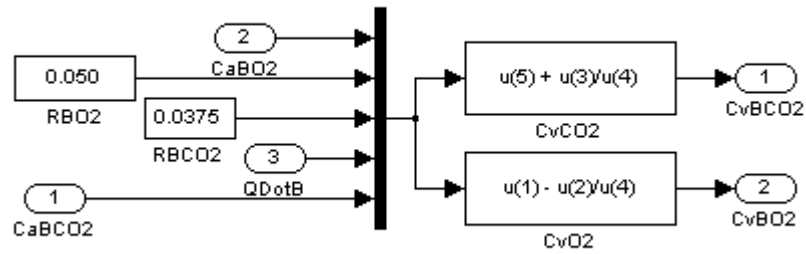


Fig B-7. Brain compartment

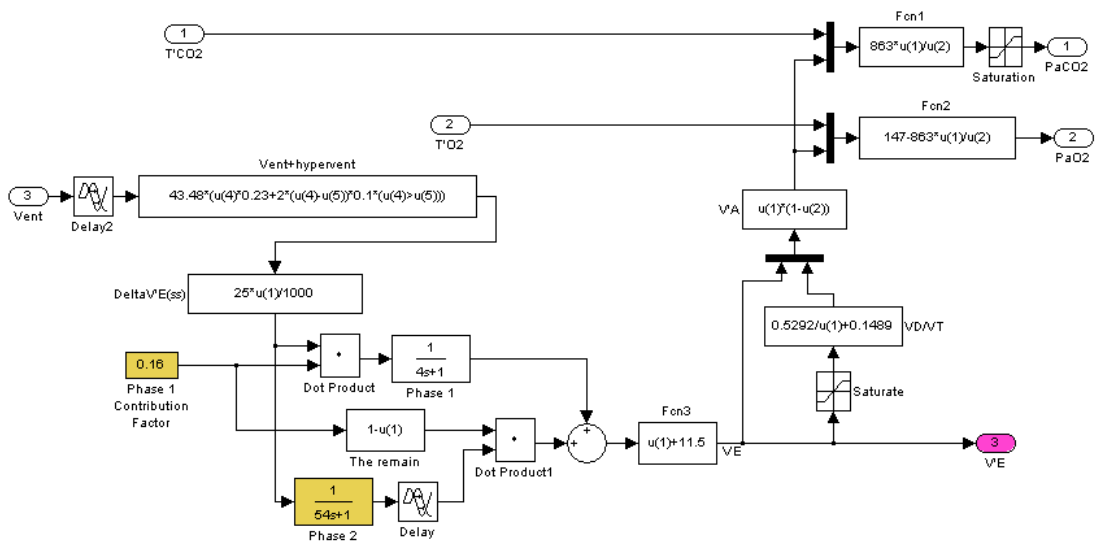


Fig B-8. Ventilation controller and alveolar compartment

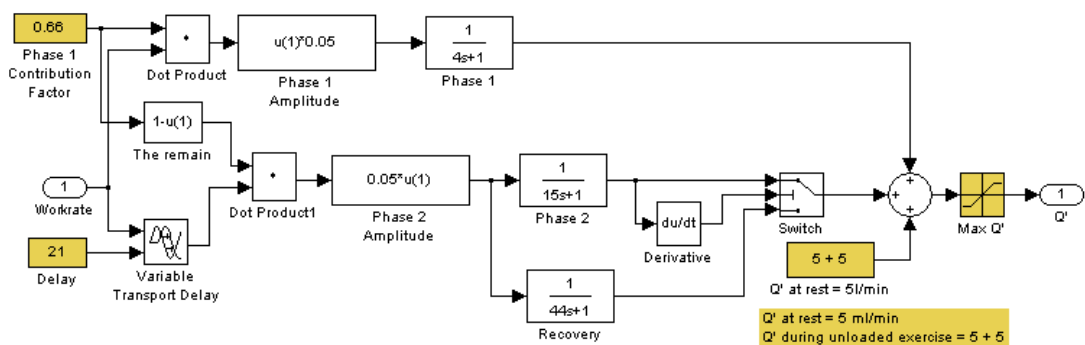


Fig B-9. Cardiac output

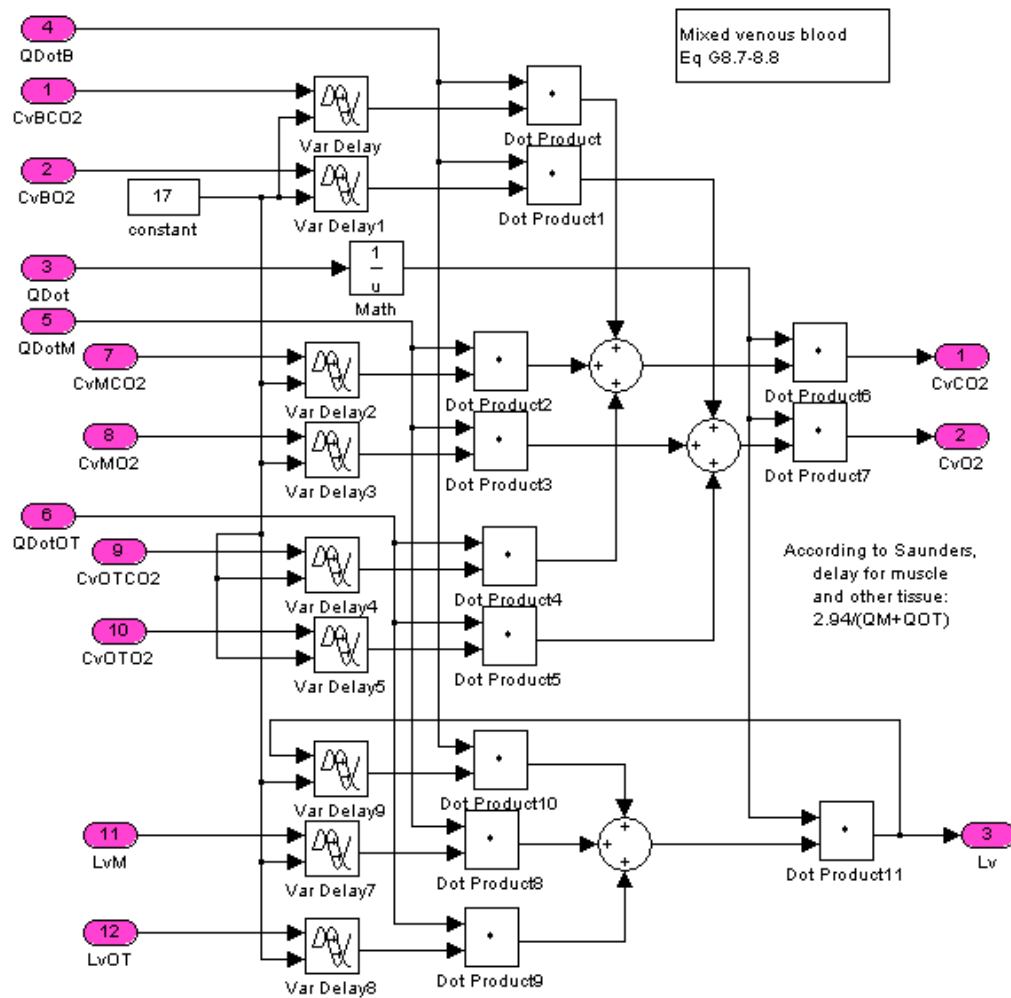


Fig B-10. Mixed-venous blood

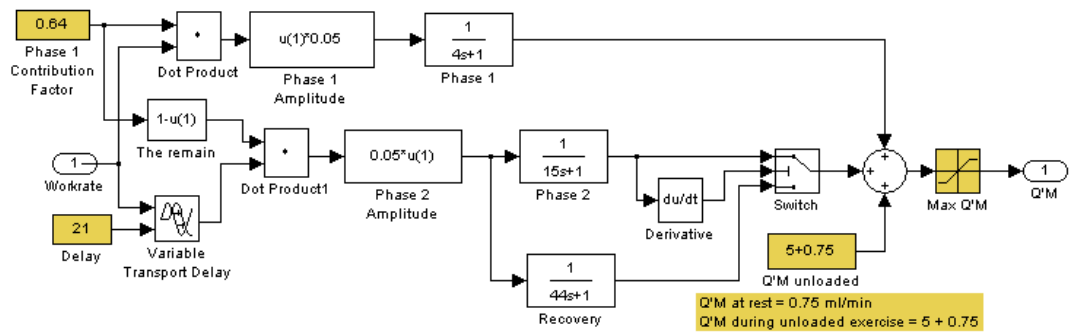


Fig B-11. Muscle blood flow

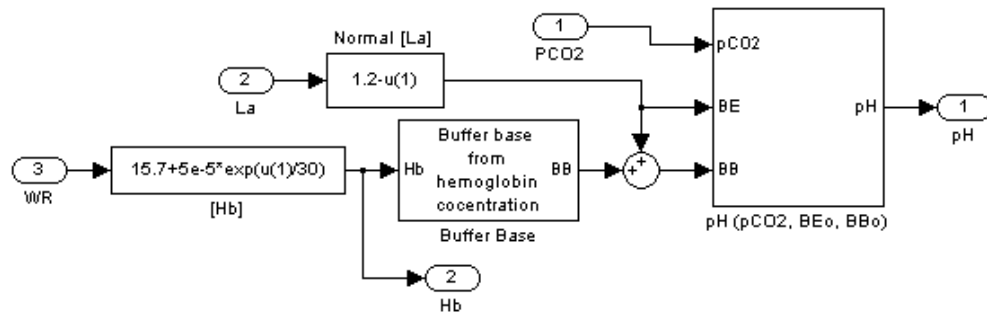


Fig B-12. Hb and pH calculation

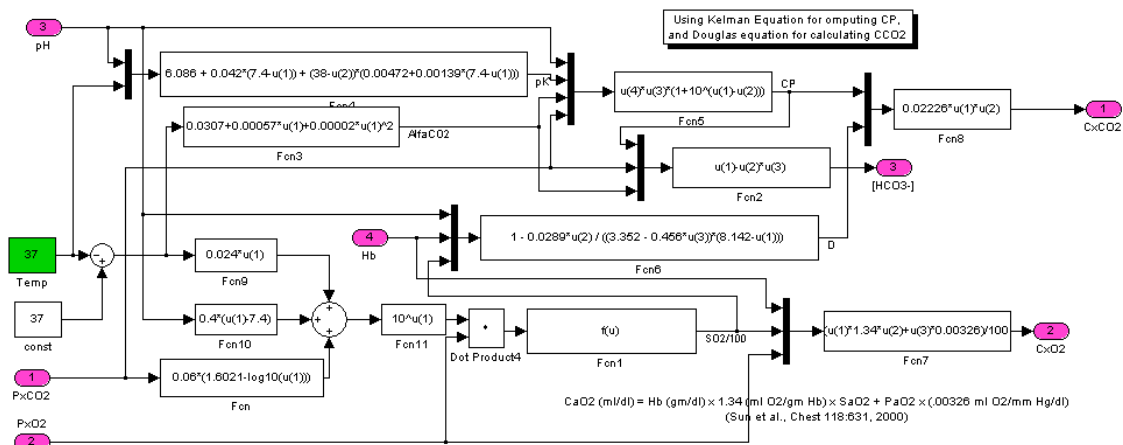


Fig B-13. Blood gas pressure-content relationship

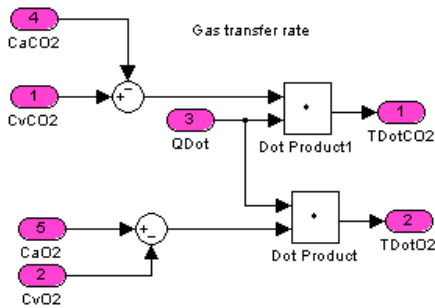


Fig B-14. Gas exchange rate

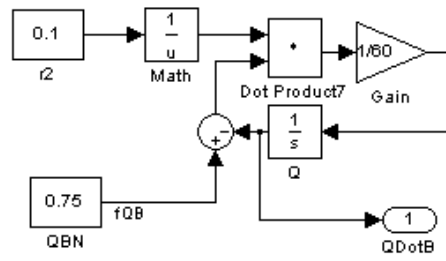


Fig B-15. Brain blood flow

C. Parameter values

Symbol	unit	value	Notes
Muscle oxygen consumption ($Q'O_2$)			
$\Delta Q'O_2/\Delta WR$	ml/min/ml/min	10	Ratio of oxygen consumption to work rate 10.3 – Sun et al. (2001)
$Q'O_{2,bl}$	ml/min	300	Base line value at unloaded exercise (“0” watt)
τ_f	s	32	Fundamental time constant
τ_s	s	150	Slow component time constant
TD_s	s	0	Slow component time delay 120 – 180 – Whipp (1994a)
Muscle CO₂ production ($Q'CO_2$)			
$Q'CO_{2,bl}$	ml/min	287.5	Base line value at unloaded exercise (“0” watt)
τ_c	s	1/15	CO ₂ storage capacity
Other tissues			
RO_{O_2}	ml/min	150	Other tissue O ₂ consumption
RO_{CO_2}	ml/min	112.5	Other tissue CO ₂ production
RBO_2	ml/min	50	Brain O ₂ consumption
$RBCO_2$	ml/min	37.5	Brain CO ₂ production
Lactate			
V_M	l	8.1	Muscle fluid volume 8.1 – Rowlands et al. (2004)
V_{OT}	l	26.17	Other tissue fluid volume
τ_c	s	125	Muscle storage capacity
Ventilation ($V'E$)			
$V'E_{bl}$	l/min	11.5	Base line value at unloaded exercise (“0” watt)
τ_i	s	4	Initial (phase 1) component time constant
τ_f	s	54	Fundamental time constant
TD_f	s	21	Fundamental component time delay
Φ_1		0.16	Phase 1 relative magnitude
Cardiac output (Q')			
$\Delta Q'/\Delta WR$	ml/min/ml/min	0.05	Ratio of cardiac output to work rate
Q'_{bl}	l/min	10	Base line value at unloaded exercise (“0” watt)
τ_i	s	4	Initial (phase 1) component time constant
τ_f	s	15	Fundamental time constant
TD_f	s	21	Fundamental component time delay
Φ_1		0.66	Phase 1 relative magnitude

Appendix C. Parameter Values

Symbol	unit	value	Notes
Muscle blood flow (Q'M)			
Q'M _{bl}	l/min	5.75	Base line value at unloaded exercise ("0" watt)
τ_i	s	4	Initial (phase 1) component time constant
τ_f	s	15	Fundamental time constant
TD _f	s	21	Fundamental component time delay
Φ_1		0.66	Phase 1 relative magnitude
Other variables			
[Hb]	g/dl	15.7	Haemoglobin concentration
T	°C	37	Body temperature
LT	watt	100	The lactate threshold Or LT=125 at incremental exercise simulation

D. Lactate Model in Tissue Compartments

Cabrera et al. (1999) proposed a mass balanced model of a compartment as a system of three parallel compartments: a blood capillary compartment, an interstitial space compartment and a tissue cell compartment. In this system, convective mass transport occurs within the capillaries and diffusion occurs through the capillary wall between the blood and the interstitial fluid (ISF) and through the cell membranes between the ISF and the tissue cells.

Figure has been removed
due to Copyright restrictions.

Fig D-1. Compartmental model of tissue compartment; F is blood flow through the compartment; C is concentration of a species; P and U are production and utilization rate of a species respectively.

Mass balance equations that apply for this system are:

$$V_{cb} \frac{dC_{cb}}{dt} = QC_a - \kappa (C_{cb} - C_{if}) - QC_v$$

$$V_{if} \frac{dC_{if}}{dt} = \kappa (C_{cb} - C_{if}) - \pi (C_{if} - \sigma C_{tc})$$

$$V_{tc} \frac{dC_{tc}}{dt} = \pi (C_{if} - \sigma C_{tc}) + P_{tc}(t) - U_{tc}(t)$$

where V_{cb} , V_{if} , and V_{tc} are the compartment volumes, C_{cb} , C_{if} , and C_{tc} are the substrate concentrations in the capillary blood (cb), interstitial fluid (if), and tissue cell (tc) compartments, respectively; C_a is the arterial blood substrate concentration; C_v is the substrate concentration in the venous blood draining tissue compartment; $P_{tc}(t)$ and $U_{tc}(t)$ are, respectively, the rates of substrate production and utilization by the tissue cells; κ and π are the substrate permeability through the capillary wall and cell membrane respectively, and σ is the partition coefficient which represent the ability of the species to diffuse (or transported) between two compartments.

When κ and π are sufficiently large, equilibrium conditions occur between the capillary blood and the interstitial space ($C_{cb} \approx C_{if}$) and between the interstitial space and the tissue cell space ($C_{if} \approx C_{tc}$). Also assuming a perfectly mixed blood compartment, the output concentration from the capillary compartment is $C_v = C_{cb} = \sigma C_{tc}$. Consequently, the three equations are not independent and can be summed to obtain

$$V \frac{dC}{dt} = P(t) - U(t) + Q(C_a - \sigma C)$$